

UCSF

UC San Francisco Electronic Theses and Dissertations

Title

Essential roles for Galpha13 in endothelial cells and neural crest during embryonic development

Permalink

<https://escholarship.org/uc/item/11v1q92d>

Author

Willison, L. David

Publication Date

2005

Peer reviewed|Thesis/dissertation

Essential roles for Galpha13 in endothelial cells and neural crest during
embryonic development

by

L. David Willison

DISSERTATION

Submitted in partial satisfaction of the requirements for the degree of

DOCTOR OF PHILOSOPHY

in

Cell Biology

in the

GRADUATE DIVISION

of the

UNIVERSITY OF CALIFORNIA, SAN FRANCISCO

UCSF LIBRARY

Date

University Librarian

Degree Conferred:.....

IPCCE LIBRARY

Copyright (2005)
by
L. David Willison

Acknowledgements

The work detailed in this thesis was conducted with Dr. Kathleen M. Ruppel and was published in *The Proceedings of the National Academy of Sciences*, volume 102, pages 8281-8286 (June 7, 2005).

We thank Drs. Tom Sato and Mashashi Yanagisawa of U.T. Southwestern at Dallas; J. Miyazaki of Osaka University Medical School, Osaka, Japan; Marc Tessier-Lavigne, Hilary Beggs, Louis Reichardt and Gail Martin, UCSF (MTL now at Genentech); S.M. Dymecki, Carnegie Institute of Washington; Mel Simon of California Institute of Technology; and Andrew McMahon of Harvard University for certain plasmids and transgenic mouse lines (see Methods).

UCSF LIBRARY

ESSENTIAL ROLES FOR $G\alpha_{13}$ IN ENDOTHELIAL CELLS AND NEURAL CREST DURING EMBRYONIC DEVELOPMENT

L. David Willison

Abstract

Toward identifying the G protein pathways that mediate the actions of the thrombin receptor PAR1 and other G protein-coupled receptors in vascular development, we investigated the role of $G\alpha_{13}$ in endothelial cells and other cell types. *lacZ* inserted into $G\alpha_{13}$ exon 1 was highly expressed in endothelial and presumptive neural crest cells in the mouse embryo at midgestation. Endothelium-specific knockout of $G\alpha_{13}$ caused embryonic lethality at E9.5-11.5 that resembled the *Par1* null phenotype. Conversely, restoration of $G\alpha_{13}$ expression in endothelial cells in $G\alpha_{13}$ null embryos by use of a Tie2 promoter/enhancer-driven $G\alpha_{13}$ transgene rescued the E9.5 vascular phenotype in such embryos. Thus, $G\alpha_{13}$ signaling in endothelial cells plays a critical role in vascular development. Roles in other cell types were also uncovered. The Tie2 promoter/enhancer- $G\alpha_{13}$ transgene completely rescued development of endothelium-specific $G\alpha_{13}$ knockout embryos but not $G\alpha_{13}$ global knockouts; transgene-positive $G\alpha_{13}$ null embryos developed for several days beyond their transgene-negative littermates and then manifested a new phenotype that included intracranial bleeding and exencephaly. Knockout of $G\alpha_{13}$ in the neural crest using *Wnt1-Cre* phenocopied these endothelial-rescued $G\alpha_{13}$ nulls. Taken together, our results suggest a critical role for G protein-coupled receptor signaling via $G\alpha_{13}$ in endothelial cells and neural crest during mammalian embryonic development.

JICCE LIBRARY

Table of Contents

Copyright.....	ii
Acknowledgements.....	iii
Abstract	iv
Table of Contents.....	v
List of Tables	vi
List of Figures.....	vii
Chapter	
I. Introduction.....	1
II. Results.....	34
III. Discussion.....	65
Materials and Methods.....	73
Bibliography	82

IICSE LIBRARY

List of Tables

Table		Page
1	Impaired viability of endothelium-specific $G\alpha_{13}$ knockout mice.....	49
2	Genotype and gross phenotype of embryos from $Tie2p/e-Cre^{Tg/Tg}; G\alpha_{13}^{+/-}$ X $G\alpha_{13}^{flax/-}$ intercrosses.....	49
3	Frequency of hemorrhage and pericardial dilation in $Tie2p/e-Cre^{Tg/o}; G\alpha_{13}^{-/-}$, $Tie2p/e-Cre^{Tg/o}; G\alpha_{13}^{flax/-}$, and $Tie2p/e-Cre^{Tg/o}; G\alpha_{13}^{flax/+}$ embryos	49
4	Endothelial $G\alpha_{13}$ transgene rescue of early $G\alpha_{13}^{-/-}$ lethality. Genotype and gross phenotype of embryos from $Tie2p/e- G\alpha_{13}^{Tg/o}; G\alpha_{13}^{+/-}$ X $G\alpha_{13}^{+/-}$ intercrosses	58
5	$Tie2p/e- G\alpha_{13}$ transgene rescues development of endothelium-specific $G\alpha_{13}$ knockout mice	58
6	Oligonucleotides used for the generation and genotyping of mice	81

UCSF LIBRARY

List of Figures

Figure		Page
1	Generation of a $G\alpha_{13}^{lacZ}$ allele	36
2	Phenotype of $G\alpha_{13}^{lacZ/lacZ}$ embryos and expression of $G\alpha_{13}$ -lacZ in endothelium and neuroepithelium	37
3	Expression of $G\alpha_{13}^{lacZ}$ in adult tissues	38
4	Analysis of the contribution of $G\alpha_{13}^{lacZ/lacZ}$ cells to the endothelium in midgestation embryos.....	41
5	Generation of a floxed $G\alpha_{13}$ allele.....	43
6	Excision of the floxed $G\alpha_{13}$ allele	44
7	Gross phenotype of $G\alpha_{13}$ endothelium-specific and $G\alpha_{13}^{-/-}$ knockouts.....	50
8	Vascular phenotype of $G\alpha_{13}$ endothelium-specific and $G\alpha_{13}^{-/-}$ knockouts.....	51
9	Yolk sac vascular phenotype of $G\alpha_{13}$ endothelium-specific and $G\alpha_{13}^{-/-}$ knockouts	52
10	Rescue of early $G\alpha_{13}^{-/-}$ lethality with an endothelium-specific $G\alpha_{13}^{-/-}$ transgene..	59
11	Deletion of $G\alpha_{13}$ in neuronal cell populations with <i>Nestin-Cre</i> and <i>Wnt1-Cre</i>	60
12	Exencephaly and hemorrhage in embryos in which $G\alpha_{13}$ is absent in neural crest cell populations	61
13	$G\alpha_{13}$ -deficient endothelial cells fail to form a network on Matrigel	64

UCSF LIBRARY

Chapter I:
INTRODUCTION

Chapter Ia: Description of vasculogenesis and angiogenesis:

Formation of blood vessels during mammalian embryonic development is a complex and highly regulated process. Angioblasts proliferate, migrate, and differentiate to form primitive vascular structures composed of endothelial cells. These structures remodel by sprouting, branching, growing, and regressing, and mature by the recruitment and differentiation of pericytes and smooth muscle cells. Studies to define the molecular signals that orchestrate vascular development have focused mainly on receptor tyrosine kinases and integrins, and their ligands. Less is known regarding the roles of G protein-coupled receptors (GPCRs) in this process. In this thesis I will present data that advances our understanding of how GPCR signaling, specifically how the heterotrimeric G protein $G\alpha_{13}$, contributes to vascular development. In Chapter 1 I will provide an overview of some of the processes that control vasculogenesis and angiogenesis, and discuss some of the genes and signaling pathways involved.

Blood vessel formation can be divided into two broad categories, vasculogenesis and angiogenesis. Vasculogenesis refers to the *in situ* differentiation of endothelial cells from mesodermal precursors and their subsequent organization into a network, or plexus, of blood vessels. Angiogenesis refers to the processes that occur after this initial vascular plexus is formed and includes sprouting angiogenesis and intussusceptive angiogenesis.¹ Sprouting angiogenesis occurs when new vessels grow out from preexisting ones, and

UCSF LIBRARY

involves localized proteolytic degradation of the vessel wall and the surrounding extracellular matrix proteins followed by migration and proliferation of endothelial cells as the nascent vessel forms. In the adult, sprouting angiogenesis is thought to coincide with the recruitment of bone marrow derived endothelial stem cells to the site of sprouting, though it is not established whether this also occurs in the embryo.^{2,4} Intussusceptive angiogenesis occurs when a preexisting vessel is subdivided into two or more smaller vessels by “transcapillary pillars” and does not require proliferation.^{5,6} In concert these angiogenic processes transform the relatively uniform vascular bed created during vasculogenesis into an expanded, hierarchical tree of vessels. Subsequent vessel maturation involves selective pruning of the vascular tree and the recruitment and differentiation of pericytes and vascular smooth muscle cells to and around the vessel wall, followed by the formation of an extracellular matrix.⁷ Without support cells or the extracellular matrix, the vessel is unstable and prone to regression.⁸

Chapter 1b: The Hemangioblast:

The first step in the development of the cardiovascular system is the differentiation of endothelial cells. Accumulating evidence suggests that endothelial cells are derived from a bipotential progenitor cell, the hemangioblast, which has both hematopoietic and endothelial potential. Support for this idea has its roots in classical histological studies conducted nearly a century ago by Florence Sabin.⁹ Further evidence of the hemangioblast’s existence has come from recent *in vitro* studies in which single cells from mouse embryonic stem cell-derived embryoid bodies gave rise to blast

UCSF LIBRARY

colonies containing both hematopoietic and endothelial cells.^{10, 11} Further work both *in vitro* and *in vivo* suggests that recently gastrulated mesodermal precursor cells defined by the expression of the mesodermal marker Brachyury (*T*) and the vascular endothelial growth factor (VEGF) receptor Flk1¹² or by the expression of the transcription factor SCL/TAL1 and Flk1^{13, 14} are the precursors to the hemangioblast. The application of this model is not restricted to mammals as work in chick embryos has shown that VEGF can direct recently gastrulated SCL/TAL1⁺ mesoderm cells toward an endothelial cell fate.¹⁵ Other signaling factors have been shown to be important in determining or supporting the murine hemangioblast lineage including fibroblastic growth factors (FGF),¹⁶⁻¹⁸ bone morphogenetic proteins (BMP),¹⁹ and Hedgehog (Hh) ligands.²⁰

Pinpointing the timing and location of hemangioblast commitment in the mouse embryo has proved difficult, though one recent study has shown that the commitment to a hemangioblast fate can occur intraembryonically at the primitive streak early during mouse development (around embryonic day E7.0) in cells that co-express Brachyury and Flk1.²¹ At this point it is unclear whether these early hemangioblasts are capable of seeding the entire embryo, or if hemangioblasts form independently elsewhere at later stages in the yolk sac. Interestingly, the existence of the hemangioblast, or of hemangioblast-like cells, has also been suggested in the analysis of SCL/TAL1 function in *Danio rerio* and in cell fate studies in *Drosophila melanogaster* where the FGF-Receptor (FGFR) homologue *heartless* is involved in patterning the mesoderm and in maintaining cardiocytes (which are analogous to vertebrate endothelial cells).^{22, 23} These

UCSF LIBRARY

data point to the conserved nature of endothelial cell fate decision across multiple animal phyla.

Historically, the first site of vasculogenesis in the mouse embryo was thought to be the blood islands of the extraembryonic yolk sac beginning at around E6.5-7.0.²⁴ Blood islands are initially isolated foci of SCL/TAL1⁺; Flk1⁺ cells that can be visualized as individual, hollow spheres of endothelial cells surrounding a loose inner mass of hematopoietic precursors.²⁵ Blood islands are formed by E7.3 and then coalesce into a uniform vascular plexus by E8.5. They then remodel into a branched, arborized tree that connects to the embryo proper via the vitelline vessels by E9.5 to supply the embryo with yolk sac nutrients. The first intraembryonic vascular structures to form are the heart and the great vessels.* At around E7.3 the endocardial primordia are formed as a bilateral crescent of migrating angioblasts in the cranial mesoderm that connects through the midline. Between E8.2-8.5 these bilateral heart fields are brought to the midline and remodeled into endocardial tubes. Simultaneously, at around E7.8 the angioblasts in bilateral aortic primordia become visible in the para-aortic splanchnopleuric mesoderm (known later in development as the aorta-gonad mesonephros or AGM). By E8.5 these have formed a primitive vascular network which is bidirectionally remodeled into the bilateral embryonic aortae.¹³ By E8.5 a rudimentary embryonic circulation is established,

* Historically it has been accepted that extraembryonic vasculogenesis does not contribute to intraembryonic vasculogenesis (*i.e.*, that intraembryonic angioblasts differentiate *in situ*) though recent work suggests that blood island-derived extraembryonic cells can contribute to vascular structures within the embryo proper.

[LaRue, A. C., Lansford, R. & Drake, C. J. Circulating blood island-derived cells contribute to vasculogenesis in the embryo proper. *Dev Biol* 262, 162-72 (2003).]

though the extent to which the intra- and extraembryonic vascular compartments communicate at this developmental stage is still debated.^{26, 27}

Chapter Ic: Molecules involved with vessel assembly:

What are the molecular signals that orchestrate the processes just described? VEGF (also known as VEGF-A) was initially discovered in the 1970s based on its ability to cause an increase in vascular permeability in guinea pig skin.²⁸ It was the first factor discovered that causes an angiogenic effect selectively on endothelial cells. As alluded to in the above discussions of hemangioblast and endothelial cell fate determination, VEGF plays a central role in the control of vascular development. VEGF is a ~40-kilodalton disulfide-linked dimeric glycoprotein that shares homology to platelet derived growth factor-B (PDGF-B) and to other VEGF-related proteins including VEGF-B, VEGF-C, VEGF-D, and placental growth factor (PlGF).²⁹ VEGF exists as a variety of splice-variant isoforms that have different signaling characteristics,³⁰ though in this discussion these distinctions will not be addressed and “VEGF” will refer to any or all VEGF-A isoforms collectively. VEGF binds to three cell surface receptor tyrosine kinases; the fms-like tyrosine kinase (VEGFR1 or Flt1)^{31, 32} and fetal liver kinase-1 (VEGFR2 or Flk1)³³ which are both expressed on embryonic vascular endothelium, and VEGFR3 or Flt4 which is expressed on lymphatic endothelium.^{34, 35} VEGF can also bind to neuropilin-1 and neuropilin-2 (NP1 and NP2) which have previously described roles in axon guidance as cell surface receptors for class III semaphorins. Though these receptors do not have tyrosine kinase activity and are also expressed on neurons, NP1 enhances the

UCSF LIBRARY

binding of VEGF to Flk1.³⁶ Interestingly, mice lacking NP1 suffer from transposition of the great vessels and both *NP1* and *NP1/NP2* double null mice have defects in yolk sac angiogenesis and in neural vascularization in addition to the defects in axon guidance that would be expected due to their interaction with class III semaphorins.^{37, 38} Mice lacking NP2 show absence or reduction of small lymphatic vessels and capillaries, but larger lymphatic vessels, arteries, and veins are intact.³⁹

Heterozygosity for a deletion of the VEGF gene (*Vegfa*) in mice results in lethality between E11.0 and E12.0 with defects in blood island formation, sprouting angiogenesis, lumen formation, the formation of large vessels, and in plexus remodeling.^{40, 41} In addition, using tetraploid aggregation to generate embryos in which the extraembryonic tissues were derived entirely from *Vegfa*^{+/-} cells while the embryo proper was derived from *Vegfa*^{+/+} cells resulted in abnormal angiogenesis and death at midgestation. Deletion of *Vegfa* in neonatal mice results in growth arrest and lethality with structural alterations and increased endothelial cell death in the liver vascular bed indicating that VEGF is not only required for proliferation but also endothelial cell survival.⁴² Deletion of the genes encoding for the VEGF receptors Flk1 and Flt1 also results in embryonic lethality and severe alterations in the vasculature.

Embryos lacking Flk1, or lacking one specific tyrosine residue in the cytoplasmic tail of the Flk1 receptor, fail to form blood islands and have widespread defects in vasculogenesis and hematopoiesis.^{43, 44} Using chimera analysis it was shown that *Flk1* null cells fail to migrate from the primitive streak into the yolk sac suggesting a

role for VEGF and Flk1 in the chemotaxis/migration of endothelial cells.⁴⁵ This hypothesis has been supported by other studies including one in which VEGF/Flk1 signaling was shown to guide the tip of endothelial cell filopodia during angiogenic sprouting in the retina.⁴⁶ The regulation of Flk1 transcription/expression is complex and involves many players, some of which have been mentioned above (e.g., Brachyury). As described above, SCL/TAL1 is a transcription factor expressed in hemangioblasts and in endothelial cells, and its deletion in mice results in defects in the yolk sac vasculature as well as in embryonic and adult hematopoiesis.⁴⁷⁻⁵¹ SCL/TAL1 apparently acts in concert with other transcription factors like serum response factor, GATA, and ETS to induce Flk1 expression.⁵² Another early signal that acts to promote vasculogenesis is FGF produced by the paraxial mesoderm⁵³⁻⁵⁵ and, in the case of FGF2 signaling through FGFR1 acts to upregulate Flk1 expression.⁵⁶ The identity of the Zebrafish *cloche* gene is not yet known but it apparently acts cell-autonomously in endothelial cells downstream of SCL/TAL1 and upstream of Flk1 to regulate endothelial cell differentiation.⁵⁷⁻⁵⁹ Flk1 expression is also regulated by environmental oxygen availability by hypoxia inducible factor-1 α (HIF-1 α), which will be discussed in more detail later.

Unlike *Flk1* null embryos, those lacking Flt1 are capable of forming blood islands and endothelial cells but have severe defects in vascular organization that results from a dysregulation of endothelial cell proliferation. In *Flt1* null embryos excess endothelial cells fill the lumen of vessels in both the extra- and intraembryonic tissues.^{60, 61} Although Flt1 is capable of binding VEGF, previous work has not been able to show that the

receptor actually signals in response to VEGF in endothelial cells* and mice lacking the Flt1 cytoplasmic tyrosine kinase domain have no vascular phenotype.⁶² It appears that at least in endothelial cells Flt1 functions to tune the threshold for VEGF signaling⁶³ in a similar, but opposite way as NP1 (see above). VEGFR3, a receptor for the VEGF family member VEGF-C, might also perform a similar role in “tuning” angiogenesis and lymphangiogenesis.^{64, 65} Less is known regarding the regulation of Flt1 transcription than there is about the regulation of Flk1 transcription, though possible players include the zinc-finger transcription factor early growth response-1, or Egr1^{66, 67} and the endothelial PAS domain protein (which has high homology to HIF-1 α).⁶⁸ VEGF signaling through Flk1, and PlGF which is thought to signal through Flt1, have been shown to increase expression of Flt1 under certain conditions.⁶⁹

Chapter Id: Molecules involved with vessel stabilization and maturation:

Until this point, I have described the molecular basis to early events in vascular development: the commitment to the hemangioblast lineage followed by the differentiation of endothelial cells and the formation of the first vascular beds. Next, I will discuss some of the processes and molecules involved with vessel remodeling, and stabilization, which are often referred to as vessel maturation or the “resolution phase” of angiogenesis.

* Previous work *has* suggested that VEGF can signal through Flt1 in monocytes. [Clauss, M. et al. The vascular endothelial growth factor receptor Flt-1 mediates biological activities. Implications for a functional role of placenta growth factor in monocyte activation and chemotaxis. J Biol Chem 271, 17629-34 (1996).]

Tie1^{70, 71} and Tie2 (or *Tek*)⁷² define another family of receptor tyrosine kinases that are expressed in endothelial cells in the developing vasculature of mouse embryos and at adult sites of neovascularization.⁷³⁻⁷⁵ *Tie1* null embryos have a normal vessel pattern at E12.5-E13.5 but show reduced survival of endothelial cells and defects in the vascular integrity of endothelial cells that results in edema and hemorrhage that is apparent late in gestation. These animals die at birth with breathing difficulties presumably resulting from defects in the lung vasculature.^{74, 76} Two studies in which Tie2 signaling is abrogated or reduced show conflicting results. In the first study, *Tie2* null embryos and embryos in which a dominant negative Tie2 protein is expressed both died *in utero* and showed defects in vascular integrity and a decrease in the number of endothelial cells leading the authors to propose a role for Tie2 in endothelial cell proliferation and survival.⁷⁷ The second study showed that *Tie2* null embryos were dead by E10.5 with obvious defects in vascular patterning and angiogenesis by E9.5, including dilated head vessels, a lack of angiogenic sprouting into the neuroectoderm, and a failure of vascular remodeling and maintenance of the vascular capillaries (leading to hemorrhage), but this study did not find defects in endothelial cell survival.⁷⁸ The basis for this difference in phenotypes is thought to be in the construction of the groups' respective targeting vectors, and subsequent studies by others have shown that Tie2 is in fact essential for endothelial cell survival and in its absence these cells undergo apoptosis.^{75, 76, 79}

Tie2 null embryos have defects in endocardial and heart development. These defects include a decreased complexity of the ventricular endocardium and a collapsed endothelial lining of the atria. Mosaic analysis has shown an absolute requirement for

Tie2 in endocardium. Tie1 and Tie2 are each dispensable for the initial assembly of the embryonic vasculature, however both Tie1 and Tie2 are necessary in the microvasculature later during embryogenesis, and in adults.⁸⁰ Tie2 is also required for the association of nascent vessels with perivascular cells and Tie2 appears to negatively regulate intussusceptive angiogenesis.⁸¹ Interestingly, mutation of tyrosine residue 1100 in the intracellular tail of Tie2 recapitulates the endothelial cell and heart defects of global *Tie2* ablation, but does not adversely affect the association of perivascular cells with nascent vessels.⁸²

Angiopoietin-1 (Ang1) is a soluble growth factor that is expressed adjacent to both developing and mature blood vessels, and binds to and induces tyrosine phosphorylation of Tie2.^{83, 84} Embryos lacking Ang1 exhibit a similar, if less severe, phenotype than *Tie2* null embryos and are dead by E12.5 but do exhibit the prominent endocardial and myocardial defects seen in *Tie2* null embryos. *Ang1* null embryos have a reduction in vascular complexity (*i.e.*, vessel branching and endocardial folding), the endothelial cells are poorly associated with pericytes/vascular smooth muscle cells and with the extracellular matrix, and there are reduced numbers of pericytes associated with endothelial cells.⁸⁵ This observation suggests that in addition to supporting angiogenesis, Ang1/Tie2 is involved in the recruitment and/or the stable association of endothelial cells with adjacent pericytes. The fact that mature, stable vessels in the adult consistently express tyrosine phosphorylated Tie2 supports this hypothesis⁸⁶ as does the observation that overexpression of Ang-1 results in tissues that are hypervascularized with leakage-resistant blood vessels.⁸⁷ Humans that have an activating mutation in Tie2 suffer from

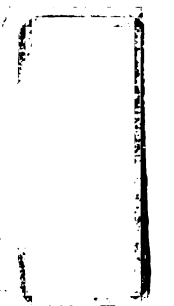
UCSF LIBRARY

autosomal dominant venous malformations; a condition resulting from hypervascularization.⁸⁸

Ang2 was identified by its sequence homology to Ang1 and it acts as an antagonist for Ang1/Tie2 signaling as it inhibits Ang1-mediated Tie2 tyrosine phosphorylation. Though the mechanism of this effect is not fully understood, Ang2 binds to Tie2 but not Tie1, possibly suggesting a direct inhibitory effect of Ang2 binding to Tie2.⁸⁹ Ang2 expression correlates with sites of active, adult vascularization where destabilization of existing vessels is necessary to allow for angiogenic sprouting. Ang2 overexpression in mouse embryos results in discontinuous vessels, separation of the endocardium from the underlying myocardium, absence of the cardinal vein, and poor arborization of vascular beds.⁹⁰ Deletion of the mouse gene for Ang2 has no embryonic phenotype but *Ang2* null adults show defects in vessel regression and sprouting in the neonatal eye, a tissue in which postnatal angiogenic remodeling has been well studied.⁹¹ Therefore, Ang2 has a critical function as a destabilizer of vessel architecture.

Stabilization and maturation of blood vessels relies to a large degree on interactions that occur between endothelial cells and the pericytes/VSMC that surround the vessel. The distinction between a pericyte and a VSMC is not absolute, though in general, pericytes are found embedded in the basement membrane on the abluminal side of the vascular endothelial cells and in some instances actually make direct contact with endothelial cells.⁹² On the other hand, VSMC are separated from this basement membrane by an additional layer of mesenchymal cells and are found mainly on larger

1877
1878
1879
1880
1881
1882
1883
1884
1885
1886
1887
1888
1889
1890
1891
1892
1893
1894
1895
1896
1897
1898
1899
1900



1901
1902
1903
1904
1905
1906
1907
1908
1909
1910
1911
1912
1913
1914
1915
1916
1917
1918
1919
1920
1921
1922
1923
1924
1925
1926
1927
1928
1929
1930
1931
1932
1933
1934
1935
1936
1937
1938
1939
1940
1941
1942
1943
1944
1945
1946
1947
1948
1949
1950
1951
1952
1953
1954
1955
1956
1957
1958
1959
1960
1961
1962
1963
1964
1965
1966
1967
1968
1969
1970
1971
1972
1973
1974
1975
1976
1977
1978
1979
1980
1981
1982
1983
1984
1985
1986
1987
1988
1989
1990
1991
1992
1993
1994
1995
1996
1997
1998
1999
2000

vessels. One intriguing possibility is that while VSMC are organized to better effect vascular tone, the close proximity of pericytes to endothelial cells serves to integrate intercellular communication.⁹³ The heterogeneity of pericyte/VSMC populations is highlighted by the fact that 1) pericytes are able to differentiate into VSMC and *vice versa*, and 2) these cells have multiple embryonic origins depending upon the vessel's location in the embryo where they differentiate. Pericytes are most often thought of as being derived from mesenchyme as is the case with pericytes that develop around the trunk vessels,⁹⁴ however the cephalic neural crest has been shown to contribute VSMC/pericytes to the vessels of the face and forebrain⁹⁵ and the mural cells in the coronary arteries have been shown to derive (via an epithelial-mesenchymal transformation) from epicardial cells that in turn derive from the splanchnic mesoderm.⁹⁶ It has also been proposed that pericytes can transdifferentiate from endothelial cells.⁹⁷

UCSF LIBRARY

How are pericytes/VSMCs determined and localized around developing vessels in the embryo? One central player in this that has been well studied is transforming growth factor- β (TGF β). Mice in which the gene for TGF β 1 has been deleted die around 20 days after birth from a multifocal inflammatory response with associated tissue necrosis^{98, 99} however, a later study showed that, at least in some genetic backgrounds, 50% of TGF β 1^{-/-} and 25% of TGF β 1^{+/-} embryos die at around E10.5. These embryos have defects in the yolk sac vasculature including reduced endothelial cell differentiation and vessel number suggesting a role in vasculogenesis.¹⁰⁰ Transgenic expression of TGF β 1 from a vascular smooth muscle promoter results in dilated blood islands and a possible vasculogenesis defect that is restricted to the extraembryonic tissues.¹⁰¹ In contrast,

animals deficient in either TGF β 2 or TGF β 3 survive to parturition though both result in perinatal death from lung and various other defects.¹⁰²⁻¹⁰⁴ Deletion of the gene for TGF β Receptor II (TGF β RII) results in an embryonic phenotype identical to *TGF β I* knockouts.¹⁰⁵ Analysis of tetraploid embryos in which the extraembryonic tissues, including the yolk sac endothelial cells, lacked TGF β RII showed that TGF β I signaling is not required for endothelial cell differentiation *per se*, but is necessary for the deposition of Fibronectin (Fn) into the extracellular matrix. Reduced Fn in the yolk sac extracellular matrix results in yolk sac instability.¹⁰⁶

Other TGF β Receptor knockouts also exhibit vascular phenotypes. Embryos lacking activin-receptor-like kinase-5, or ALK5, a member of the class I TGF β receptor family have prominent defects in the remodeling and branching of the yolk sac vessels and these embryos die by around E10.5. Endothelial cells from *ALK5*^{-/-} embryos also show increased proliferation and migration in culture, along with decreased Fn synthesis.¹⁰⁷ Embryos deficient in ALK1 (another class I TGF β receptor family member) have similar defects, and pericytes/VSMC in these embryos show delayed differentiation and fail to be recruited to the vessel walls.¹⁰⁸ *ALK1*^{-/-} embryos also show abnormal fusion of the capillary beds throughout the embryo resulting in large cavernous vessels as well as arteriovenous malformations (AVMs) that form between the cardinal vein and the dorsal aorta. These AVMs are associated with reduced expression of EphrinB2 (see below for a discussion of EphrinB2) suggesting a role for ALK1 in arterial-venous identity.¹⁰⁹ Interestingly, disruption of the Zebrafish ALK1 homologue, *violet beaugarde*, also causes AVMs.¹¹⁰ Mutations in the human gene for ALK1 cause

UCSF LIBRARY

hereditary hemorrhagic telangiectasia type 2 (HHT-2), an autosomal dominant disorder characterized by recurrent hemorrhage, especially in the nasal mucosa and the gastrointestinal tract, and dermal and visceral telangiectases often leading to AVMs in the lungs, brain, and other organs.¹¹¹ ALK1 signals through Smad1 and Smad5 and deletion of either of these genes also leads to comparable vascular phenotypes.^{19, 112}

Endoglin, or CD105, is a cell surface accessory protein expressed on endothelial cells that binds TGF β ligands when associated with TGF β RII.^{113, 114} Mutations in the human gene for Endoglin cause hereditary hemorrhagic telangiectasia type 1 (HHT-1) which, in comparison to HHT-2 tends to cause more pulmonary AVMs, a later onset of epistaxis, and carries an increased risk for pulmonary hypertension.¹¹⁵ Vasculogenesis occurs in mice lacking Endoglin (in contrast to *TGF β 1* null embryos) but these animals die by ~E10.5 with defects in yolk sac vessel remodeling, embryonic and extraembryonic hemorrhage, heart defects including absence of the endocardial cushion and failure of the endocardium to undergo epithelial-mesenchymal transformation at the atrioventricular boundary, and a reduction in pericyte/VSMC numbers and their failed recruitment to vessels.¹¹⁶⁻¹¹⁸ Similar to *ALK1* null embryos, *Endoglin* null embryos show arteriovenous malformations between the cardinal vein and dorsal aorta.¹¹⁹

ALK1 and ALK5 are both expressed on endothelial cells and it appears that TGF β signaling from each of these receptors has mutually antagonistic roles in endothelial cell behavior. Signaling through TGF β /ALK5 inhibits endothelial cell proliferation and migration and promotes differentiation of pericytes/VSMC while

UCSF LIBRARY

TGF β /ALK1 signaling promotes endothelial cell proliferation and migration and therefore the balance between the relative activity of these signaling pathways determines the effects of TGF β on endothelial cells.¹²⁰ Analysis of immortalized *Endoglin* null endothelial cell lines by two separate groups suggests that Endoglin plays a key role in determining this balance. One study suggests that loss of Endoglin expression leads to an increase in ALK5 expression resulting in the recruitment of more high affinity ALK1 receptors on the cell surface and hence an increase in endothelial cell proliferation.¹²¹ The other seemingly disparate study showed that loss of Endoglin expression decreased ALK5 expression apparently shifting the balance in favor of TGF β /ALK1 signaling and resulting in decreased endothelial cell proliferation suggesting that Endoglin serves to promote endothelial cell proliferation.¹²² Since ALK5 helps recruit ALK1 into TGF β signaling complexes and is essential for ALK1 activation, one interpretation of these results is that given this requirement of ALK5 for ALK1 signaling, subtleties in the set up of these two experiments or in the relative expression of ALK1/ALK5 in individual cell lines could lead to opposite results.

Using intact yolk sacs from embryos with either a global *Endoglin* knockout or an endothelial cell-specific knockout of *ALK5* it was shown that *Endoglin* null animals have a defect in paracrine TGF β signaling from endothelial cells to adjacent pericytes that results in the failure of pericyte differentiation and association with endothelial cells. Addition of exogenous TGF β 1 to cultured *Endoglin* null yolk sacs rescues this phenotype.¹²³ Embryos with endothelial cell-specific knockouts of either *TGF β RII* or *ALK5* develop similar yolk sac defects as the global knockouts suggesting that the effects

of global disruption of these genes is attributable to their function in endothelial cells at this developmental stage. Neural crest cell specific ablation of TGF β RII results in a DiGeorge syndrome-like phenotype characterized, in part, by a failure of neural crest smooth muscle derivatives to differentiate into VSMC in the cardiac outflow tract, thus providing further evidence that TGF β signaling is crucial within VSMC for their differentiation in some tissues.¹²⁴

A further level of complexity is added to this system when one appreciates that TGF β is secreted by endothelial cells in an inactive form that associates with the extracellular matrix and must be proteolytically activated for signaling.^{125, 126} One player in this process is the gap-junction protein Connexin43 (Cx43). Gap junctions are membrane protein aggregates that connect the cytoplasm of adjacent cells, allowing the passage of second messengers and other signaling molecules.^{127, 128} Cx43 knockout mice die at birth with defects in the patterning of the coronary vessels including decreased complexity of vessel branching and decreased investment of these vessels with VSMC.¹²⁹ *In vitro* studies suggest that although Cx43 null VSMC precursors synthesize latent TGF β 1 and can differentiate upon addition of exogenous activated TGF β 1, they are unable to form gap-junctions with adjacent endothelial cells and this somehow results in an inability to activate latent TGF β 1.¹³⁰ Another connexin family member, Connexin45, is expressed predominantly in the embryonic vasculature, and mice in which this gene has been deleted show vascular remodeling defects and die by ~E10.5.¹³¹ It is tempting to propose that the death of Cx45 null mice is triggered by similar defects in gap-junction communication between endothelial cells and pericytes/VSMC and the subsequent loss of

UCSF LIBRARY

activation of latent TGF β , as in *Cx43* knockouts, though this hypothesis has not yet been addressed.

Platelet-derived growth factor (PDGF) receptors are a family of tyrosine kinase receptors that, like TGF β and Tie2/Ang1, are involved with increasing the stability of nascent vessels. Knockout of the genes for PDGF-B and PDGF receptor- β (PDGFR β) result in perinatal lethality characterized by renal/glomerular defects, cardiovascular defects in which some large arteries are dilated, and hemorrhage.^{132, 133} The unifying defect that explains these phenotypes is a defect in signaling within pericytes/VSMC. This is in contrast to other signaling pathways that regulate pericyte/VSMC function such as Tie2/Ang1, TGF β /Endoglin/ALK1/5, and Edg1 (see below for a discussion of Edg1) in which the primary signaling defect is in endothelial cells. PDGF-B is expressed in immature capillary endothelial cells during angiogenesis and PDGFR β is normally expressed on pericyte/VSMC progenitors that surround the vessels. Pericytes in mice lacking either gene show lower rates of proliferation and fail to migrate toward vessel walls resulting in the decreased mechanical stability of the vessel.^{134, 135} Analysis of chimeras in which *PDGFR β* null cells were introduced into wild type embryos showed that *PDGFR β* null cells were significantly less capable of contributing to pericyte populations (8 fold less capable) than wild type cells.¹³⁶

Endothelial cell-specific ablation of the *PDGF-B* gene recapitulates the pericyte phenotype seen in the global knockout, albeit with less severity, suggesting that this phenotype is a result of loss of endothelial cell secretion of PDGF-B.¹³⁷ Unlike the

UCSF LIBRARY

PDGF-B global knockouts which die perinatally, the endothelial cell-specific knockouts live to adulthood but show persistent pathologies including microhemorrhages and a proliferative retinopathy that resembles that seen in diabetic patients.¹³⁸ Interestingly, it appears that *PDGF-B*^{+/-} mice also show proliferative retinopathy.¹³⁹ Additional work has shown that correct localization of PDGF-B to heparin sulphate proteoglycans* in the extracellular matrix via a C-terminal retention sequence is required for proper pericyte investment of the microvascular wall during normal development and tumor vascularization.^{140, 141} Certain isoforms of VEGF also contain a similar C-terminal retention sequence, and defects in angiogenic sprouting and branching are observed in embryos in which this sequence is deleted.^{142, 143}

Additional regulation of PDGF signaling has been shown to depend upon the interaction of PDGFR β with other membrane bound proteins. The expression of membrane type 1 matrix metalloproteinase (MT1-MMP) in *cis* with PDGFR β enhances the induction of PDGF-B signaling in VSMCs leading to VSMC proliferation and chemotaxis, possibly by releasing matrix-bound PDGF-B and making it accessible for signaling.¹⁴⁴ MT1-MMP apparently also regulates TGF β 1 signaling. Newly secreted TGF β 1 exists in a latent state by the non-covalent association of its active domain with

* In Zebrafish, the heparin sulphate proteoglycan (HSPG) syndecan-2 is required for sprouting angiogenesis of the intersomitic vessels and potentiates VEGF signaling. Loss of function mutations in *Drosophila* HSPGs result in the disruption of various signaling pathways including FGF, Wingless, and Hedgehog. These results support the argument that localization of secreted signaling factors by the extracellular matrix is essential for normal development.

[Chen, E., Hermanson, S. & Ekker, S. C. Syndecan-2 is essential for angiogenic sprouting during zebrafish development. *Blood* 103, 1710-9 (2004).] & [Nybakken, K. & Perrimon, N. Heparan sulfate proteoglycan modulation of developmental signaling in *Drosophila*. *Biochim Biophys Acta* 1573, 280-91 (2002).]

UCSF LIBRARY

11
12
13
14
15
16
17
18
19
20
21
22
23
24
25
26
27
28
29
30
31
32
33
34
35
36
37
38
39
40
41
42
43
44
45
46
47
48
49
50
51
52
53
54
55
56
57
58
59
60
61
62
63
64
65
66
67
68
69
70
71
72
73
74
75
76
77
78
79
80
81
82
83
84
85
86
87
88
89
90
91
92
93
94
95
96
97
98
99
100

its N-terminal propeptide termed latency-associated peptide- β 1 (LAP- β 1). Integrin $\alpha_v\beta_8$ binds to an RGD motif in LAP- β 1 allowing its cleavage by MT1-MMP which releases active TGF β 1 that is capable of engaging in autocrine and paracrine signaling.¹⁴⁵ In the embryo, integrin β_8 is expressed on yolk sac endodermal cells and on periventricular cells of the neuroepithelium, and mice in which the β_8 gene is deleted die in two waves: the first group dies at midgestation from deficient vascularization of the yolk sac, and the second group dies perinatally from brain hemorrhage.¹⁴⁶ It is not known whether defects in TGF β 1 signaling are the underlying cause for the defects observed in β_8 null mice or whether loss of β_8 on endothelial cells or some other cell population is responsible for this phenotype, but this is an intriguing possibility.

Some elegant *in vivo* studies have analyzed the contributions of individual signaling components that are downstream of PDGFR β such as Shc, PI3-kinase, phospholipase-C γ , and Ras-GAP.¹⁴⁷⁻¹⁴⁹ In these studies, specific tyrosine residues in the cytoplasmic tail of PDGFR β that allow binding of various downstream signaling modules were deleted. The resulting phenotypes suggest that there is an additive effect of PI3K and PLC γ binding/signaling on the proliferation of pericytes/VSMC in that by decreasing these downstream signals there is a corresponding decrease in pericyte/VSMC proliferation. Ablation of tyrosine residues that mediate Ras-GAP binding produced the opposite effect and led to an *increase* in the population of these cells. Global deletion of *Ras-GAP* in mice causes lethality at midgestation with vascular patterning defects and hemorrhage.¹⁵⁰ Human patients with inactivating mutations in *Ras-GAP* have AVMs,¹⁵¹

but whether the mouse or human *Ras-GAP* phenotypes are attributable to defects in endothelial cell or in pericyte/VSMC function is unclear.

Edg, or endothelial differentiation gene, receptors constitute a G protein-coupled receptor family that signals in response to phospholipids and in some instances, as their name implies, are upregulated in differentiating endothelial cells.^{152, 153} Edg1, Edg3, Edg5, Edg6, and Edg8 are receptors for the bioactive lipid sphingosine-1 phosphate (S1P) whereas Edg2, Edg4, and Edg7 are receptors for lysophosphatidic acid.¹⁵⁴ Moreover, Edg1, Edg3, and Edg5 are expressed widely, including on embryonic endothelial cells, while Edg6 and Edg8 expression is restricted mainly to immune and nervous systems¹⁵⁵ and Edg7 is expressed in the prostate.¹⁵⁷ Signaling through Edg1 induces the formation of adherens junctions between cells and increases cadherin expression leading to cellular clumping *in vitro*.¹⁵⁴ Deletion of *Edg1* in mice causes embryonic lethality by E14.5, and *Edg1*^{-/-} embryos have intraembryonic hemorrhages and edematous yolk sacs that, while showing apparently normal branched vessels, are filled with fewer blood cells.¹⁵⁸ Edg1 was found to be expressed in the endothelial cells of arteries and capillaries and not in veins. The large, intraembryonic arteries in *Edg1*^{-/-} embryos have a striking defect in which VSMCs are grouped together on the ventral side of the vessel and fail to completely envelop the vessel. This suggests a role for Edg1 in coordinating VSMC migration. Endothelium-specific ablation of the *Edg1* gene, but not VSMC-specific ablation, recapitulates the phenotype of global *Edg1* deletion suggesting that S1P acting on endothelial cells is required for proper VSMC localization/function.¹⁵⁹

UCSF LIBRARY

Further work has shown that S1P signaling through Edg1 in endothelial cells is required for endothelial cells to interact and tightly bind to VSMCs. Normally this is accomplished by homotypic interactions between endothelial cell N-cadherin and VSMC N-cadherin. *Edg1* null endothelial cells have a defect in the proper intracellular trafficking and activation of N-cadherin which is the cause of this phenotype.¹⁶⁰ The importance of S1P regulation of N-cadherin may also manifest itself in additional ways. Endothelium-specific deletion of N-cadherin results in vascular defects and embryonic lethality by around E9.5, with a phenotype that is reminiscent of *VE-cadherin* knockout embryos.¹⁶¹ VE-cadherin is expressed in endothelial cell adherens junctions¹⁶² and is required for preventing the disassembly of embryonic vessels.¹⁶³ Endothelium-specific ablation of β -catenin, a protein that signals downstream of VE-cadherin, also results in poorly organized and branched, fragile vessels and embryonic death at midgestation.¹⁶⁴ Surprisingly, *N-cadherin* null embryos showed a reduction in VE-cadherin expression at adherens junctions. Thus N-cadherin acts upstream of VE-cadherin in endothelial cells raising the possibility that loss of S1P signaling in the various Edg knockouts might adversely effect endothelial cell/endothelial cell interactions via VE-cadherin as well as endothelial cell/VSMC interactions via N-cadherin.¹⁶⁵

The gene that is defective in the Zebrafish mutant, *miles apart*, is a homologue of the S1P receptor Edg5. *Miles apart* embryos have a non-cell autonomous defect in the migration of heart precursor cells.¹⁶⁶ Mice lacking Edg5 or both Edg3/5 do not show embryonic lethality and die perinatally of unknown causes,¹⁶⁷ though this finding may depend upon genetic background or other factors as another group has reported that *Edg5*

11
12
13
14
15
16
17
18
19
20
21
22
23
24
25
26
27
28
29
30
31
32
33
34
35
36
37
38
39
40
41
42
43
44
45
46
47
48
49
50
51
52
53
54
55
56
57
58
59
60
61
62
63
64
65
66
67
68
69
70
71
72
73
74
75
76
77
78
79
80
81
82
83
84
85
86
87
88
89
90
91
92
93
94
95
96
97
98
99
100

null mice exhibit spontaneous seizures.¹⁶⁸ In order to clarify the roles of Edg receptor signaling in mouse embryos the group that generated the *Edg1* knockouts also generated (in a mouse breeding *tour de force*!) *Edg1/5* and *Edg1/3* double knockouts and *Edg1/3/5* triple nulls.¹⁶⁹ While *Edg1/3* null animals showed no change in phenotype compared to *Edg1* knockouts, *Edg1/5* null animals showed a more severe, earlier embryonic phenotype than single *Edg1* knockouts that is characterized by abnormal and immature branching of vessels in the head, hemorrhage, and lethality by E13.5. The triple knockout displayed an even more severe, but similar phenotype, resulting in death by E11.5. Since *Edg1* signals through $G\alpha_i$, and *Edg3* and *Edg5* signal through $G\alpha_i$, $G\alpha_q$, and $G\alpha_{12/13}$ ¹⁷⁰ it is possible that the severe triple knockout phenotype is due to loss of redundant downstream signals such as those that emanate from $G\alpha_i$. One important question that remains to be settled is whether, like in *Edg1* nulls, the triple null phenotype results from VSMC dysfunction secondary to loss of S1P signaling in endothelial cells, or whether there are additional requirements for other Edg receptors in endothelial cells and/or VSMC for angiogenesis.

Indeed, there is evidence that S1P signaling has direct effects on endothelial cell function and on angiogenesis. Endothelial cell-specific *Edg1* null mice show defects in limb development including abnormal chondrocyte condensation and digit formation. There was excessive vascularization in these limbs and a coincident upregulation of VEGF and HIF-1 α (see below for discussion of HIF-1 α).¹⁷¹ One interesting study showed that S1P (signaling through *Edg1* and/or *Edg3*) potentiates the effects of VEGF on angiogenesis and that S1P increases the maturation of these neovessels as indicated by

UCSF LIBRARY

their increased production of extracellular matrix and VE-cadherin-containing adherens junctions.¹⁷² By itself, VEGF has been shown to disrupt VE-cadherin adherens junctions and thus it is possible that the balance between the stabilizing effects of S1P signaling and the destabilizing effects of VEGF on these junctions plays an important role in angiogenesis and vascular remodeling.¹⁷³ S1P/Edg signaling is also required for EC chemotaxis possibly by playing a role in priming the cortical actin cytoskeleton to correctly respond to additional chemotactic clues.¹⁷⁴ Not to be left out, it appears that S1P also has effects on PDGF signaling. S1P signaling has been found to upregulate PDGF-B expression in VSMCs.¹⁷⁵ S1P treatment of adult rat VSMC inhibits PDGF-mediated chemotaxis¹⁷⁶ and PDGF signaling can, in some instances, increase the production of S1P,¹⁷⁷ though it is not currently known if interactions between the PDGF and S1P signaling pathways account for the observed phenotypes in either Edg or PDGF receptor knockouts. Taken together, these data suggest that S1P signaling through Edg receptors play a central role in coordinating the functions of endothelial cells and VSMCs during angiogenesis at least in part by modulating their responses to other angiogenic factors such as VEGF and PDGF.

Chapter 1e: Additional molecules involved in the regulation of angiogenesis, including G protein-coupled receptors:

The above discussion, though relatively thorough, does neglect some interesting and important players that act primarily in the regulation of angiogenesis. In the next few paragraphs, I will discuss these molecules. I will then end Chapter I with a brief

UCSF LIBRARY



overview of G protein-coupled receptor signaling, and in particular the role of thrombin signaling through one of its receptors, PAR1, in vascular development,

HIF-1 α is a transcription factor that plays a fundamental role in how cells and tissues perceive and regulate oxygen homeostasis. It is therefore not surprising that HIF-1 α is a central regulator of angiogenesis. The *Drosophila* tracheal system is in some ways analogous to the vertebrate vascular system. Trachea form when cells on the larval surface invaginate to form tubules which then extend and branch into the larval body to supply target tissues with oxygen. Null mutations in the *Drosophila HIF-1 α* gene, *tracheless*, fail to form trachea.¹⁷⁸ The *Drosophila* FGF homologue, *branchless*, has been shown to be downstream of the HIF-1 α signal and is thought to be secreted by oxygen-deprived tissues as a chemotactic cue for tracheal tip cells.¹⁷⁹ Mouse embryos lacking HIF-1 α exhibit defects in vascular patterning that are visible as early as E8.5 including the absence of cephalic and branchial arch vascularization, perhaps due to the fact that the head vasculature is formed by angiogenic sprouting from vessels in the trunk.^{180, 181}

HIF-1 α forms active heterodimers with the basic-helix-loop-helix transcription factor arylhydrocarbon-receptor-nuclear translocator, or ARNT. Mice in which ARNT is deleted show a similar phenotype, with the additional observation that the embryonic component of the placenta fails to vascularize.^{182, 183} This decrease in placental vascularization is associated with decreased expression of Flk1 and Tie2 in the embryonic placental vasculature. It has been known for some time that reduced oxygen



tension increases VEGF expression¹⁸⁴ and it is now known that HIF-1 α mediates this effect by stimulating VEGF gene expression.^{185, 186} A closely related hypoxia inducible factor, HIF-2 α , which also forms active heterodimers with ARNT is capable of activating transcription of VEGF as well as the genes for Flk1 and Tie2.¹⁸⁷⁻¹⁸⁹ Thus, the association of HIF-1 α and/or HIF-2 α with ARNT seems to be a crucial regulatory step for multiple stages in angiogenesis.

Integrin signaling is also required at multiple stages of angiogenesis. $\alpha_v\beta_3$ integrin has historically been thought to be crucial for blood vessel formation as it is predominantly expressed on endothelial cells and since blockade of $\alpha_v\beta_3$ with monoclonal antibodies inhibits blood vessel formation.¹⁹⁰ The engagement of $\alpha_v\beta_3$ integrins with extracellular matrix components (*i.e.*, vitronectin) *in vitro* has been shown to enhance, *in cis*, VSMC proliferation and migration, though the mechanism of this is not clear.¹⁹¹ It also appears that $\alpha_v\beta_3$ surface expression is upregulated by HIF-1 α in hypoxic conditions in certain tumors though it is not known whether this regulation is by direct transcriptional activation of the genes for $\alpha_v\beta_3$ by HIF-1 α or whether this is important for embryonic angiogenesis.¹⁹² Coexpression of $\alpha_v\beta_3$ with Flk1 has also been shown to increase the ability of VEGF to activate Flk1 and downstream mediators such as PI3-kinase.¹⁹³ Conversely, VEGF has been shown to activate $\alpha_v\beta_3$ and other integrins in cancer cells.¹⁹⁴ Coexpression of $\alpha_v\beta_3$ with PDGFR β also potentiates the signaling activity of PDGF-B.¹⁹¹ Counterintuitively, ablation of α_v integrins either globally or in endothelial cells has no effect on angiogenesis or on vessel stability, but α_v deletion in glia and neurons using a *Nestin-Cre* transgene leads to brain hemorrhages and axonal

degradation.^{195, 196} And in β_3 null and β_3/β_3 double null animals there are no embryonic angiogenesis defects and there are actually increased tumor angiogenic responses to hypoxia and VEGF coincident with increased expression of Flk1 on endothelial cells.¹⁹⁷
¹⁹⁸ Given our current knowledge, it not clear how to resolve the discrepancy between these apparently incongruous effects of $\alpha_v\beta_3$ function in these various systems and assays.

An interesting body of work has emerged in recent years describing another facet of vascular development, the establishment of arteriovenous identity. Arteries and veins are defined by the direction of blood flow and by their morphology and function. It is now clear that arterial and venous endothelial cells also differ in their molecular characteristics. Notch signaling is required nearly ubiquitously in the animal kingdom for its role in determining cell fate decisions in such tissues as muscle, neurons, hematopoietic cells, and epithelium. It is probably not surprising that it also plays a role in cell fate decisions in vascular development. Notch is a cell surface receptor for its cell surface ligands, including Delta and Jagged. Activation of Notch results in its proteolytic cleavage by extra- and intracellular proteases, resulting in the release of an intracellular Notch domain that can then enter the nucleus and directly participate in transcriptional activation of target genes including, in mice, the transcriptional repressors Hey1 and Hey2. Notch expression is thought to be induced on arterial endothelial cells by VEGF binding to Flk1 and NP1.^{199, 200} Compound deletion of Notch1/Notch4 from mice results in defects in angiogenic remodeling in the embryo proper, the yolk sac, and the placenta and these embryos fail to form the dorsal aortae and cardinal veins.²⁰¹ Embryos with a

UCSF LIBRARY

gain of function Notch4 also show vascular defects, primarily in the head vessels though the significance of this in terms of the role of Notch signaling in the vasculature is not known.²⁰²

Deletion of the Notch1 ligand Jagged1 in mice also results in vascular defects,^{*} and interestingly the carotid vessels form (in contrast to Notch1 nulls) but they subsequently collapse.²⁰³ The murine Notch ligand Delta-like ligand-4 (Dll4) is expressed primarily in large arteries of the embryos. Haploinsufficiency of Dll4 results in defects in arterial specification and angiogenesis.^{204, 205} Double knockout of the downstream transcriptional repressors *Hey1* and *Hey2* results in a similar reduction in arterial specification in the mouse²⁰⁶ as does reduced expression of *gridlock*, a gene that is downstream of Notch in Zebrafish.²⁰⁷ The Notch pathway is not active in veins, so how is venous identity determined? Deletion of the orphan nuclear receptor COUP-TII results in defects in vascular development that are associated with an increased expression of Notch1 and Notch signaling mediators.^{208, 209} COUP-TFII expression was found to be restricted to veins, and ectopic expression of COUP-TFII throughout the endothelium was found to suppress Notch signaling leading to a suppression of arterial identity. Previous models have proposed that venous identity is, by default, determined by the

* Mutations in human Jagged1 cause Alagille syndrome, an early onset autosomal dominant disease characterized by defects in multiple organ systems. Cardiovascular system defects include congenital heart defects, pulmonary stenosis, and coarctation of the aorta.

[Li, L. et al. Alagille syndrome is caused by mutations in human Jagged1, which encodes a ligand for Notch1. *Nat Genet* 16, 243-51 (1997)] & [Oda, T. et al. Mutations in the human Jagged1 gene are responsible for Alagille syndrome. *Nat Genet* 16, 235-42 (1997).]

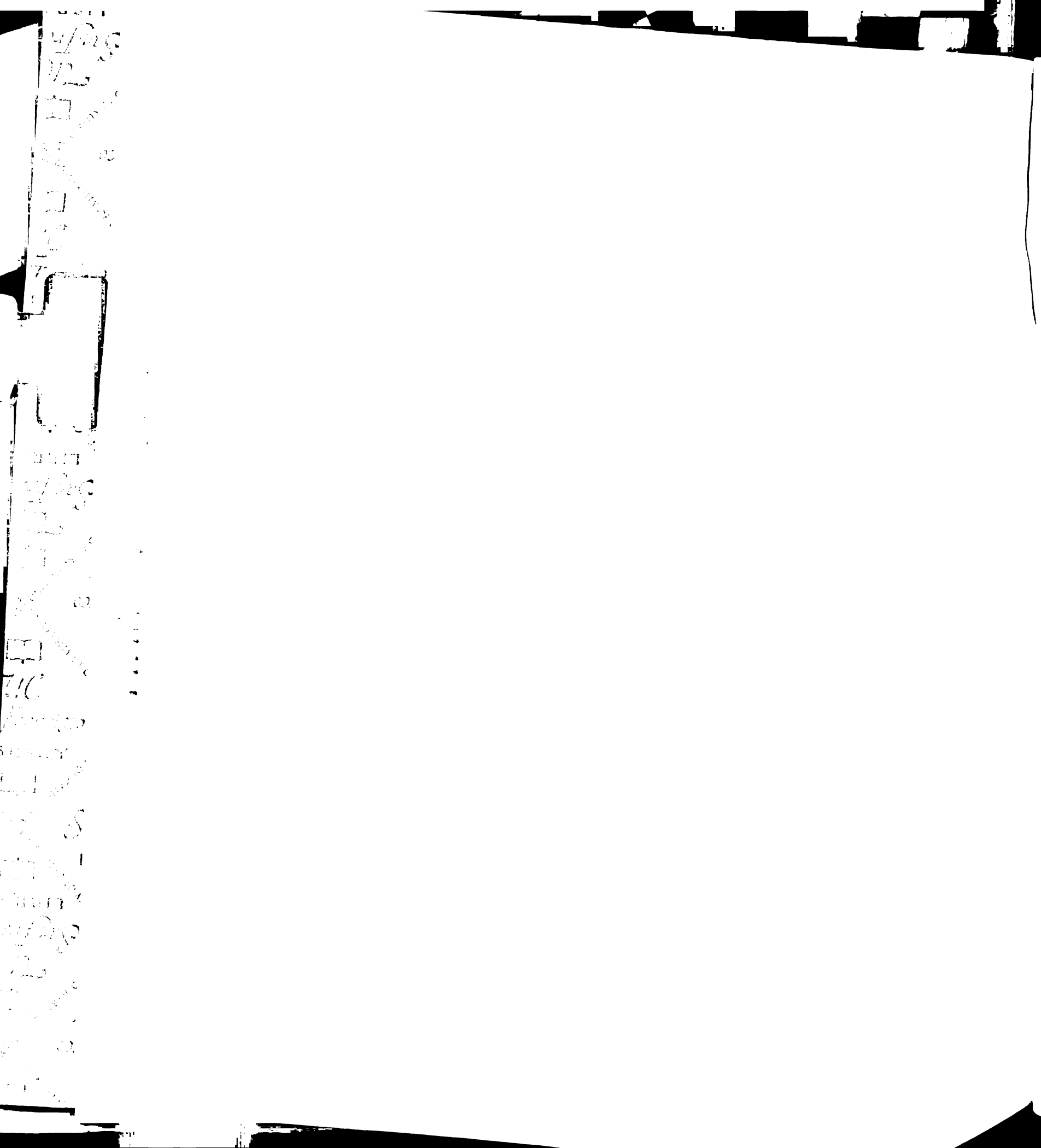
WEST LIBRARY

absence of Notch signaling. These results, however, suggest that venous identity is regulated by active repression of Notch by COUP-TFII in venous endothelial cells.

Notch also is involved in VSMC fate determination. Notch-3 has been shown to be required for arterial VSMC determination, but not endothelial cell determination. Arteries in certain vascular beds in *Notch-3* null adults show reduced VSMC numbers.²¹⁰ Some mutations in human Notch-3 are associated with an inherited vascular dementia, “cerebral autosomal dominant arteriopathy with subcortical infarcts and leukoencephalopathy” (“CADASIL”), which is characterized by the progressive degeneration of VSMC in small cerebral arteries.²¹¹

Ephrins and their Eph receptors are cell surface proteins that have, at least initially, been mainly studied as axon guidance cues in the developing nervous system.²¹² Ephrin/Eph signaling is also involved in arteriovenous identity, and likely acts downstream of Notch to control the spatial organization of arteries and veins. EphrinB2 and its receptor EphB4 also have been found to have a role in delineating the arteriovenous boundary early in embryogenesis. EphrinB2 is expressed in the endothelial cells of arteries while EphB4 is expressed in endothelial cells of veins and deletion of either gene in mice leads to death by ~E10.0 with widespread defects in angiogenesis throughout the embryonic and extraembryonic tissues.²¹³⁻²¹⁶ The roles of EphrinB2/EphB4 interactions in vascular development may not be limited to endothelial cells. There is evidence from studies in chick embryos that suggests that EphrinB2/EphB4 signaling may also involve pericyte/VSMC interactions with endothelial cells.²¹⁷ In

WEST LIBRARY



Xenopus laevis EphrinB2/EphB4 signaling is required for the migration of intersomitic vessels, a defect that was also observed in the mouse knockouts.²¹⁸ Interestingly, this study found that in *Xenopus* EphB4 is expressed in endothelial cells while the EphrinB ligands are expressed in the somites *adjacent* to the migratory paths followed by these vessels. Therefore, Ephrin/Eph interactions not only help define arteriovenous boundaries, but are also likely involved in mediating guidance cues to migrating vessels/endothelial cells in a way that is analogous to the role of Ephrin/Eph interactions in guiding axonal migrations.

Chapter 1f: G protein-coupled receptors in vascular development:

With the exception of Edg receptor family signaling, which has already been discussed, significantly less is known regarding the roles of G protein-coupled receptors (GPCRs) in cardiovascular development despite their diversity and ubiquity. In the following section, I will discuss several additional GPCRs that are involved in vascular development.

Endothelins are soluble factors that were discovered by virtue of their powerful vasoconstrictive effects.²¹⁹ Three isoforms exist, ET1, ET2, and ET3 and all are synthesized as precursors which are proteolytically cleaved and activated by the membrane-bound metalloproteases, endothelin-converting enzymes (ECE1 and ECE2). ETs signal through two GPCRs, ET_A which preferentially binds ET1, and ET_B which binds all three.²²⁰ Additional roles for ET signaling were revealed in mice lacking the

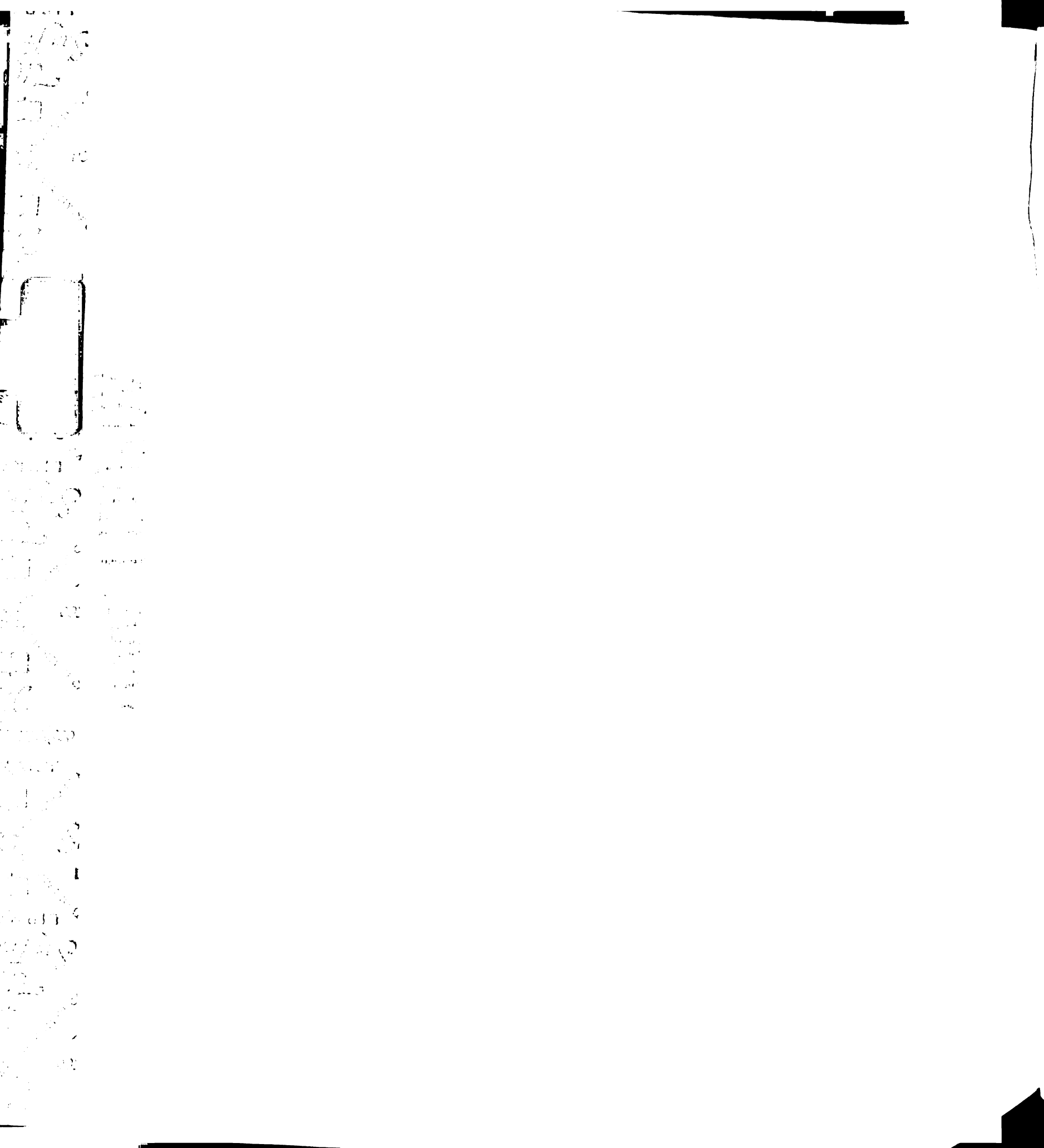
converting enzymes, the receptors, or the endothelins themselves. ET_B null mice show defects in gut autonomic innervation resulting in aganglionic megacolon which resembles the human condition Hirschprung's disease.²²¹ ET_A knockouts have defects in neural crest cell (NCC) derivatives resulting in craniofacial and cardiac outflow tract abnormalities.²²² ET-1 is expressed in the pharyngeal arch epithelium, the paraxial mesoderm-derived arch core, and the arch vessel endothelium whereas ET_A is reciprocally expressed in NCCs suggesting that paracrine signaling of ET-1 from multiple tissues is essential in patterning NCC derived cells. Mice in which ECE1 and ECE2 are deleted have comparable defects to ET_A knockouts.²²³ In the embryo, each branchial arch artery forms bilaterally but then undergoes assymetrical regression in order to establish correct circulation. The branchial arch arteries in ET_A and ECE-1 null embryos form properly and symmetrically but exhibit an abnormal pattern of asymmetrical regression thus providing an anatomic basis for the observed cardiac outflow tract defects.²²⁴

The chemokine receptor CXCR4 is a GPCR for stromal-derived factor-1, or SDF1. Embryos that lack CXCR4 or SDF1 die between E15.5 and just after birth with defects in the generation of the large vessels supplying the gastrointestinal tract in addition to defects in neuronal migration and the formation of the ventricular septum of the heart.²²⁵⁻²²⁷ SDF1 and CXCR4 are expressed by endothelial cells, and their expression is increased by VEGF. In an *in vitro* Matrigel-based model of tube formation and branching morphogenesis showed that blockade of SDF1 or CXCR4 with inhibitory antibodies or pertussis toxin (which inhibits $G\alpha_i$) prevents network, and purportedly tube,

formation.²²⁸ Additional studies could determine whether SDF1 and CXCR4 also function in branching morphogenesis and tubulogenesis in embryonic angiogenesis.

The Hedgehog signaling pathway has also been shown to play a role in vascular development. Hedgehog signaling has been shown to be essential for the proper patterning and morphogenesis in many species.²²⁹ In the mouse there are three Hedgehog homologues, Sonic Hedgehog (*Shh*), Desert Hedgehog (*Dhh*), and Indian Hedgehog (*Ihh*). These bind to a 12-pass membrane protein, Patched, which associates with a G protein receptor-like membrane protein, Smoothened (*Smo*). Binding of Hedgehog ligands to Patched is thought to release its inhibition on Smoothened thus allowing *Smo* to signal to downstream mediators to effect transcriptional changes. The immediate downstream effectors of Smoothened are unknown though there is some evidence that these are heterotrimeric G proteins.²³⁰ The yolk sacs of *Smo*^{-/-} embryos contain endothelial tubes that fail to remodel beyond the primary plexus stage and therefore appear stunted at ~E8.5. *Smo*^{-/-} embryos also fail to form the dorsal aortae, suggesting an early, central role for *Smo* in vessel formation.²³¹ Yolk sacs from *Ihh*^{-/-} embryos show a less severe phenotype, in that there is remodeling of the primary vascular plexus, but there are fewer and smaller vessels.²³² *Shh* null Zebrafish embryos also show defects in axial vessels which are even more severe than those seen in *VEGF* null embryos.²³³ Hedgehog ligands are secreted from the mouse yolk sac visceral endoderm at early embryonic stages, and it appears that hedgehog signaling is an early step in a signaling cascade that leads to increased VEGF signaling and ultimately Notch signaling which participates in determining arterial fate.²³⁴

WEST LIBRARY



We recently showed that protease-activated receptor-1 (PAR1), a GPCR for thrombin, plays an important role in the proper formation and/or maintenance of blood vessels in mouse embryos.^{235, 236} In the embryo, PAR1 is expressed predominantly in the endothelium and endocardium, but is also found to be expressed in circulating blood cells, the mesenchyme of the hindlimbs, and the septum transversum which is the precursor of the diaphragm. About half of *Par1* null embryos die at midgestation with grossly normal embryonic vascular patterning but with defective yolk sac remodeling, hemorrhage in multiple tissues, and dilated pericardium. *Par1* null embryos that do not die *in utero* survive to adulthood with no obvious phenotype. Rescue of these embryonic defects by endothelium-specific expression of PAR1 from a Tie2 promoter/enhancer transgene suggests that the vascular defects observed in *Par1* null embryos result from loss of PAR1 in endothelial cells. Thus, PAR1 function is required at an earlier stage in angiogenesis than any other classical (*i.e.*, not including Patched/Smoothed) GPCR discussed here.

Heterotrimeric G proteins transduce signals from GPCRs and can be divided into four families based on sequence and functional similarity: $G\alpha_i$, $G\alpha_s$, $G\alpha_q$ and $G\alpha_{12/13}$. PAR1 can trigger a host of cellular responses by activating heterotrimeric G proteins of the $G\alpha_{q/11}$, $G\alpha_{i/o}$, and $G\alpha_{12/13}$ families.²³⁷⁻²⁴⁰ The $G\alpha_{12/13}$ family consists of two proteins, $G\alpha_{12}$ and $G\alpha_{13}$ which share about 70% amino acid identity.²⁴¹ Although the signaling pathways that are regulated by $G\alpha_{12}$ and $G\alpha_{13}$ are incompletely understood, studies in cell culture have shown that $G\alpha_{12/13}$ can regulate actin stress fiber formation,²⁴² focal

UCST LIBRARY

112
113
114
115
116
117
118
119
120
121
122
123
124
125
126
127
128
129
130
131
132
133
134
135
136
137
138
139
140
141
142
143
144
145
146
147
148
149
150
151
152
153
154
155
156
157
158
159
160
161
162
163
164
165
166
167
168
169
170
171
172
173
174
175
176
177
178
179
180
181
182
183
184
185
186
187
188
189
190
191
192
193
194
195
196
197
198
199
200

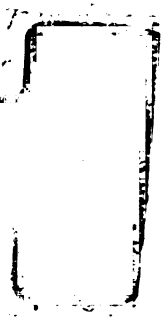
[Faint, illegible text covering the main body of the page]

adhesions
apoptosis
also call
chemotax
C
midgesta
sac vasc
vessels
occurre
Gα₁₃ is
using a
endothe
and ske
downst
sufficie
GPCR
studies
consiste
neural c

adhesions,^{243, 244} Na⁺/H⁺ exchange,²⁴⁵ transcription,²⁴⁶ transformation,^{238, 247, 248} and apoptosis.^{249, 250} The best characterized downstream mediator of Gα₁₃ signaling is Lsc (also called p115RhoGEF) which links Gα₁₃ to Rho^{251, 252} to regulate cell shape and chemotaxis.²⁵³

Gα₁₃-deficient mice fail to form a functional vascular system and die at midgestation.²⁵⁴ Discontinuities in the endothelial lining, a failure to remodel their yolk sac vascular plexus into a branched vascular tree, and abnormally large and ectopic head vessels were noted in Gα₁₃-deficient embryos. These phenotypes are reminiscent of, but occurred with more penetrance than, those seen in *Par1* deficient embryos. Although Gα₁₃ is reported to be widely expressed in the embryonic and adult mouse tissues,^{254, 255} using a Gα₁₃^{lacZ} knockin allele we observed relatively high expression of Gα₁₃ in endothelial cells and other specific cell types at midgestation, including cardiac, smooth, and skeletal muscle, and in platelets. Accordingly, we asked whether Gα₁₃ function downstream of PAR1 or other GPCRs in endothelial cells might play a necessary or sufficient role in vascular development. Our results strongly suggest a key role for GPCR signaling via Gα₁₃ in endothelial cells in this critical process. In addition, our studies uncovered an important function for Gα₁₃ in lineages where *Wnt1* is expressed, consistent with a role for GPCR signaling in the development of structures derived from neural crest.

18011
172
173
174
175
176
177
178
179
180



181
182
183
184
185
186
187
188
189
190
191
192
193
194
195
196
197
198
199
200

Go, ex
mouse
of the
of Ge
widesp
staini
throu
vasc
an e
end
20
us
n
d
im

Chapter II:

RESULTS

$G\alpha_{13}$ expression in the mouse embryo and in the adult:

Toward characterizing $G\alpha_{13}$ expression in the mouse embryo, we generated a mouse in which the coding sequence for β -galactosidase (*lacZ*) was inserted into exon 1 of the $G\alpha_{13}$ gene ($G\alpha_{13}^{lacZ}$ allele; Figure 1) such that *lacZ* transcription would mimic that of $G\alpha_{13}$. Whole mount X-gal staining of an E10.5 $G\alpha_{13}^{+lacZ}$ embryo suggested widespread expression, but analysis of tissue sections from these embryos revealed the staining to be non-uniform (Figure 2B). While faint staining was indeed present throughout the mesenchyme and elsewhere, relatively strong staining was noted in vascular endothelial cells and in the dorsal neuroepithelium; analysis of embryos bearing an endothelium-specific *Tie2-promoter/enhancer-lacZ* transgene showed similar endothelial staining but not neuroepithelial or widespread mesenchymal staining (Figure 2C). $G\alpha_{13}$ expression in endothelial cells was also readily detected by Northern blot using endothelial cells immunopurified from neonatal mice as a source of RNA²⁵⁶ (data not shown) and by staining for β -galactosidase in such cells from $G\alpha_{13}^{+lacZ}$ mice (Figure 2B e,f). While these results confirm widespread expression of $G\alpha_{13}$ in the mouse embryo at midgestation²⁵⁴ they suggest relatively higher expression of $G\alpha_{13}$ in endothelial cells and in the dorsal neuroepithelium in the region where neural crest cells arise and delaminate (Figure 2B g,h). These findings supported our initial focus on defining the importance $G\alpha_{13}$ function in endothelial cells and our subsequent focus on neural crest.

1950
1951
1952
1953
1954
1955
1956
1957
1958
1959
1960
1961
1962
1963
1964
1965
1966
1967
1968
1969
1970
1971
1972
1973
1974
1975
1976
1977
1978
1979
1980
1981
1982
1983
1984
1985
1986
1987
1988
1989
1990
1991
1992
1993
1994
1995
1996
1997
1998
1999
2000
2001
2002
2003
2004
2005
2006
2007
2008
2009
2010
2011
2012
2013
2014
2015
2016
2017
2018
2019
2020
2021
2022
2023
2024
2025



1950
1951
1952
1953
1954
1955
1956
1957
1958
1959
1960
1961
1962
1963
1964
1965
1966
1967
1968
1969
1970
1971
1972
1973
1974
1975
1976
1977
1978
1979
1980
1981
1982
1983
1984
1985
1986
1987
1988
1989
1990
1991
1992
1993
1994
1995
1996
1997
1998
1999
2000
2001
2002
2003
2004
2005
2006
2007
2008
2009
2010
2011
2012
2013
2014
2015
2016
2017
2018
2019
2020
2021
2022
2023
2024
2025

As stated above, $G\alpha_{13}$ expression was found to be non-uniform in embryos at midgestation. To further characterize $G\alpha_{13}$ expression, frozen sections of various tissues from control and $G\alpha_{13}^{+/lacZ}$ mice were stained for β -galactosidase (Figure 3). Indeed $G\alpha_{13}$ is also expressed non-uniformly in adult tissues. Strikingly, $G\alpha_{13}$ appears to be strongly expressed in all muscle lineages as we observed expression in cardiomyocytes and in multiple smooth muscle and skeletal muscle populations (Figure 3 B,C,D,E,G,H,J). Expression was found in vascular smooth muscle cells lining the aorta as well as in other arteries (Figure 3 E,F,G). Smooth muscle lining the trachea and the small bowel expresses $G\alpha_{13}$ (Figure 3 C,D) as does the smooth muscle capsule and trabeculae that surrounds and extends into the mouse spleen (Figure 3 G,H). Skeletal muscle in the trachea and the intercostal muscles also were β -galactosidase positive (Figure 3 C,J). Megakaryocyte expression of $G\alpha_{13}$ was observed in the splenic red pulp (Figure 3 H,I). Using FACS analysis to identify β -galactosidase-expressing cells, $G\alpha_{13}$ was also found to be expressed in all major adult hematopoietic lineages including B and T lymphocytes, macrophages, granulocytes (data not shown). Strong $G\alpha_{13}$ expression was also observed in the epidermis and hair shaft (Figure 3 K). These results suggest that $G\alpha_{13}$ has roles on multiple tissues in the embryo and the adult though analysis of these roles was beyond the scope of this project.

1722
1723
1724
1725
1726
1727
1728
1729
1730
1731
1732
1733
1734
1735
1736
1737
1738
1739
1740
1741
1742
1743
1744
1745
1746
1747
1748
1749
1750
1751
1752
1753
1754
1755
1756
1757
1758
1759
1760
1761
1762
1763
1764
1765
1766
1767
1768
1769
1770
1771
1772
1773
1774
1775
1776
1777
1778
1779
1780
1781
1782
1783
1784
1785
1786
1787
1788
1789
1790
1791
1792
1793
1794
1795
1796
1797
1798
1799
1800

Figure 1: Generation of a $G\alpha_{13}^{lacZ}$ allele

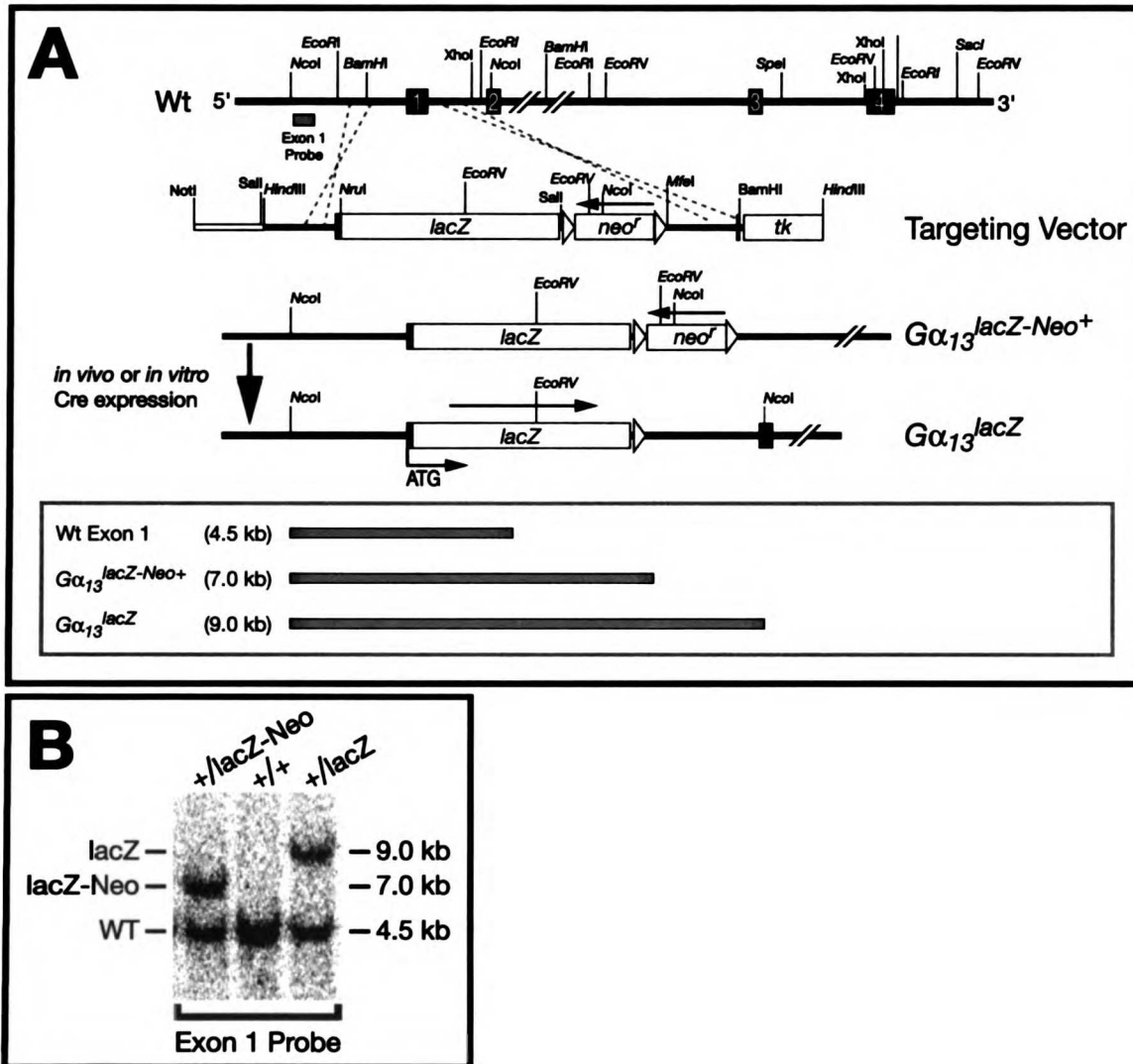
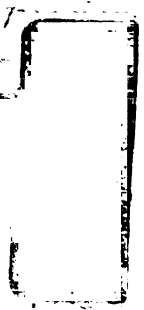


Figure 1 Legend:

A. Diagram of the wild-type (Wt) $G\alpha_{13}$ locus, the $G\alpha_{13}^{lacZ}$ targeting vector, and the recombined locus. Exons (coding in black, untranslated in open boxes), loxP sites (open triangles), and neomycin resistance (*neo^r*) and thymidine kinase negative selection (*tk*) cassettes are shown. The targeting vector contains a *lacZ*-Sv40pA cassette fused in frame to the first 45 base pairs of exon 1 (including the native start codon). Homologous recombination in embryonic stem (ES) cells resulted in the replacement of exon 1 with the $G\alpha_{13}::lacZ$ -Sv40pA fusion sequence, thus generating a null $G\alpha_{13}$ allele. The *neo^r* cassette was excised *in vivo* by breeding homozygous $G\alpha_{13}^{lacZ-Neo^+}$ mice to β -actin-*Cre^{Tg/Tg}* mice. (see **Materials and Methods**)

B. Southern blot analysis of tail DNA from adult mice with the indicated $G\alpha_{13}$ genotypes. Location of the "Exon 1" probe and the expected sizes of DNA fragments detected by this probe after an *Nco*I digest are indicated in (A).

Handwritten text on the left margin, including a large '7' and various illegible characters.



Vertical text on the left margin, possibly a list or index.

Handwritten text on the left margin, including the word 'REPLY' and other illegible characters.

Figure 2: Phenotype of $G\alpha_{13}^{lacZ/lacZ}$ embryos and expression of $G\alpha_{13}-lacZ$ in endothelium and neuroepithelium.

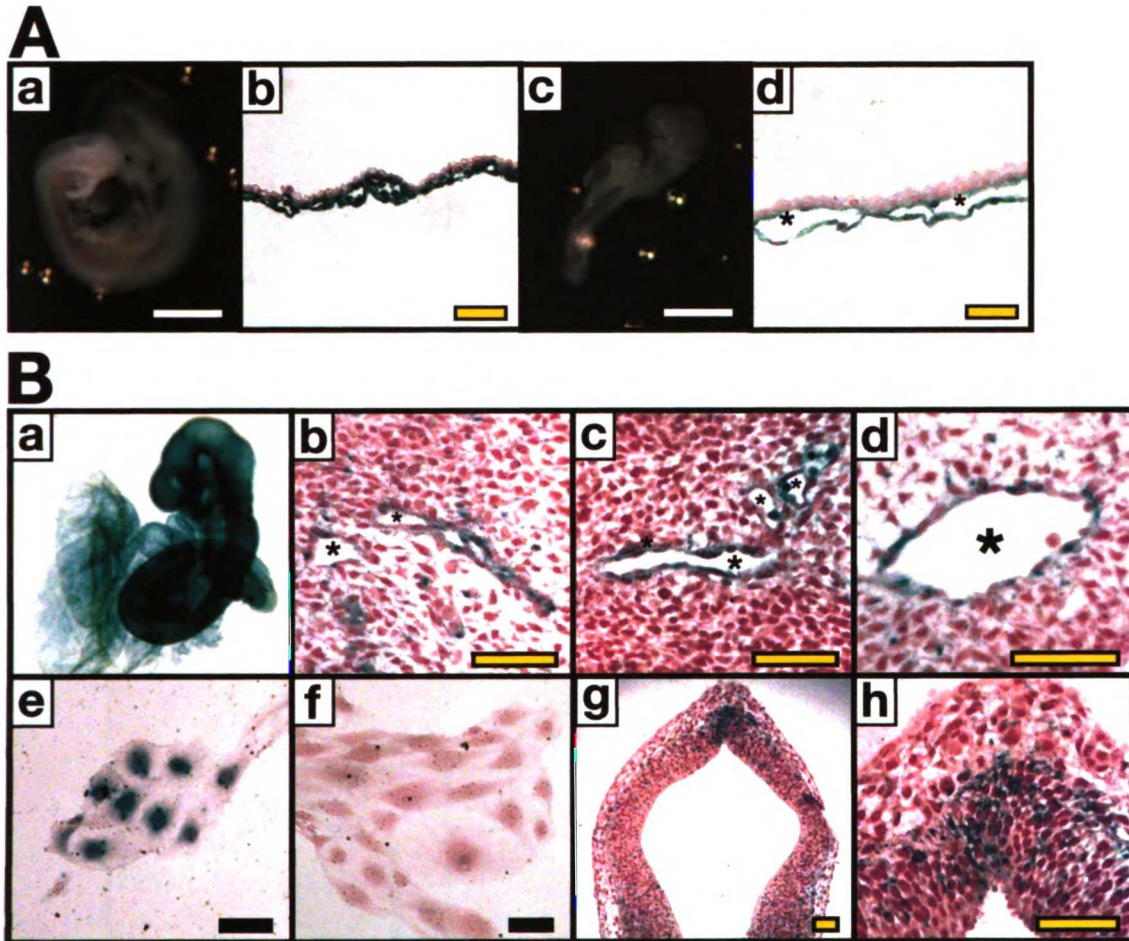
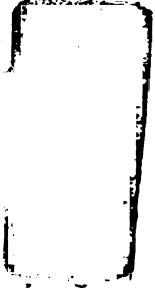


Figure 2 Legend:

A. $G\alpha_{13}^{lacZ/lacZ}$ embryos (c) and yolk sacs (d) phenocopy $G\alpha_{13}^{-/-}$ embryos (see **Figures 7, 8, and 9** for $G\alpha_{13}^{-/-}$ photos). Compare to littermate control embryo (a) and yolk sac (b). Additionally, the yolk sacs were stained with X-gal for β -galactosidase activity and reveal $G\alpha_{13}^{lacZ}$ expression in the endothelium. Vessel lumina are indicated with an asterisk in (d) and in **Figure 2B, (b,c,d)**.

B. (a) $G\alpha_{13}^{lacZ}$ expression in an X-gal stained E9.5 $G\alpha_{13}^{+/lacZ}$ embryo appears to be ubiquitous in whole mount. (b,d) However, analysis of tissue sections from an E10.5 $G\alpha_{13}^{+/lacZ}$ embryo revealed weak staining throughout the mesenchyme and stronger staining in the endothelium of (b) intersomitic and (d) carotid vessels. (c) By comparison, staining of a $Tie2p/e-Cre^{Tg/o}; ROSA26R$ embryo showed endothelial but not mesenchymal staining. (e,f) Strong staining of endothelial cells purified from neonatal $G\alpha_{13}^{+/lacZ}$ mice (e) compared to those purified from $G\alpha_{13}^{+/+}$ mice (f). (g,h) Relatively strong X-gal staining was also seen in the dorsal neuroepithelium of E9.5 $G\alpha_{13}^{+/lacZ}$ embryos consistent with $G\alpha_{13}$ expression in neural crest cells. (Yellow bars = 100 μ m; White bars = 1 mm; Black bars = 10 μ m.)

Handwritten notes on the left margin, including the word "FRANCIS" and other illegible text.



Faint vertical text on the left margin, possibly a page number or reference code.

Figure 3: Expression of $G\alpha_{13}^{lacZ}$ in adult tissues.

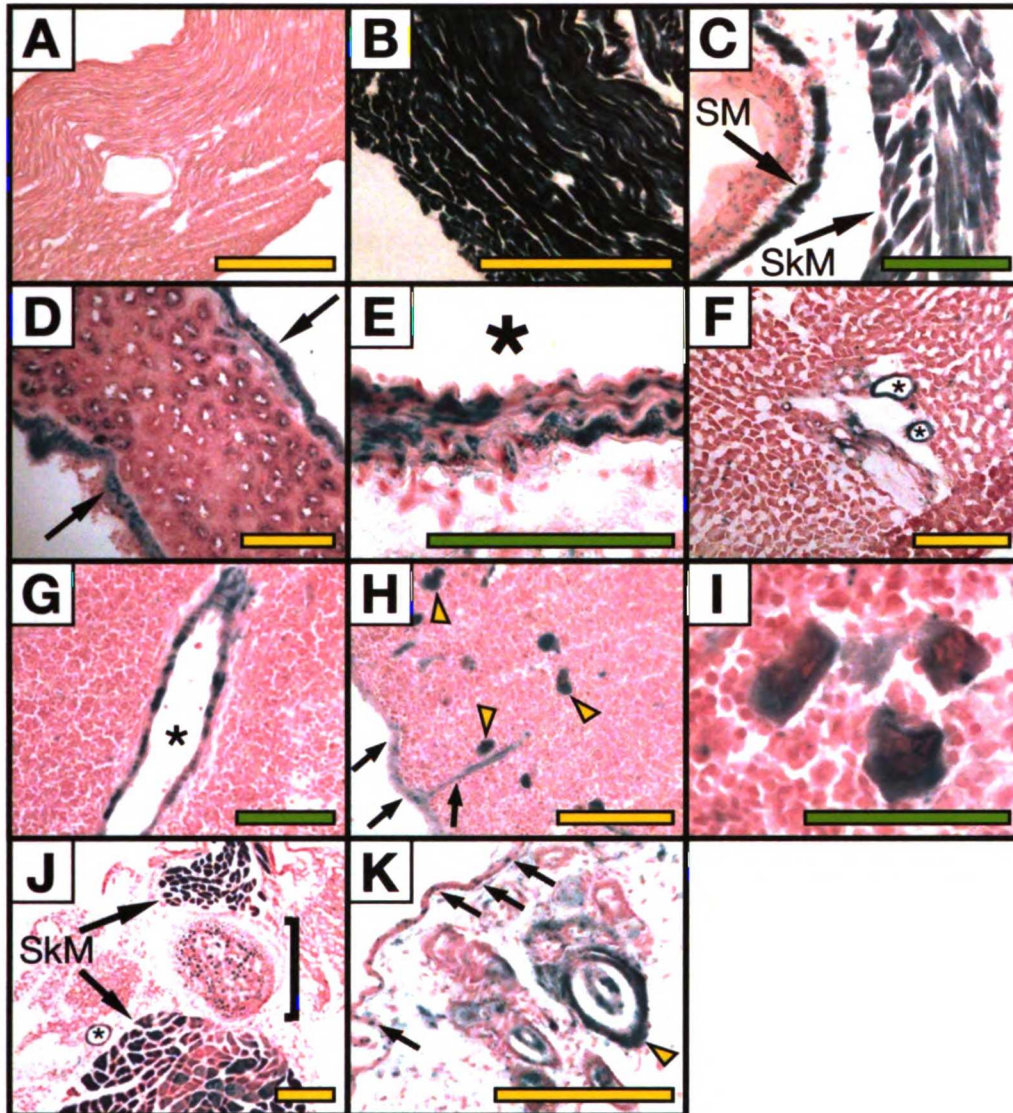


Figure 3 Legend:

X-gal-stained frozen sections from a Wt mouse (A), and from $G\alpha_{13}^{lacZ/+}$ mice (B-K). (A,B) Myocardium. (C) Trachea showing smooth muscle (SM) and skeletal muscle (SkM) expression. (D) Longitudinal small bowel section showing predominately smooth muscle staining (arrows). (E) Aorta, showing smooth muscle cell expression. Vessel lumina are indicated with an asterisk in all appropriate panels. (F) Liver showing vascular smooth muscle staining, and no detectable hepatocyte staining. (G,H,I) Spleen with vascular smooth muscle staining (G), capsular smooth muscle (H, arrows), and megakaryocytes (yellow arrowheads in H, and magnified in I). (J) Cross section through rib-cage showing skeletal and arterial smooth muscle staining, as well as staining within the rib (bracket). (K) Cross section of skin showing expression predominately in the root and hair sheath (yellow arrowhead), in addition to punctuate staining in keratinocytes (arrows). (Yellow bars = 200 μm; Green bars = 100 μm.)

1871
1872
1873
1874
1875
1876
1877
1878
1879
1880
1881
1882
1883
1884
1885
1886
1887
1888
1889
1890
1891
1892
1893
1894
1895
1896
1897
1898
1899
1900

Chimera analysis:

To begin to address the role of $G\alpha_{13}$ in embryonic development we generated embryonic stem cells (ES cells) homozygous for the targeted $G\alpha_{13}^{lacZ}$ allele. $G\alpha_{13}^{lacZ/lacZ}$ embryos phenocopied $G\alpha_{13}$ null embryos suggesting that our *lacZ* knockin allele is in fact a null allele (Figure 2A). Homozygous $G\alpha_{13}^{lacZ}$ ES cells were generated by selecting for a gene conversion event among heterozygous $G\alpha_{13}^{lacZ}$ ES cells (see Materials and Methods, and reference²⁵⁷). Embryonic chimeras were generated by blastocyste injection using 2 homozygous $G\alpha_{13}^{lacZ}$ ES clones ("4A3" and "4C1") and 1 heterozygous $G\alpha_{13}^{lacZ}$ ES clone ("B3"). The neomycin resistance cassette was removed from the targeted $G\alpha_{13}^{lacZ}$ locus in each of these 3 clones. Embryos with 90% or greater chimerism for $G\alpha_{13}^{lacZ/lacZ}$ cells phenocopied global $G\alpha_{13}$ null embryos (data not shown) and analysis was centered on embryos with 20-75% chimerism (Figure 4).

Analysis of 4A3 and 4C1 chimeras suggests that $G\alpha_{13}$ null cells are capable of differentiating into endocardial cells or endothelial cells in the embryonic or extraembryonic tissues. On gross, histological inspection these $G\alpha_{13}$ null endothelial cells were morphologically normal. In fact 4A3 $G\alpha_{13}$ null cells were often observed to constitute the majority of endothelial cells in some vessels (Figure 4 B,C,E,F,H,I). Whether or not this is a generalized feature of $G\alpha_{13}$ null cells is not apparent from this analysis as $G\alpha_{13}$ null cell chimeras from a second ES clone, 4C1, although able to contribute to normal endothelium did so in a reduced capacity compared to 4A3 chimeras (Figure 4 J-L). A likely reason for this is that, among the limited number of chimeric embryos generated with 4C1 cells, there were no high % chimeras (which were routinely

Faint, illegible text and markings along the left edge of the page, possibly bleed-through from the reverse side. Some faint shapes and lines are visible, but no legible characters are present.

observed in 4A3 chimeras) and as a result there were simply fewer $G\alpha_{13}$ null cells available to contribute to endothelium. Another possibility is that there were phenotypic differences between the 4A3 and 4C1 ES clones. In heterozygous $G\alpha_{13}^{lacZ}$ ES clone ("B3") chimeras we also observed normal incorporation into EC populations, although again the limited number of chimeras obtained with this clone were of low % (Figure 4 M,N).

$G\alpha_{13}$ null and heterozygous ES cells were also able to contribute to various other cell types including the neuroectoderm (Figure 4 D,E,G,H) and mesenchyme (Figure 4 A-L). $G\alpha_{13}$ null ES cells did not appear to contribute to circulating cell populations even in high percentage chimeras (Figure 4 A-C, F,L). β -galactosidase-positive rounded cells that resemble hematopoietic cells but are associated with or adherant to the endothelium/endocardium were observed in $G\alpha_{13}$ null ES chimeras (Figure 4 A,J; arrowheads). This raises the possibility that $G\alpha_{13}$ plays a role in embryonic hematopoiesis though our work did not pursue this possibility. In sum, we were unable to find any cell-autonomous or cell-non-autonomous defects in $G\alpha_{13}$ null cells in contributing to normal endothelial cell populations. One possibility is that $G\alpha_{13}$ has functions that are required after the endothelium is already formed and that cannot be discerned by histological analysis alone.

WEST LINDSEY



Figure 4: Analysis of the contribution of $G\alpha_{13}^{lacZ/lacZ}$ cells to the endothelium in midgestation embryos.

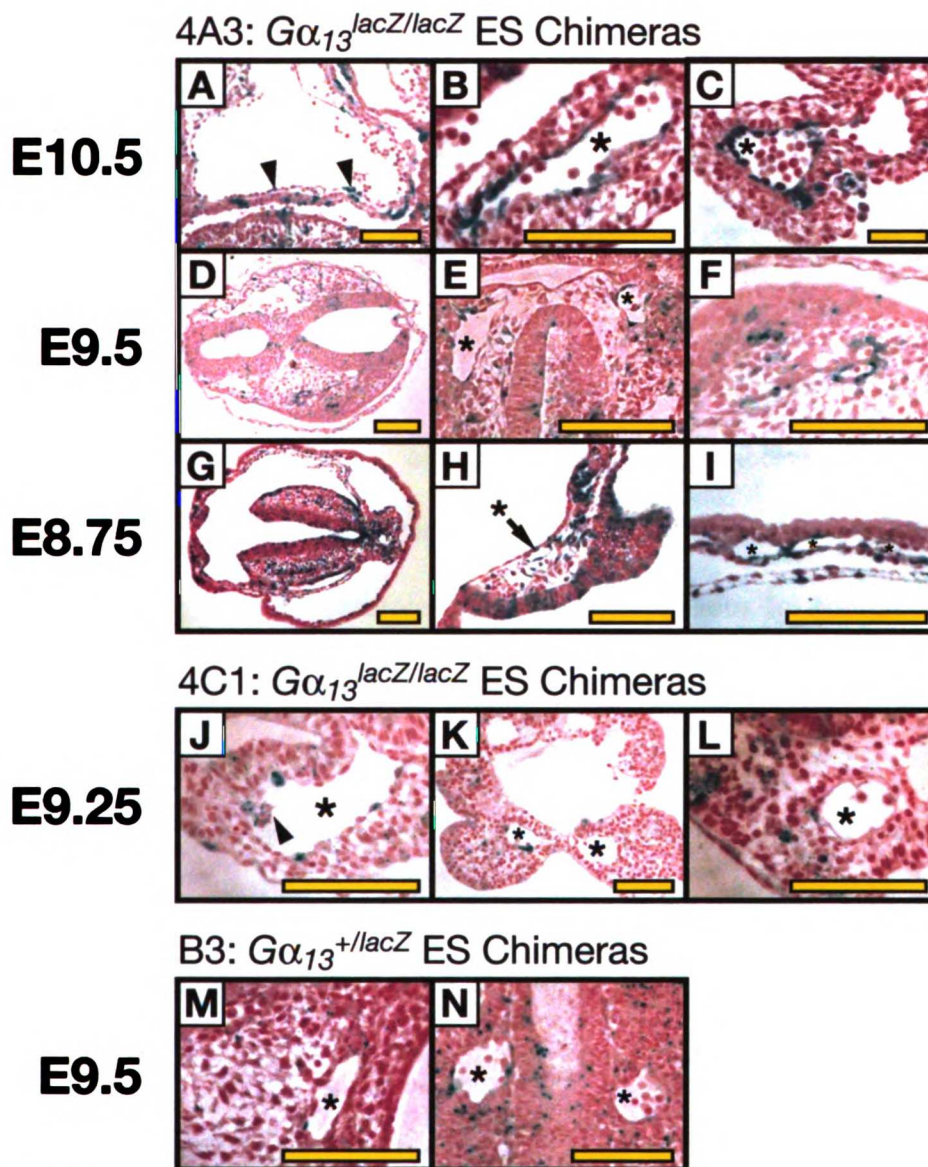


Figure 4 Legend:

Sections of whole-mount β -galactosidase stained $G\alpha_{13}^{lacZ/lacZ}$ (A-L) and $G\alpha_{13}^{+/lacZ}$ (M,N) embryonic chimeras of the indicated age that were generated by injecting ES cells of the indicated genotypes into Wt blastocysts. $G\alpha_{13}^{lacZ/lacZ}$, and hence $G\alpha_{13}$ null, cells in chimeras derived from ES clone 4A3 (A-I) are capable of contributing to normal looking endocardium (A, arrowheads) and endothelium (B,C,E,F,H,I). Vessels are indicated by an asterisk. $G\alpha_{13}^{lacZ/lacZ}$ null cells also contribute to mesenchyme and neuroepithelium. $G\alpha_{13}^{lacZ/lacZ}$ cells are also able to contribute to the endothelium in chimeras derived from a separate ES clone 4C1 (J-L). In control experiments, heterozygous $G\alpha_{13}^{+/lacZ}$ cells in chimeras made from clone B3 ES cells were also observed to incorporate into endothelium (M,N). (Yellow bars = 100 μ m.)



Characterization of a conditional $G\alpha_{13}$ allele:

We generated mice bearing a $G\alpha_{13}$ allele in which the coding portion of exon 4 was flanked by loxP sites (Figure 5). Mice with one such “floxed” and one wild-type allele ($G\alpha_{13}^{+/lox}$) were mated to each other and to mice heterozygous for the conventional exon 1 knockout $G\alpha_{13}$ allele ($G\alpha_{13}^{+/-}$)²⁵⁴ to generate $G\alpha_{13}^{lox/lox}$ and $G\alpha_{13}^{lox/-}$ offspring. These were born at or near the expected Mendelian rate and had no obvious abnormalities. Thus, insertion of loxP sites did not appear to disrupt necessary functions of the $G\alpha_{13}$ gene.

To determine whether deletion of exon 4 coding sequence would yield a null allele as predicted, $G\alpha_{13}^{lox/lox}$ mice were mated to mice carrying a β -actin promoter-driven *Cre* recombinase transgene²⁵⁸ to generate offspring heterozygous for the $G\alpha_{13}$ exon 4 deletion ($G\alpha_{13}^{+/Δ4}$). Southern blot and PCR analysis confirmed excision of exon 4, and crosses of $G\alpha_{13}^{+/Δ4}$ with $G\alpha_{13}^{+/-}$ mice showed that the $G\alpha_{13}^{Δ4/-}$ embryos died at ~E9.5 with a phenotype grossly indistinguishable from that previously reported for embryos homozygous for a $G\alpha_{13}$ allele made by deletion of exon 1 (Figure 6D).²⁵⁴ $G\alpha_{13}^{Δ4/Δ4}$ embryos also exhibited the $G\alpha_{13}^{-/-}$ phenotype (not shown). In addition, infection of endothelial cells cultured from $G\alpha_{13}^{lox/lox}$ neonates with an adenovirus that drove expression of *Cre* caused a marked drop in the level of $G\alpha_{13}$ mRNA in the cultures (Figure 6C). Thus, *Cre* can excise the floxed exon 4 resulting in a $G\alpha_{13}$ allele that is functionally null.

WEST LINDSEY



Figure 5: Generation of a floxed $G\alpha_{13}$ allele

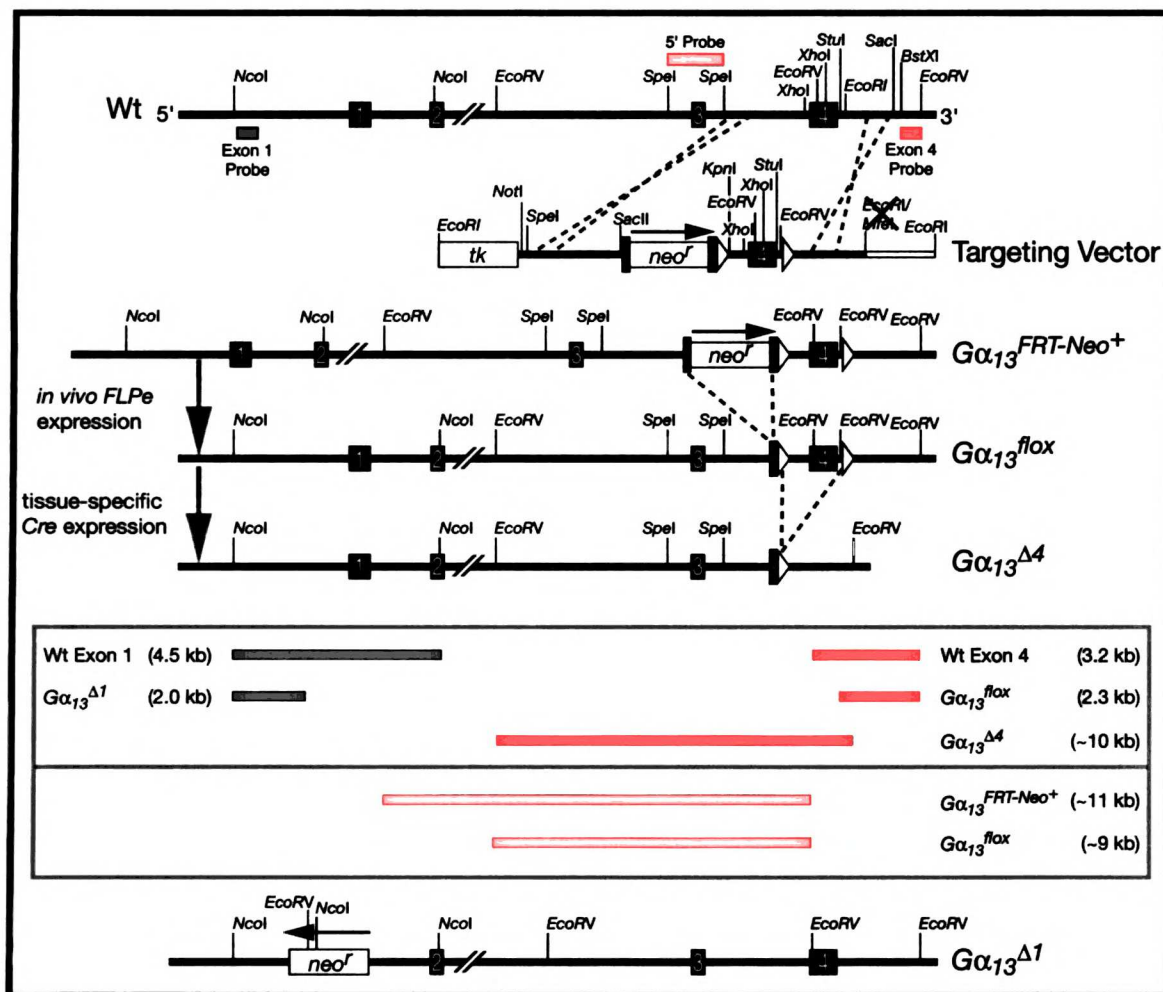


Figure 5 Legend:

Diagram of the Wt $G\alpha_{13}$ locus, targeting vector, and recombined locus. Shaded rectangles indicate FRT sites; other conventions are as in **Figure 1**. *In vivo* FLPe-mediated excision of the *neo^r* cassette generated the " $G\alpha_{13}^{flox}$ " allele which contains one residual 5' FRT site, and loxP sites flanking exon 4. Cre-mediated excision of the floxed allele generated a null $G\alpha_{13}$ allele (" $G\alpha_{13}^{\Delta 4}$ "), transcription of which gives rise to an mRNA fragment encoding a truncated $G\alpha_{13}$ protein that is predicted to be inactive and short-lived. Shown at the bottom is a previously described global null $G\alpha_{13}$ allele (" $G\alpha_{13}^{\Delta 1}$ ", or " $G\alpha_{13}^{-}$ " in other figures) in which exon 1 was replaced by a *neo^r* cassette through homologous recombination (Offermanns *et al.*, 1997). Sizes of the DNA fragments generated by the various alleles after *NcoI/EcoRV* digestion and Southern hybridization with either Exon 1 (blue) or Exon 4 (red) probe are shown at the bottom. Southern analysis after *EcoRV* digestion and hybridization with the "5' Probe" (yellow) was used to verify FLPe-mediated excision of the *neo^r* cassette (see **Materials and Methods**).

11
12
13
14
15
16
17
18
19
20
21
22
23
24
25
26
27
28
29
30
31
32
33
34
35
36
37
38
39
40
41
42
43
44
45
46
47
48
49
50
51
52
53
54
55
56
57
58
59
60
61
62
63
64
65
66
67
68
69
70
71
72
73
74
75
76
77
78
79
80
81
82
83
84
85
86
87
88
89
90
91
92
93
94
95
96
97
98
99
100
101
102
103
104
105
106
107
108
109
110
111
112
113
114
115
116
117
118
119
120
121
122
123
124
125
126
127
128
129
130
131
132
133
134
135
136
137
138
139
140
141
142
143
144
145
146
147
148
149
150
151
152
153
154
155
156
157
158
159
160
161
162
163
164
165
166
167
168
169
170
171
172
173
174
175
176
177
178
179
180
181
182
183
184
185
186
187
188
189
190
191
192
193
194
195
196
197
198
199
200
201
202
203
204
205
206
207
208
209
210
211
212
213
214
215
216
217
218
219
220
221
222
223
224
225
226
227
228
229
230
231
232
233
234
235
236
237
238
239
240
241
242
243
244
245
246
247
248
249
250
251
252
253
254
255
256
257
258
259
260
261
262
263
264
265
266
267
268
269
270
271
272
273
274
275
276
277
278
279
280
281
282
283
284
285
286
287
288
289
290
291
292
293
294
295
296
297
298
299
300
301
302
303
304
305
306
307
308
309
310
311
312
313
314
315
316
317
318
319
320
321
322
323
324
325
326
327
328
329
330
331
332
333
334
335
336
337
338
339
340
341
342
343
344
345
346
347
348
349
350
351
352
353
354
355
356
357
358
359
360
361
362
363
364
365
366
367
368
369
370
371
372
373
374
375
376
377
378
379
380
381
382
383
384
385
386
387
388
389
390
391
392
393
394
395
396
397
398
399
400
401
402
403
404
405
406
407
408
409
410
411
412
413
414
415
416
417
418
419
420
421
422
423
424
425
426
427
428
429
430
431
432
433
434
435
436
437
438
439
440
441
442
443
444
445
446
447
448
449
450
451
452
453
454
455
456
457
458
459
460
461
462
463
464
465
466
467
468
469
470
471
472
473
474
475
476
477
478
479
480
481
482
483
484
485
486
487
488
489
490
491
492
493
494
495
496
497
498
499
500
501
502
503
504
505
506
507
508
509
510
511
512
513
514
515
516
517
518
519
520
521
522
523
524
525
526
527
528
529
530
531
532
533
534
535
536
537
538
539
540
541
542
543
544
545
546
547
548
549
550
551
552
553
554
555
556
557
558
559
560
561
562
563
564
565
566
567
568
569
570
571
572
573
574
575
576
577
578
579
580
581
582
583
584
585
586
587
588
589
590
591
592
593
594
595
596
597
598
599
600
601
602
603
604
605
606
607
608
609
610
611
612
613
614
615
616
617
618
619
620
621
622
623
624
625
626
627
628
629
630
631
632
633
634
635
636
637
638
639
640
641
642
643
644
645
646
647
648
649
650
651
652
653
654
655
656
657
658
659
660
661
662
663
664
665
666
667
668
669
670
671
672
673
674
675
676
677
678
679
680
681
682
683
684
685
686
687
688
689
690
691
692
693
694
695
696
697
698
699
700
701
702
703
704
705
706
707
708
709
710
711
712
713
714
715
716
717
718
719
720
721
722
723
724
725
726
727
728
729
730
731
732
733
734
735
736
737
738
739
740
741
742
743
744
745
746
747
748
749
750
751
752
753
754
755
756
757
758
759
760
761
762
763
764
765
766
767
768
769
770
771
772
773
774
775
776
777
778
779
780
781
782
783
784
785
786
787
788
789
790
791
792
793
794
795
796
797
798
799
800
801
802
803
804
805
806
807
808
809
810
811
812
813
814
815
816
817
818
819
820
821
822
823
824
825
826
827
828
829
830
831
832
833
834
835
836
837
838
839
840
841
842
843
844
845
846
847
848
849
850
851
852
853
854
855
856
857
858
859
860
861
862
863
864
865
866
867
868
869
870
871
872
873
874
875
876
877
878
879
880
881
882
883
884
885
886
887
888
889
890
891
892
893
894
895
896
897
898
899
900
901
902
903
904
905
906
907
908
909
910
911
912
913
914
915
916
917
918
919
920
921
922
923
924
925
926
927
928
929
930
931
932
933
934
935
936
937
938
939
940
941
942
943
944
945
946
947
948
949
950
951
952
953
954
955
956
957
958
959
960
961
962
963
964
965
966
967
968
969
970
971
972
973
974
975
976
977
978
979
980
981
982
983
984
985
986
987
988
989
990
991
992
993
994
995
996
997
998
999
1000



Figure 6: Excision of the floxed $G\alpha_{13}$ allele

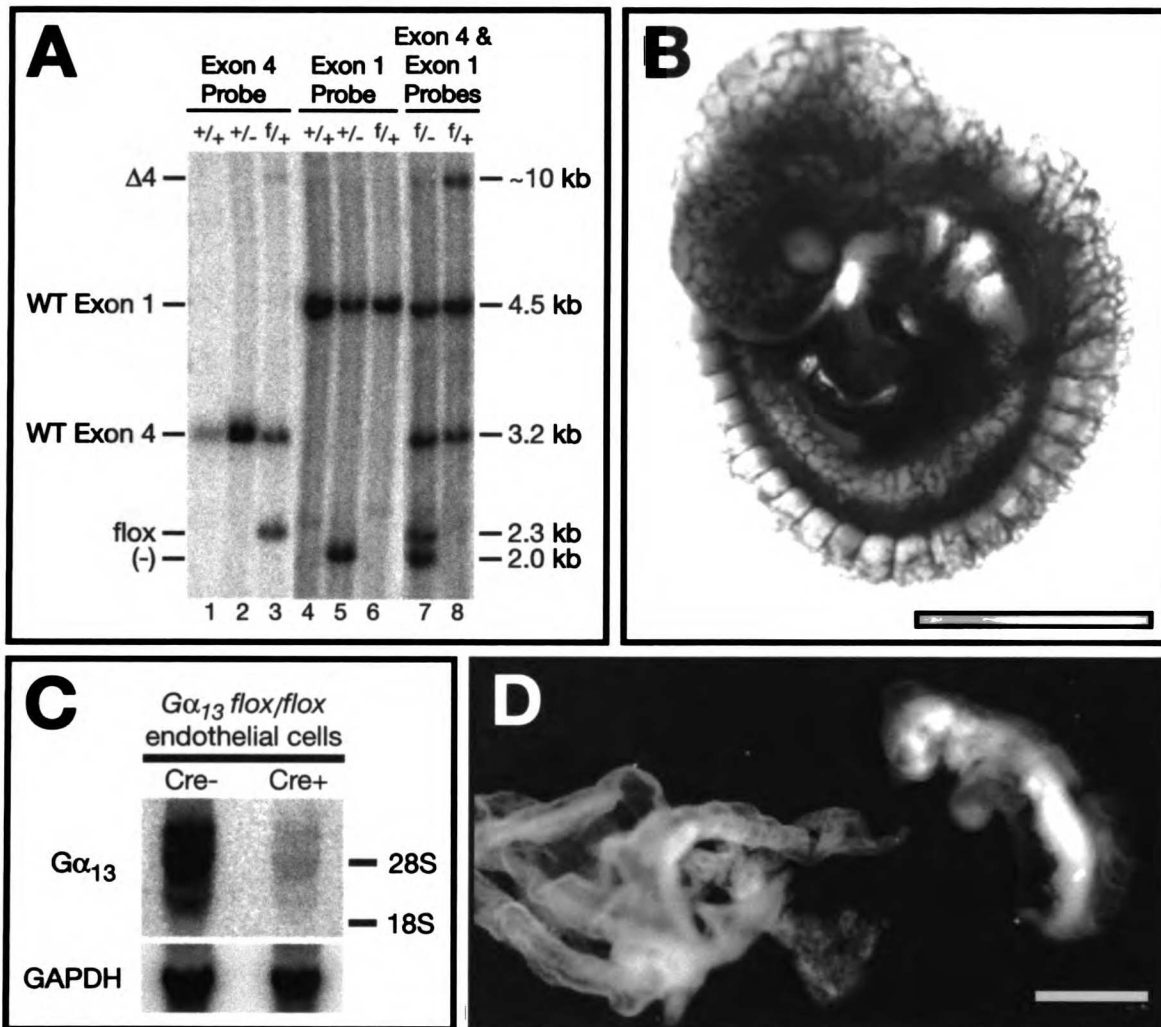


Figure 6 Legend:

A. Southern blot analysis of tail DNA from adult mice with the indicated $G\alpha_{13}$ genotypes: wild-type (+), exon 1 global null (-), flox (f), exon 4 deletion null ($\Delta 4$). The probes used are indicated at top (and see **Figure 5**). The mouse from which the DNA in lane 8 was obtained carried one copy of a β -actin-Cre transgene such that Cre recombinase was expressed globally; note the disappearance of the 2.3-kb band predicted for the $G\alpha_{13}^{flox}$ allele and the appearance of a ~10.0-kb band that corresponds to the $G\alpha_{13}^{\Delta 4}$ allele.

B. Efficiency of endothelium-specific Cre-mediated excision by a $Tie2p/e$ -Cre transgene (see Kisanuki, *et al.*, 2001). Tie2-Cre transgenic mice were crossed to $ROSA26R^{Tg/Tg}$ lacZ Cre-reporter mice; embryos collected at E9.5 were stained for β -galactosidase activity. Virtually all endothelial cells were β -galactosidase positive.

C. Endothelial cells isolated from the lungs of neonatal $Tie2-Cre^{Tg/o}; G\alpha_{13}^{flox/flox}$ mice showed complete excision of the flox allele by Northern analysis and Southern analysis (not shown).

D. $G\alpha_{13}^{\Delta 4/-}$ embryo dissected at ~E10.5 phenocopies $G\alpha_{13}^{-/-}$ embryos (see **Figure 7**) suggesting that the $G\alpha_{13}^{\Delta 4}$ allele is, in fact, a null allele.

(Yellow bars = 1mm.)



Inactivation of the $G\alpha_{13}$ gene in endothelial cells causes embryonic lethality:

To ablate $G\alpha_{13}$ expression in endothelium, we utilized a transgenic mouse line in which expression of *Cre* recombinase was driven in the vascular endothelium by the *Tie2* promoter/enhancer (*Tie2p/e-Cre*).^{259, 260} The *Tie2p/e-Cre* transgene yielded efficient gene excision in endothelial cells at midgestation as assessed by *Cre*-dependent activation of β -galactosidase expression by the *ROSA26R Cre*-excision reporter²⁶¹ (Figure 6B), consistent with previous reports.²⁵⁹ $G\alpha_{13}^{lox/-}$ mice were crossed with $G\alpha_{13}^{+/-}$ mice that were hemizygous for the *Tie2p/e-Cre* transgene (*Tie2p/e-Cre*^{Tg/o}; $G\alpha_{13}^{+/-}$), and offspring were genotyped ~10 days after birth (Table 1). Live $G\alpha_{13}^{lox/+}$ or $G\alpha_{13}^{+/-}$ offspring were produced at similar rates in the presence or absence of the transgene. By contrast, *Tie2p/e-Cre*^{Tg/o}; $G\alpha_{13}^{lox/-}$ mice were markedly underrepresented compared to their *Cre*-negative counterparts (3 vs. 25; $P < 0.005$), and the few *Cre*-positive $G\alpha_{13}^{lox/-}$ mice that were born were runted. Thus, ablation of $G\alpha_{13}$ function in endothelial cells resulted in a highly penetrant embryonic lethal phenotype.

To characterize this phenotype, embryos from *Tie2p/e-Cre*^{Tg/Tg}; $G\alpha_{13}^{+/-}$ X $G\alpha_{13}^{lox/-}$ matings were collected at E8.5, E9.5, E10.5, and E11.5 (Table 2). At E8.5, $G\alpha_{13}^{+/-}$, $G\alpha_{13}^{+/lox}$, $G\alpha_{13}^{lox/-}$, and $G\alpha_{13}^{-/-}$ embryos were indistinguishable in gross appearance (not shown). At E9.5, ~half of $G\alpha_{13}^{-/-}$ embryos were dead and all showed delayed or abnormal development. $G\alpha_{13}^{lox/-}$ endothelial-conditional knockout embryos were also severely affected at this time; 36% were dead and 76% were affected. By E10.5, ~90% of $G\alpha_{13}^{-/-}$ and 50% of $G\alpha_{13}^{lox/-}$ embryos were dead; all $G\alpha_{13}^{-/-}$ embryos and 81% of $G\alpha_{13}^{lox/-}$ embryos

WGT LIDIANI

1971
1972
1973
1974
1975
1976
1977
1978
1979
1980
1981
1982
1983
1984
1985
1986
1987
1988
1989
1990
1991
1992
1993
1994
1995
1996
1997
1998
1999
2000
2001
2002
2003
2004
2005
2006
2007
2008
2009
2010
2011
2012
2013
2014
2015
2016
2017
2018
2019
2020
2021
2022
2023
2024
2025

were affected (Figure 7). By E11.5, all $G\alpha_{13}^{-/-}$ and 88% of $G\alpha_{13}^{floxed}$ embryos were dead. Thus, ablation of $G\alpha_{13}$ function by *Tie2^{pl}/e-Cre*-mediated excision of the $G\alpha_{13}$ floxed allele resulted in a highly penetrant embryonic lethality at midgestation.

To further characterize the potential causes for lethality in $G\alpha_{13}^{-/-}$ and $G\alpha_{13}^{floxed}$ embryos we segregated the two most obvious phenotypes, pericardial dilation and hemorrhage, away from lack of heartbeat in affected embryos and tallied the results (Table 3). In the embryo, pericardial dilation is thought to be an indicator of general cardiovascular stress and/or failure. At E9.5 24% of $G\alpha_{13}^{-/-}$ embryos had a dilated pericardium while half, or 12%, of $G\alpha_{13}^{floxed}$ embryos did. At E10.5, 46% of $G\alpha_{13}^{-/-}$ embryos and 61% of $G\alpha_{13}^{floxed}$ embryos had a dilated pericardium. Embryonic hemorrhage is a more specific phenotype and suggests defects in the structure and/or stability of embryonic blood vessels. In many previous studies hemorrhage has been shown to result from decreased mechanical stability of endothelial cells¹⁶³ or from defective pericyte/VSMC investment of neovessels.^{82, 116, 137, 158} At E9.5 67% of $G\alpha_{13}^{-/-}$ embryos showed evidence of hemorrhage, most often in the head, while in $G\alpha_{13}^{floxed}$ embryos no evidence of hemorrhage was seen. At E10.5, 69% of $G\alpha_{13}^{-/-}$ embryos had hemorrhages while only 23% of $G\alpha_{13}^{floxed}$ embryos did. The higher observed frequency of dilated pericardium in E10.5 $G\alpha_{13}^{floxed}$ embryos vs. E10.5 $G\alpha_{13}^{-/-}$ embryos might simply reflect the fact that more $G\alpha_{13}^{floxed}$ embryos survive intact (*i.e.*, without extensive necrosis) long enough to allow observation of this phenotype, and in any case this phenotype is relatively non-specific. The observation that $G\alpha_{13}^{floxed}$ embryos show significantly less hemorrhage at E9.5 and E10.5 than $G\alpha_{13}^{-/-}$ littermates is more intriguing. Perhaps the

WWT LIBRARY



expression of $G\alpha_{13}$ in a cell type(s) that does not express *Tie2p/e-Cre* (i.e., pericytes/vascular smooth muscle), results in a milder bleeding phenotype of $G\alpha_{13}^{lox/-}$ embryos.

Abnormal vascular development in endothelium-specific $G\alpha_{13}$ knockout embryos.

Endothelium-specific $G\alpha_{13}$ knockout embryos showed a gross phenotype that was similar to, but less severe than, that reported for the conventional $G\alpha_{13}$ knockout.²⁵⁴ Both showed wrinkled yolk sacs with a paucity of blood-filled vessels as well as pale and delayed embryos with pericardial swelling and variable amounts of bleeding into cavities and tissues (Figures 7 and 9). The onset and penetrance of developmental delay and pericardial dilatation was similar in $G\alpha_{13}^{-/-}$ embryos and $G\alpha_{13}^{lox/-}$ endothelium-specific knockout embryos, but gross hemorrhage was more evident in the former (Figure 7, and Table 3).

The structure of the yolk sacs of *Tie2p/e-Cre^{Tg/o}; G $\alpha_{13}^{lox/-}$* embryos was strikingly abnormal. At E9.5 and E10.5, wild-type yolk sacs contain an arborized vasculature with large and small vessels evident by gross examination and by PECAM staining. By contrast, large vessels were lacking from *Tie2p/e-Cre^{Tg/o}; G $\alpha_{13}^{lox/-}$* yolk sacs, and unusually large vascular spaces were apparent on cross section (Figure 9 E-H). This was even more obvious in $G\alpha_{13}^{-/-}$ yolk sacs (Figure 9 I-L). Whole mount β -galactosidase staining of E9.5 *Tie2p/e-Cre^{Tg/o}; G $\alpha_{13}^{lox/-}$* embryos that carried the *ROSA26R Cre*-excision reporter revealed a grossly normal vascular pattern in the trunk (see intersomitic vessels,

UWAT LIBRARY

100
101
102
103
104
105
106
107
108
109
110
111
112
113
114
115
116
117
118
119
120
121
122
123
124
125
126
127
128
129
130
131
132
133
134
135
136
137
138
139
140
141
142
143
144
145
146
147
148
149
150
151
152
153
154
155
156
157
158
159
160
161
162
163
164
165
166
167
168
169
170
171
172
173
174
175
176
177
178
179
180
181
182
183
184
185
186
187
188
189
190
191
192
193
194
195
196
197
198
199
200



branchial arch vessels, and endocardium in Figure 8). However, head vessels were delayed and disorganized compared to those seen in littermate controls (Figure 8 C,F,I). Thus, endothelial cell differentiation occurred and early vasculogenesis and patterning were relatively normal in embryos that lacked $G\alpha_{13}$ function in endothelial cells, but subsequent remodeling of the vasculature was markedly impaired.

UWOT LIBRARY

11
12
13
14
15
16
17
18
19
20
21
22
23
24
25
26
27
28
29
30
31
32
33
34
35
36
37
38
39
40
41
42
43
44
45
46
47
48
49
50
51
52
53
54
55
56
57
58
59
60
61
62
63
64
65
66
67
68
69
70
71
72
73
74
75
76
77
78
79
80
81
82
83
84
85
86
87
88
89
90
91
92
93
94
95
96
97
98
99
100

1
2
3
4
5
6
7
8
9
10
11
12
13
14
15
16
17
18
19
20
21
22
23
24
25
26
27
28
29
30
31
32
33
34
35
36
37
38
39
40
41
42
43
44
45
46
47
48
49
50
51
52
53
54
55
56
57
58
59
60
61
62
63
64
65
66
67
68
69
70
71
72
73
74
75
76
77
78
79
80
81
82
83
84
85
86
87
88
89
90
91
92
93
94
95
96
97
98
99
100

Table 1. Impaired viability of endothelium-specific $G\alpha_{13}$ knockout mice.

	+/ <i>flox</i>	+/-	-/-	<i>flox</i> /-
Tie2p/e-Cre ^{Tg/o}	38	29	0	3
Tie2p/e-Cre ^{o/o}	40	33	0	25

Genotypes of 168 progeny from ♀ Tie2p/e-Cre^{Tg/o}; $G\alpha_{13}^{+/-}$ X ♂ $G\alpha_{13}^{flox/-}$ intercrosses alive at ~postnatal day 10.

Table 2. Genotype and gross phenotype of embryos from Tie2p/e-Cre^{Tg/Tg}; $G\alpha_{13}^{+/-}$ X $G\alpha_{13}^{flox/-}$ intercrosses.

Age	Total	+/ <i>flox</i>	+/-	-/-	<i>flox</i> /-
E9.5	102	27/32 (13%)	29/34 (9%)	11/21 (100%)	16/25 (76%)
E10.5	80	21/23 (9%)	20/22 (9%)	2/19 (100%)	8/16 (81%)
E11.5	86	17/20 (15%)	27/29 (10%)	0/13 (100%)	3/24 (92%)

Alive/total number of embryos recovered and the percent of abnormal embryos for each genotype at the indicated gestational age are shown. Alive is defined as having a heartbeat. Abnormal included embryos showing pericardial dilation, hemorrhage, developmental delay, or absence of a heartbeat. collected at the indicated day of gestation. The percentage of "affected" embryos, including those without a heartbeat is indicated in parentheses.

Table 3. Frequency of hemorrhage and pericardial dilation in Tie2-Cre^{Tg/o}; $G\alpha_{13}^{-/-}$, Tie2-Cre^{Tg/o}; $G\alpha_{13}^{flox/-}$, and Tie2-Cre^{Tg/o}; $G\alpha_{13}^{flox/+}$ embryos.

	-/-; Tie2-Cre ^{Tg/o}		<i>flox</i> /-; Tie2-Cre ^{Tg/o}		<i>flox</i> /+; Tie2-Cre ^{Tg/o}	
	E9.5	E10.5*	E9.5	E10.5*	E9.5	E10.5
Hemorrhage	67% (14/21)	69% (9/13)	0% (0/25)	23% (3/13)	0% (0/35)	0% (0/23)
Pericardial Dilation	24% (5/21)	46% (6/13)	12% (3/21)	61% (8/13)	0% (0/35)	0% (0/35)

* Necrotic E10.5 embryos are excluded from the data in these columns.

UNIVERSITY OF CALIFORNIA

1
2
3
4
5
6
7
8
9
10
11
12
13
14
15
16
17
18
19
20
21
22
23
24
25
26
27
28
29
30
31
32
33
34
35
36
37
38
39
40
41
42
43
44
45
46
47
48
49
50
51
52
53
54
55
56
57
58
59
60
61
62
63
64
65
66
67
68
69
70
71
72
73
74
75
76
77
78
79
80
81
82
83
84
85
86
87
88
89
90
91
92
93
94
95
96
97
98
99
100

Figure 7: Gross phenotype of $G\alpha_{13}$ endothelium-specific and $G\alpha_{13}^{-/-}$ knockouts

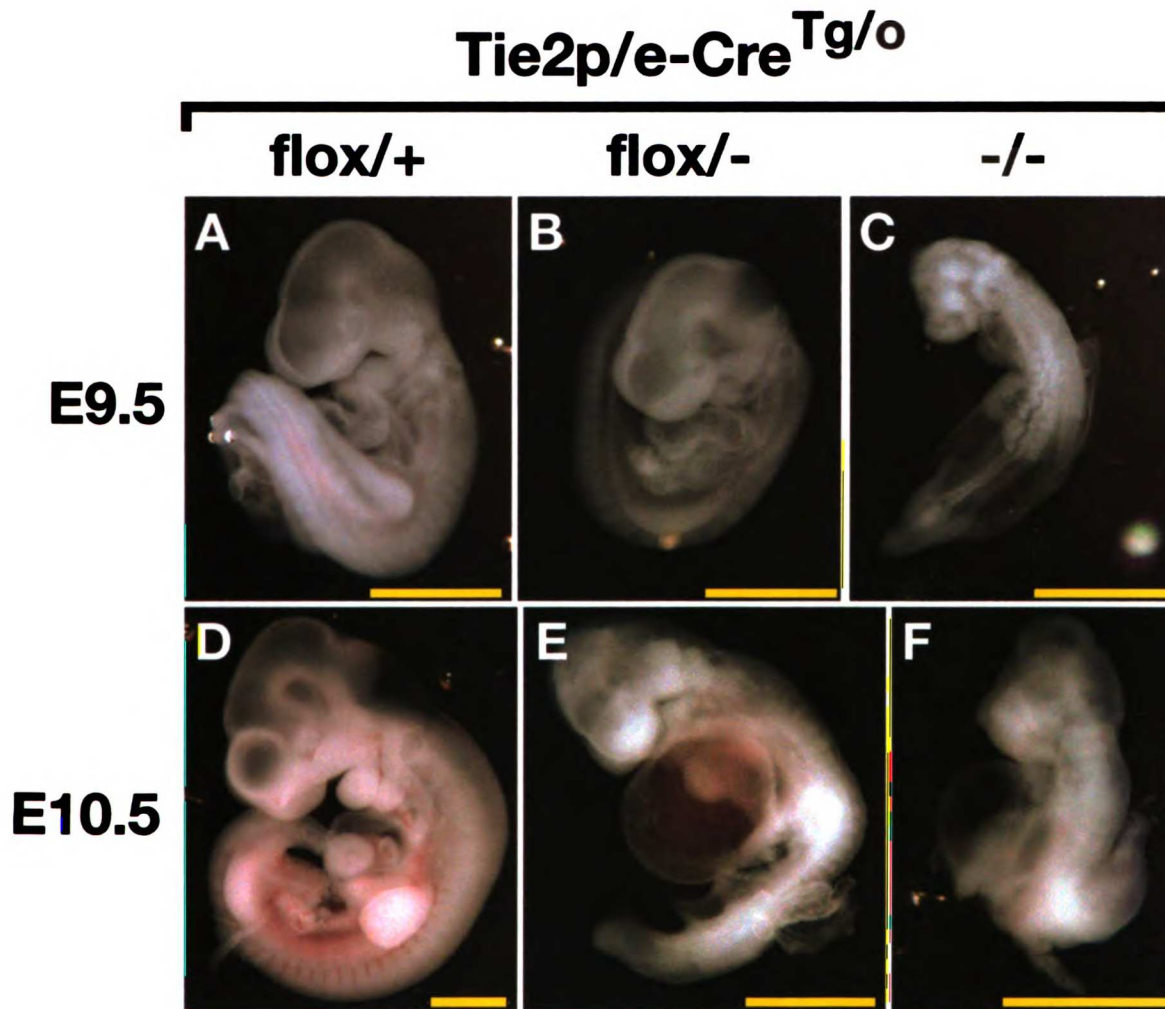


Figure 7 Legend:

Phenotype of $G\alpha_{13}$ endothelium-specific knockout and $G\alpha_{13}^{-/-}$ embryos. $G\alpha_{13}^{flox/+}$ embryos (**A,D**), $G\alpha_{13}^{flox/-}$ embryos (**B,E**), and $G\alpha_{13}^{-/-}$ embryos (**C,F**). All embryos (**A-F**) are $Tie2p/e-Cre^{Tg/o}$ and had a heartbeat at the time of photography. At E9.5, $G\alpha_{13}^{-/-}$ embryos (**C**) were significantly delayed compared to control embryos (**A**); the time of developmental arrest appeared to be ~E8.5 as previously reported (Offermanns, *et al.*, 1997). At E9.5, $G\alpha_{13}^{flox/-}$ embryos (**B**) had turned but appeared arrested at ~E9.0. By E10.5, >80% of $G\alpha_{13}^{flox/-}$ embryos (**E**) were either dead or morphologically abnormal, and all $G\alpha_{13}^{-/-}$ embryos are dead and/or grossly abnormal. Dilated pericardial sacs, consistent with cardiovascular failure, were a prominent feature in both $G\alpha_{13}^{flox/-}$ and $G\alpha_{13}^{-/-}$ embryos (also see **Table 3**). (Yellow bars = 1 mm.)

1
2
3
4
5
6
7
8
9
10
11
12
13
14
15
16
17
18
19
20
21
22
23
24
25
26
27
28
29
30
31
32
33
34
35
36
37
38
39
40
41
42
43
44
45
46
47
48
49
50
51
52
53
54
55
56
57
58
59
60
61
62
63
64
65
66
67
68
69
70
71
72
73
74
75
76
77
78
79
80
81
82
83
84
85
86
87
88
89
90
91
92
93
94
95
96
97
98
99
100

en

ES

Figure 8: Vascular phenotype of $G\alpha_{13}$ endothelium-specific and $G\alpha_{13}^{-/-}$ knockouts

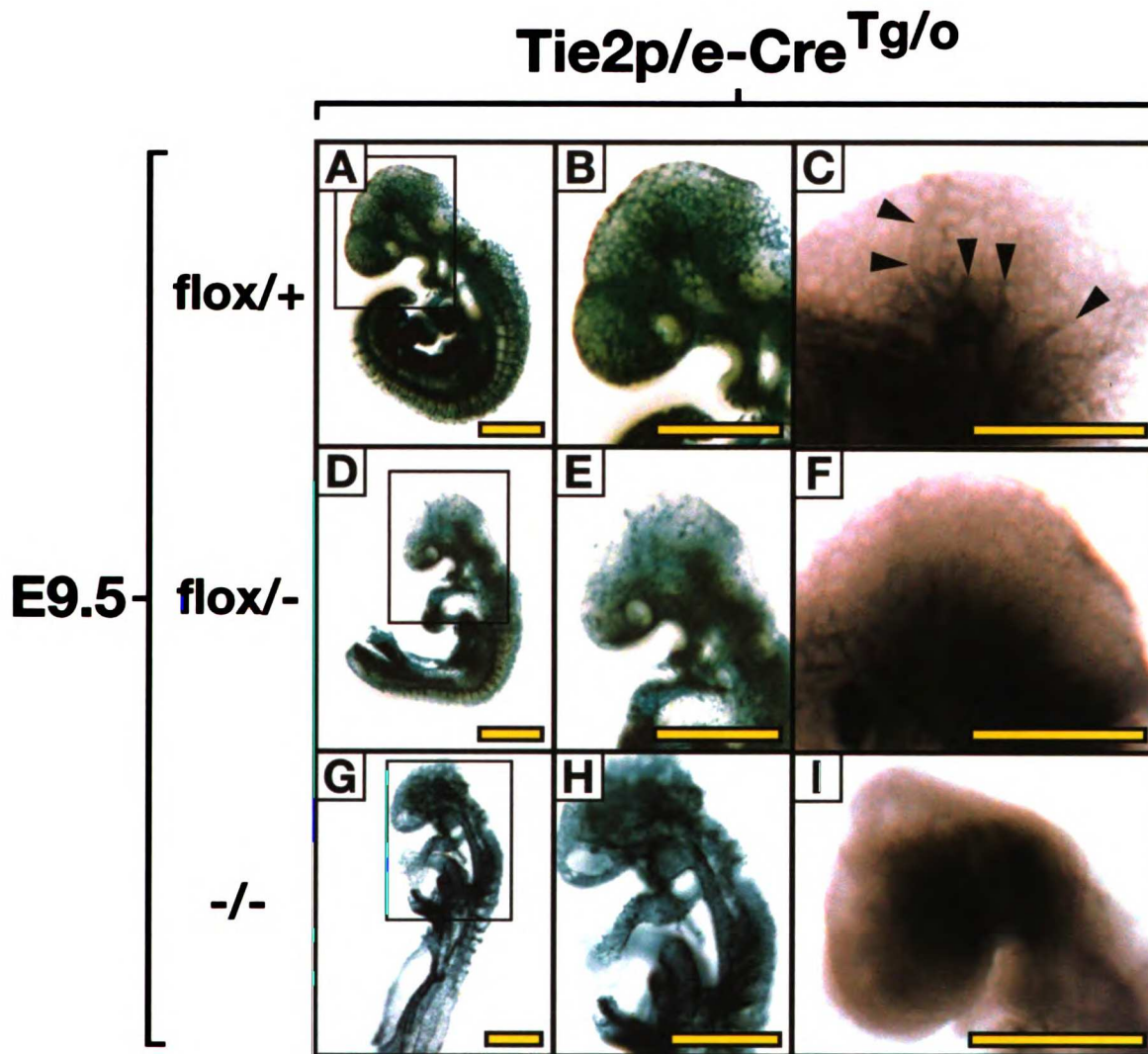


Figure 8 Legend:

Whole mount β -galactosidase staining of *Tie2p/e-Cre^{Tg/o}; ROSA26R* embryos (A,B,D,E,G,H), or CD105 (a.k.a., Endoglin) immunostained *Tie2p/e-Cre^{Tg/o}* embryos (C,F,I) with the indicated $G\alpha_{13}$ genotypes collected at E9.5. Control embryos (A,B,C) show an extensive vascular network in the head. Note the arborization of large vessels (C, arrowheads). In contrast, endothelium-specific null embryos (D,E,F) and global $G\alpha_{13}$ nulls (G,H,I) displayed a more primitive vascular plexus in the head compared to controls. No difference in the vascular anatomy of control and $G\alpha_{13}^{flox/-}$ embryos was observed in the truncal regions. (Yellow bars = 1 mm.)



Figure 9: Yolk sac vascular phenotype of $G\alpha_{13}$ endothelium-specific and $G\alpha_{13}^{-/-}$ knockouts

Tie2p/e-Cre^{Tg/o}

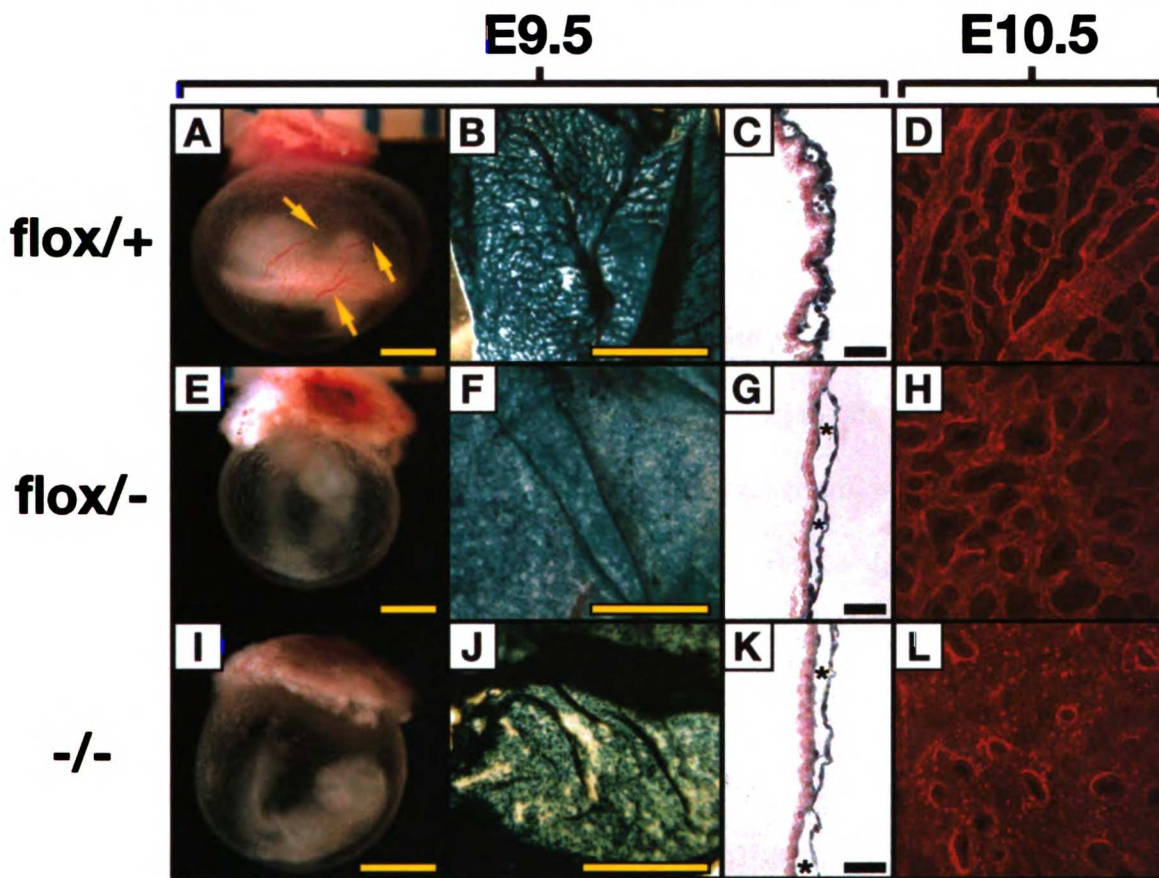


Figure 9 Legend:

Phenotype of $G\alpha_{13}$ endothelium-specific knockout and $G\alpha_{13}^{-/-}$ yolk sacs. $G\alpha_{13}$ genotypes were $G\alpha_{13}^{flox/+}$ (A-D), $G\alpha_{13}^{flox/-}$ (E-H), and $G\alpha_{13}^{-/-}$ (I-L). At E9.5 (left), large blood-filled vessels (arrows) were seen in control yolk sacs (A) but not in $G\alpha_{13}^{flox/-}$ (E) or $G\alpha_{13}^{-/-}$ (I) yolk sacs, which were pale and dimpled. X-gal staining of yolk sacs also carrying one copy of the *Tie2p/e-Cre* transgene and one copy of the *ROSA26R lacZ* reporter allele (B,C,F,G), or one copy of the *Tie2p/e-lacZ* transgene (J,K) revealed an arborized structure with large and small vessels in control yolk sacs (B) while $G\alpha_{13}^{flox/-}$ (F) and $G\alpha_{13}^{-/-}$ (J) yolk sacs exhibited a more plexus-like structure that lacked large vessels. Cross sections of such yolk sacs (C,G,K) showed blood-filled vessels spaced at regular intervals and lined with blue-stained endothelial cells in controls (C) but enlarged and often bloodless vascular spaces in $G\alpha_{13}^{flox/-}$ (G) and $G\alpha_{13}^{-/-}$ (K) yolk sacs (*). Immunofluorescence staining of E10.5 yolk sacs for the endothelial marker PECAM1 (CD31), shown at right, provides a higher resolution view of these phenotypes. (Yellow bars = 1 mm; Black bars = 100 μ m.)

1941
1942
1943
1944
1945
1946
1947
1948
1949
1950
1951
1952
1953
1954
1955
1956
1957
1958
1959
1960
1961
1962
1963
1964
1965
1966
1967
1968
1969
1970
1971
1972
1973
1974
1975
1976
1977
1978
1979
1980
1981
1982
1983
1984
1985
1986
1987
1988
1989
1990
1991
1992
1993
1994
1995
1996
1997
1998
1999
2000
2001
2002
2003
2004
2005
2006
2007
2008
2009
2010
2011
2012
2013
2014
2015
2016
2017
2018
2019
2020
2021
2022
2023
2024
2025

Generation of transgenic mice expressing $G\alpha_{13}$ in endothelial cells:

Although relatively high expression of $G\alpha_{13}$ was detected in endothelial cells during embryonic development, expression was also detected in mesenchyme, dorsal neural tube, foregut and elsewhere (Figure 2B). The results described above strongly suggest that $G\alpha_{13}$ expression in endothelial cells is required for normal vascular development and for survival in mouse embryos, but these results do not preclude a vital role for $G\alpha_{13}$ signaling in other cell types involved in vascular development or other processes. Indeed, the greater severity of the complete vs. endothelium-specific $G\alpha_{13}$ knockout phenotypes might reflect a necessary role for $G\alpha_{13}$ in other cell types. To probe for necessary roles for $G\alpha_{13}$ in cells types other than endothelium, we asked whether $G\alpha_{13}$ expression in endothelial cells might be sufficient to rescue development of $G\alpha_{13}^{-/-}$ embryos. To direct expression of $G\alpha_{13}$ to the endothelium, we used the Tie2 promoter/enhancer²⁶² to drive transcription of a $G\alpha_{13}$ -IRES-lacZ cassette in transgenic mice (Figure 10A). Whole-mount β -galactosidase staining of embryos from two $Tie2p/e$ - $G\alpha_{13}$ -IRES-lacZ (subsequently abbreviated as $Tie2p/e$ - $G\alpha_{13}$) transgenic lines confirmed expression of the transgene in vascular structures from E8.5 onward. Staining was restricted to endothelium and endocardium and to a fraction of hematopoietic cells suggesting that transgene expression was appropriately cell-type specific (Figure 10B a,b).



Endothelium-specific expression of $G\alpha_{13}$ rescues early lethality of $G\alpha_{13}^{-/-}$ embryos and reveals a new phenotype:

$G\alpha_{13}^{+/-}$ mice hemizygous for the endothelium-specific $G\alpha_{13}$ transgene (*Tie2p/e-G $\alpha_{13}^{Tg/e}$; G $\alpha_{13}^{+/-}$*) were crossed to $G\alpha_{13}^{+/-}$ mice and embryos collected at various times. As expected, approximately half of the transgene-negative $G\alpha_{13}^{-/-}$ embryos recovered at E9.5 were dead and the remainder were delayed and/or otherwise abnormal (Table 4 and Figure 10B d). In striking contrast, transgene-positive $G\alpha_{13}^{+/-}$ embryos were recovered at the expected Mendelian rate at E9.5, alive and indistinguishable from their $G\alpha_{13}^{+/+}$ and $G\alpha_{13}^{+/-}$ littermates (Table 4 and Figure 10B c,e). Analysis of $G\alpha_{13}^{-/-}$ yolks sacs at E9.5 also revealed a striking difference in the presence or absence of the transgene. In the absence of endothelial $G\alpha_{13}$ expression, $G\alpha_{13}^{-/-}$ yolk sacs showed a grossly abnormal vascular plexus (see Figure 9 J,K,L), but in the presence of the transgene, $G\alpha_{13}^{+/-}$ yolk sacs displayed a pattern of branching vessels indistinguishable from that seen in wild-type littermates (Figure 10B f,g,h,i). Thus, expression of $G\alpha_{13}$ in endothelial cells was sufficient to prevent vascular defects and death of $G\alpha_{13}^{-/-}$ embryos at E9.5.

$G\alpha_{13}^{-/-}$ embryos carrying the *Tie2p/e-G α_{13}* transgene survived for several days beyond their transgene-negative counterparts and then developed a second phenotype. By E11.5, all transgene-negative $G\alpha_{13}^{-/-}$ embryos were dead and partially resorbed, but 13 of 14 transgene-positive $G\alpha_{13}^{+/-}$ embryos were alive. Most of these had exencephaly (11/14) and/or obvious hemorrhage within the head mesenchyme or ventricles (6/14) (Figure 12 A,C and Table 4). By E12.5, no transgene-negative $G\alpha_{13}^{-/-}$ embryos were recovered in any form, while transgene-positive $G\alpha_{13}^{+/-}$ embryos were recovered at only



slightly less than the expected rate (Table 4). Most of these lacked a heartbeat and all showed exencephaly and/or hemorrhage (Figure 12 E,G and data not shown).

These results suggested that $G\alpha_{13}$ expression in endothelial cells is sufficient for proper embryonic development through E9.5-10.5. However, they did not distinguish whether the inability of the *Tie2p/e-G α_{13}* transgene to completely rescue development of $G\alpha_{13}^{-/-}$ embryos was due to a requirement for $G\alpha_{13}$ function in another cell type vs. failure of the transgene to adequately reproduce the normal level or temporal and spatial pattern of $G\alpha_{13}$ expression in endothelial cells. To address this issue, we asked whether the *Tie2p/e-G α_{13}* transgene would completely rescue the endothelium-specific $G\alpha_{13}$ knockout.

***Tie2p/e-G α_{13}* transgene rescues development of the endothelium-specific $G\alpha_{13}$ knockout:**

Mice hemizygous for the endothelium-specific $G\alpha_{13}$ transgene and bearing one floxed and one null $G\alpha_{13}$ allele (*Tie2p/e-G $\alpha_{13}^{Tg/0}$; G $\alpha_{13}^{flox/-}$*) were crossed to $G\alpha_{13}^{+/-}$ mice homozygous for the *Tie2p/e-Cre* transgene (*Tie2p/e-Cre^{Tg/Tg}; G $\alpha_{13}^{+/-}$*). Offspring were genotyped 10-15 days after birth (Table 5). No $G\alpha_{13}^{-/-}$ mice were recovered even when the endothelium-specific $G\alpha_{13}$ transgene was present. Strikingly, however, while no *Tie2p/e-Cre^{Tg/0}; G $\alpha_{13}^{flox/-}$* pups were recovered in the absence of the transgene, *Tie2p/e-G $\alpha_{13}^{Tg/0}$; Tie2p/e-Cre^{Tg/0}; G $\alpha_{13}^{flox/-}$* mice were recovered at the expected Mendelian rate. These results strongly suggest that the *Tie2p/e-G α_{13}* transgene drives $G\alpha_{13}$ expression in a

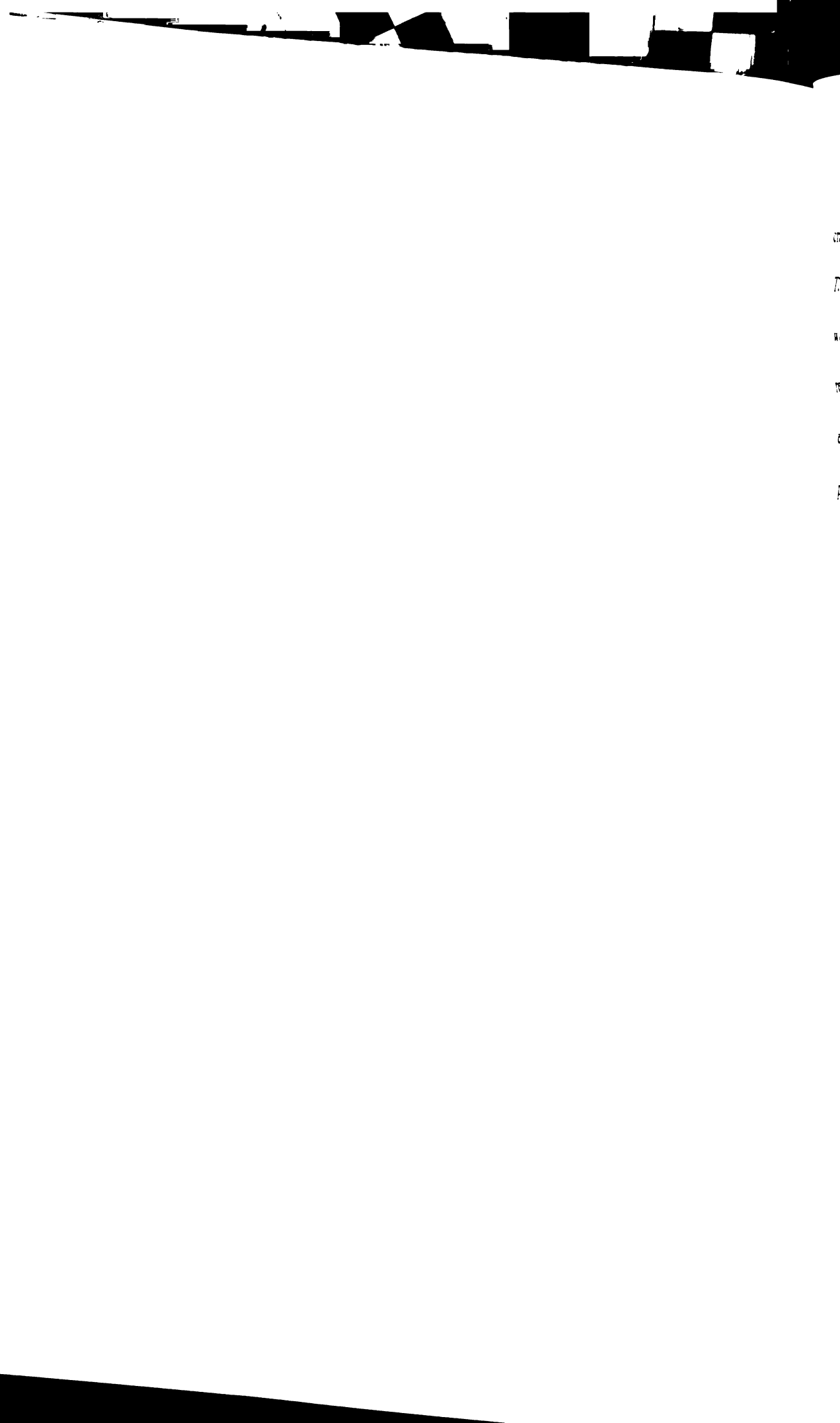
11
12
13
14
15
16
17
18
19
20
21
22
23
24
25
26
27
28
29
30
31
32
33
34
35
36
37
38
39
40
41
42
43
44
45
46
47
48
49
50
51
52
53
54
55
56
57
58
59
60
61
62
63
64
65
66
67
68
69
70
71
72
73
74
75
76
77
78
79
80
81
82
83
84
85
86
87
88
89
90
91
92
93
94
95
96
97
98
99
100
101
102
103
104
105
106
107
108
109
110
111
112
113
114
115
116
117
118
119
120
121
122
123
124
125
126
127
128
129
130
131
132
133
134
135
136
137
138
139
140
141
142
143
144
145
146
147
148
149
150
151
152
153
154
155
156
157
158
159
160
161
162
163
164
165
166
167
168
169
170
171
172
173
174
175
176
177
178
179
180
181
182
183
184
185
186
187
188
189
190
191
192
193
194
195
196
197
198
199
200
201
202
203
204
205
206
207
208
209
210
211
212
213
214
215
216
217
218
219
220
221
222
223
224
225
226
227
228
229
230
231
232
233
234
235
236
237
238
239
240
241
242
243
244
245
246
247
248
249
250
251
252
253
254
255
256
257
258
259
260
261
262
263
264
265
266
267
268
269
270
271
272
273
274
275
276
277
278
279
280
281
282
283
284
285
286
287
288
289
290
291
292
293
294
295
296
297
298
299
300
301
302
303
304
305
306
307
308
309
310
311
312
313
314
315
316
317
318
319
320
321
322
323
324
325
326
327
328
329
330
331
332
333
334
335
336
337
338
339
340
341
342
343
344
345
346
347
348
349
350
351
352
353
354
355
356
357
358
359
360
361
362
363
364
365
366
367
368
369
370
371
372
373
374
375
376
377
378
379
380
381
382
383
384
385
386
387
388
389
390
391
392
393
394
395
396
397
398
399
400
401
402
403
404
405
406
407
408
409
410
411
412
413
414
415
416
417
418
419
420
421
422
423
424
425
426
427
428
429
430
431
432
433
434
435
436
437
438
439
440
441
442
443
444
445
446
447
448
449
450
451
452
453
454
455
456
457
458
459
460
461
462
463
464
465
466
467
468
469
470
471
472
473
474
475
476
477
478
479
480
481
482
483
484
485
486
487
488
489
490
491
492
493
494
495
496
497
498
499
500
501
502
503
504
505
506
507
508
509
510
511
512
513
514
515
516
517
518
519
520
521
522
523
524
525
526
527
528
529
530
531
532
533
534
535
536
537
538
539
540
541
542
543
544
545
546
547
548
549
550
551
552
553
554
555
556
557
558
559
560
561
562
563
564
565
566
567
568
569
570
571
572
573
574
575
576
577
578
579
580
581
582
583
584
585
586
587
588
589
590
591
592
593
594
595
596
597
598
599
600
601
602
603
604
605
606
607
608
609
610
611
612
613
614
615
616
617
618
619
620
621
622
623
624
625
626
627
628
629
630
631
632
633
634
635
636
637
638
639
640
641
642
643
644
645
646
647
648
649
650
651
652
653
654
655
656
657
658
659
660
661
662
663
664
665
666
667
668
669
670
671
672
673
674
675
676
677
678
679
680
681
682
683
684
685
686
687
688
689
690
691
692
693
694
695
696
697
698
699
700
701
702
703
704
705
706
707
708
709
710
711
712
713
714
715
716
717
718
719
720
721
722
723
724
725
726
727
728
729
730
731
732
733
734
735
736
737
738
739
740
741
742
743
744
745
746
747
748
749
750
751
752
753
754
755
756
757
758
759
760
761
762
763
764
765
766
767
768
769
770
771
772
773
774
775
776
777
778
779
780
781
782
783
784
785
786
787
788
789
790
791
792
793
794
795
796
797
798
799
800
801
802
803
804
805
806
807
808
809
810
811
812
813
814
815
816
817
818
819
820
821
822
823
824
825
826
827
828
829
830
831
832
833
834
835
836
837
838
839
840
841
842
843
844
845
846
847
848
849
850
851
852
853
854
855
856
857
858
859
860
861
862
863
864
865
866
867
868
869
870
871
872
873
874
875
876
877
878
879
880
881
882
883
884
885
886
887
888
889
890
891
892
893
894
895
896
897
898
899
900
901
902
903
904
905
906
907
908
909
910
911
912
913
914
915
916
917
918
919
920
921
922
923
924
925
926
927
928
929
930
931
932
933
934
935
936
937
938
939
940
941
942
943
944
945
946
947
948
949
950
951
952
953
954
955
956
957
958
959
960
961
962
963
964
965
966
967
968
969
970
971
972
973
974
975
976
977
978
979
980
981
982
983
984
985
986
987
988
989
990
991
992
993
994
995
996
997
998
999
1000

manner adequate to support the $G\alpha_{13}$ functions in endothelial cells that are necessary for embryonic development. Thus, the contrast between the phenotypes of endothelium-specific vs. conventional $G\alpha_{13}$ knockouts carrying the *Tie2p/e-G\alpha_{13}* transgene is likely due to a necessary role for $G\alpha_{13}$ in a cell type(s) other than endothelial cells – a role that becomes apparent only when $G\alpha_{13}^{-/-}$ embryos are supported beyond E9.5 by the endothelial transgene.

Ablation of $G\alpha_{13}$ function in neural crest recapitulates the late phenotype of endothelium-rescued $G\alpha_{13}^{-/-}$ embryos:

The relatively high level of $G\alpha_{13}$ expression in the region of the neural tube that gives rise to neural crest (Figure 2 g,h) raised the possibility of an important function of $G\alpha_{13}$ in this tissue. The phenotypes seen in endothelium-rescued $G\alpha_{13}^{-/-}$ embryos were consistent with this hypothesis (see Discussion). To probe for necessary functions of $G\alpha_{13}$ in neural crest cells or their derivatives, we utilized *Wnt1-Cre* transgenic mice.²⁶³ *Wnt1-Cre* functions in the neural crest and the dorsal neural tube beginning at E8.5 (Figure 11C) and has been used to conditionally inactivate several genes in neural crest-derived tissues.²⁶⁴⁻²⁶⁷ When $G\alpha_{13}^{lox/lox}$ mice were crossed to $G\alpha_{13}^{+/-}$ mice hemizygous for the *Wnt1-Cre* transgene, only 6 *Wnt1-Cre*^{Tg/o}; $G\alpha_{13}^{lox/-}$ pups were recovered among 150 live offspring; 37 would be expected by Mendelian inheritance ($P < 0.001$ by chi-square). Thus, loss of $G\alpha_{13}$ function in *Wnt1-Cre* transgene-expressing tissues resulted in embryonic lethality ($P < .001$) with >80% penetrance.

Handwritten notes on the left margin of a page, including the number 112 and various illegible scribbles.



Analysis of *Wnt1-Cre^{Tg/o}; Gα₁₃^{flaxl}* embryos collected at E12.5 revealed both craniofacial hemorrhage and neural tube closure defects – an apparent phenocopy of the *Tie2^{p/e}-Gα₁₃^{Tg/o}; Gα₁₃^{-/-}* embryos (Figure 12 F,H). All *Wnt1-Cre^{Tg/o}; Gα₁₃^{flaxl}* embryos were affected at E12.5 and ~30% lacked a heartbeat, and by E14.5, only necrotic and resorbing *Wnt1-Cre^{Tg/o}; Gα₁₃^{flaxl}* embryos were recovered (not shown), suggesting that embryos lacking $G\alpha_{13}$ function in *Wnt1*-expressing cells die ~E12.5-14.5. Thus, $G\alpha_{13}$ plays a necessary role in *Wnt1-Cre* expressing lineages.

Wnt1-Cre can excise floxed alleles in neural crest cells but also in anterior neural tube and other cells in the developing central nervous system. To assess the necessary role of $G\alpha_{13}$ in the latter, $G\alpha_{13}$ was inactivated in neuronal and glial precursor cells using a *Nestin-Cre* transgenic line.²⁶⁸ At postnatal day 10-15, $G\alpha_{13}$ ^{flaxl} mice bearing the *Nestin-Cre* transgene were recovered at the expected Mendelian rate and were grossly normal (not shown). Southern analysis of brains from these mice confirmed virtually complete excision of $G\alpha_{13}$ exon 4 (Figure 11A). *Wnt1-Cre*-driven excision of the *ROSA26R Cre*-reporter was readily detected in the anterior and dorsal region neural tube at E8.5 and became more widely distributed by E9.5 (Figure 11C). *Nestin-Cre*-driven excision in neural tube was nearly absent at E8.5 and 9.5 but by E10.5 was detected throughout the CNS but not in neural crest derivatives (Figure 11B and not shown). Thus, we cannot exclude differences in the time of onset of excision as the basis for the different phenotypes of the between the *Wnt1-Cre*-driven and *Nestin-Cre*-driven $G\alpha_{13}$ conditional knockouts. Overall, however, our data suggest that $G\alpha_{13}$ function in neural crest-derived cells, and not in CNS neurons or glia, is necessary for proper embryonic development.

1
2
3
4
5
6
7
8
9
10
11
12
13
14
15
16
17
18
19
20
21
22
23
24
25
26
27
28
29
30
31
32
33
34
35
36
37
38
39
40
41
42
43
44
45
46
47
48
49
50
51
52
53
54
55
56
57
58
59
60
61
62
63
64
65
66
67
68
69
70
71
72
73
74
75
76
77
78
79
80
81
82
83
84
85
86
87
88
89
90
91
92
93
94
95
96
97
98
99
100

Table 4. Endothelial $G\alpha_{13}$ transgene rescue of early $G\alpha_{13}^{-/-}$ lethality. Genotype and gross phenotype of embryos from $Tie2p/e-G\alpha_{13}^{Tg/o}; G\alpha_{13}^{+/-} \times G\alpha_{13}^{+/-}$ intercrosses.

	Total	$G\alpha_{13}^{+/+}$		$G\alpha_{13}^{+/-}$		$G\alpha_{13}^{-/-}$	
		Tg ⁺	Tg ⁻	Tg ⁺	Tg ⁻	Tg ⁺	Tg ⁻
E9.5	90	11/11 (0%)	9/9 (0%)	23/23 (0%)	23/23 (0%)	11/11 (0%)	6/13 (100%)
E11.5	104	15/15 (0%)	12/12 (0%)	28/28 (0%)	25/25 (0%)	13/14 100%	0/10 (100%)
E12.5	151	21/22 (5%)	16/16 (0%)	49/49 (0%)	44/46 (4%)	2/18 (100%)	0/0 (N/A)

Number of alive/total recovered embryos and percent of embryos that were abnormal. Abnormal includes embryos showing hemorrhage, pericardial dilation, small size, developmental delay, and/or a neural tube defect in addition to those lacking a heartbeat. Note that the transgene yielded complete rescue of $G\alpha_{13}^{-/-}$ embryos through E9.5 and nearly complete rescue at the level of viability through E11.5, at which time the rescued embryos manifested a new phenotype (see text and Figures 11 and 12). NA, not applicable.

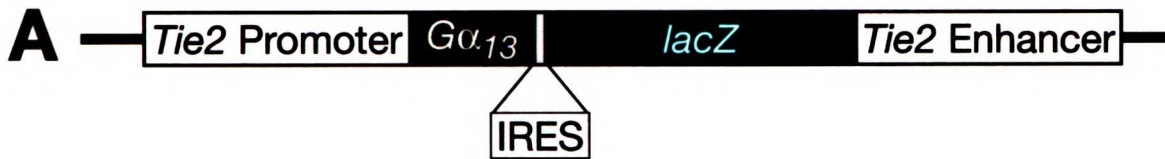
Table 5. $Tie2p/e-G\alpha_{13}$ transgene rescues development of endothelium-specific $G\alpha_{13}$ knockout mice.

	flox/+	+/-	-/-	flox/-
$Tie2p/e-G\alpha_{13}^{Tg/o}$	19	20	0	21
$Tie2p/e-G\alpha_{13}^{o/o}$	25	18	0	0

Genotypes of 103 progeny from $Tie2p/e-G\alpha_{13}^{Tg/o}; G\alpha_{13}^{flox/-} \times Tie2p/e-Cre^{Tg/Tg}; G\alpha_{13}^{+/-}$ intercrosses were determined at postnatal days 10-15. All carry the $Tie2p/e-Cre$ transgene such that all $G\alpha_{13}^{flox/-}$ are endothelium-specific knockouts. Note the complete rescue of the endothelium-specific knockouts by the transgene.

11
12
13
14
15
16
17
18
19
20
21
22
23
24
25
26
27
28
29
30
31
32
33
34
35
36
37
38
39
40
41
42
43
44
45
46
47
48
49
50
51
52
53
54
55
56
57
58
59
60
61
62
63
64
65
66
67
68
69
70
71
72
73
74
75
76
77
78
79
80
81
82
83
84
85
86
87
88
89
90
91
92
93
94
95
96
97
98
99
100
101
102
103
104
105
106
107
108
109
110
111
112
113
114
115
116
117
118
119
120
121
122
123
124
125
126
127
128
129
130
131
132
133
134
135
136
137
138
139
140
141
142
143
144
145
146
147
148
149
150
151
152
153
154
155
156
157
158
159
160
161
162
163
164
165
166
167
168
169
170
171
172
173
174
175
176
177
178
179
180
181
182
183
184
185
186
187
188
189
190
191
192
193
194
195
196
197
198
199
200
201
202
203
204
205
206
207
208
209
210
211
212
213
214
215
216
217
218
219
220
221
222
223
224
225
226
227
228
229
230
231
232
233
234
235
236
237
238
239
240
241
242
243
244
245
246
247
248
249
250
251
252
253
254
255
256
257
258
259
260
261
262
263
264
265
266
267
268
269
270
271
272
273
274
275
276
277
278
279
280
281
282
283
284
285
286
287
288
289
290
291
292
293
294
295
296
297
298
299
300
301
302
303
304
305
306
307
308
309
310
311
312
313
314
315
316
317
318
319
320
321
322
323
324
325
326
327
328
329
330
331
332
333
334
335
336
337
338
339
340
341
342
343
344
345
346
347
348
349
350
351
352
353
354
355
356
357
358
359
360
361
362
363
364
365
366
367
368
369
370
371
372
373
374
375
376
377
378
379
380
381
382
383
384
385
386
387
388
389
390
391
392
393
394
395
396
397
398
399
400
401
402
403
404
405
406
407
408
409
410
411
412
413
414
415
416
417
418
419
420
421
422
423
424
425
426
427
428
429
430
431
432
433
434
435
436
437
438
439
440
441
442
443
444
445
446
447
448
449
450
451
452
453
454
455
456
457
458
459
460
461
462
463
464
465
466
467
468
469
470
471
472
473
474
475
476
477
478
479
480
481
482
483
484
485
486
487
488
489
490
491
492
493
494
495
496
497
498
499
500
501
502
503
504
505
506
507
508
509
510
511
512
513
514
515
516
517
518
519
520
521
522
523
524
525
526
527
528
529
530
531
532
533
534
535
536
537
538
539
540
541
542
543
544
545
546
547
548
549
550
551
552
553
554
555
556
557
558
559
560
561
562
563
564
565
566
567
568
569
570
571
572
573
574
575
576
577
578
579
580
581
582
583
584
585
586
587
588
589
590
591
592
593
594
595
596
597
598
599
600
601
602
603
604
605
606
607
608
609
610
611
612
613
614
615
616
617
618
619
620
621
622
623
624
625
626
627
628
629
630
631
632
633
634
635
636
637
638
639
640
641
642
643
644
645
646
647
648
649
650
651
652
653
654
655
656
657
658
659
660
661
662
663
664
665
666
667
668
669
670
671
672
673
674
675
676
677
678
679
680
681
682
683
684
685
686
687
688
689
690
691
692
693
694
695
696
697
698
699
700
701
702
703
704
705
706
707
708
709
710
711
712
713
714
715
716
717
718
719
720
721
722
723
724
725
726
727
728
729
730
731
732
733
734
735
736
737
738
739
740
741
742
743
744
745
746
747
748
749
750
751
752
753
754
755
756
757
758
759
760
761
762
763
764
765
766
767
768
769
770
771
772
773
774
775
776
777
778
779
780
781
782
783
784
785
786
787
788
789
790
791
792
793
794
795
796
797
798
799
800
801
802
803
804
805
806
807
808
809
810
811
812
813
814
815
816
817
818
819
820
821
822
823
824
825
826
827
828
829
830
831
832
833
834
835
836
837
838
839
840
841
842
843
844
845
846
847
848
849
850
851
852
853
854
855
856
857
858
859
860
861
862
863
864
865
866
867
868
869
870
871
872
873
874
875
876
877
878
879
880
881
882
883
884
885
886
887
888
889
890
891
892
893
894
895
896
897
898
899
900
901
902
903
904
905
906
907
908
909
910
911
912
913
914
915
916
917
918
919
920
921
922
923
924
925
926
927
928
929
930
931
932
933
934
935
936
937
938
939
940
941
942
943
944
945
946
947
948
949
950
951
952
953
954
955
956
957
958
959
960
961
962
963
964
965
966
967
968
969
970
971
972
973
974
975
976
977
978
979
980
981
982
983
984
985
986
987
988
989
990
991
992
993
994
995
996
997
998
999
1000

Figure 10: Rescue of early $G\alpha_{13}^{-/-}$ lethality with an endothelium-specific $G\alpha_{13}$ transgene



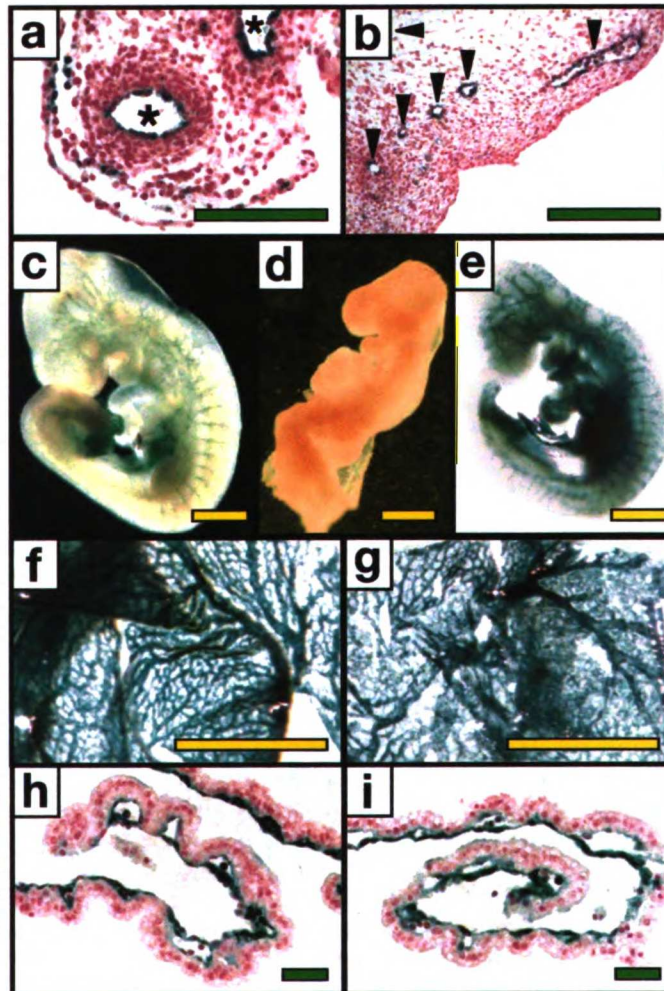
B

Figure 10 Legend:

A. Diagram of the *Tie2p/e-Gα₁₃-IRES-lacZ* construct (*Tie2p/e-Gα₁₃*) used to generate mice in which $G\alpha_{13}$ is expressed in endothelial cells.

B. X-gal staining of an E10.5 *Tie2p/e-Gα₁₃^{Tg/o}* embryo showing staining of endothelium in (a) umbilical artery and vein (*) and (b) head vessels (arrowheads). (c-e) Whole mount X-gal staining of E9.5 embryos. In the presence of the *Tie2p/e-Gα₁₃* transgene, both $G\alpha_{13}^{+/+}$ (c) and $G\alpha_{13}^{-/-}$ (e) embryos appear grossly normal and show endothelium-specific vascular staining. $G\alpha_{13}^{-/-}$ embryos that lacked the transgene (d) were all grossly abnormal at this time. Whole mount (f,g) and cross section (h,i) of X-gal stained E9.5 yolk sacs. *Tie2p/e-Gα₁₃^{Tg/o}; Gα₁₃^{+/-}* mice were mated to $G\alpha_{13}^{+/+}$ mice that were homozygous for the *Tie2p/e-lacZ* transgene to generate embryos in which endothelial cells exhibited strong X-gal expression. The yolk sac vasculature from both $G\alpha_{13}^{+/+}$ (f,h) and $G\alpha_{13}^{-/-}$ (g,i) embryos that carried the *Tie2p/e-Gα₁₃* transgene appeared normal. Note contrast to $G\alpha_{13}^{-/-}$ yolk sacs that lacked the transgene (Figure 9, J and K).

(Green bars = 100 μm; Yellow bars = 1 mm.)





Handwritten text in the top left margin, including the word "writing" and some numbers.

Handwritten text in the middle left margin, possibly a date or a list item.

A vertical column of handwritten text in the bottom left margin, containing various words and numbers.

A block of faint, illegible text in the middle left margin, possibly a list or a set of instructions.

Figure 11: Deletion of $G\alpha_{13}$ in neuronal cell populations with *Nestin-Cre* and *Wnt1-Cre*

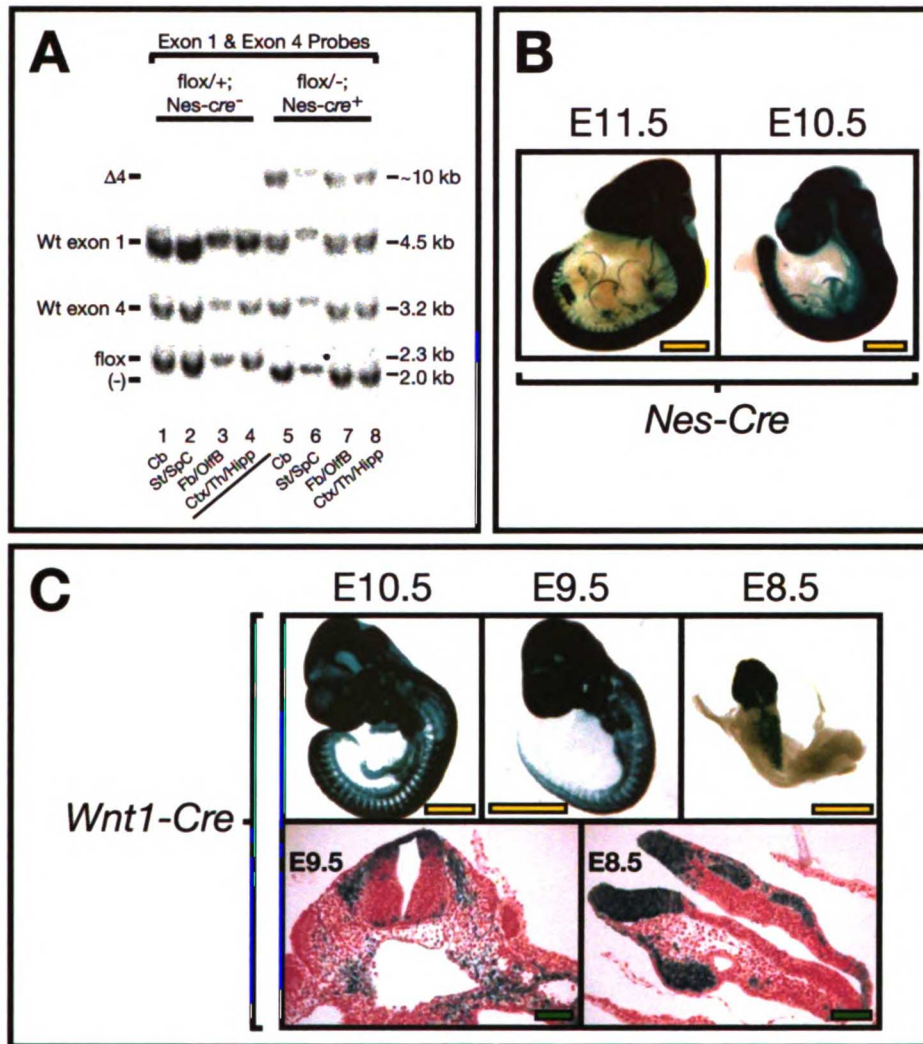


Figure 11 Legend:

A. Southern analysis of the indicated regions of mouse brain from $G\alpha_{13}^{flox/+}$ (lanes 1-4) and *Nestin-Cre*^{Tg/o}; $G\alpha_{13}^{flox/-}$ (lanes 5-8) adult animals to estimate the efficiency of excision by the *Nestin-Cre* transgene. In lanes 5, 7, and 8 there appears to be nearly 100% excision of the flox allele as judged by loss of the 2.3 kb band and appearance of the ~10 kb band. The excision of the flox allele in lane 6 appears to be less efficient (see black dot in lane 6, and **Figure 5** and **Figure 6** for details). (Cb = cerebellum; St/SpC = brain stem and spinal cord; Fb/OlfB = forebrain and olfactory bulb; Ctx/Th/Hipp = cortex, thalamus, and hippocampus).

B. β -galactosidase staining of *Nestin-Cre*^{Tg/o}; *ROSA26R* embryos at the indicated gestational age indicates that *Nestin-Cre* is expressed by E10.5 in neuronal tissues.

C. β -galactosidase staining of *Wnt1-Cre*^{Tg/o}; *ROSA26R* embryos at the indicated gestational age suggests that *Wnt1-Cre* is expressed earlier and its expression is more restricted to neural crest cells than *Nestin-Cre*. (Yellow bars = 1 mm; Green bars = 100 μ m.)

Handwritten notes and diagrams on the left margin of a page. The text is dense and includes several small diagrams and tables. At the top, there is a large number '172' and some illegible handwriting. Below this, there are several lines of text, some of which appear to be a list or a series of entries. There are also several small diagrams, some of which are rectangular boxes with internal lines, possibly representing a grid or a table. The handwriting is cursive and somewhat difficult to read. The overall appearance is that of a handwritten manuscript or a set of notes.

Figure 12: Exencephaly and hemorrhage in embryos in which $G\alpha_{13}$ is absent in neural crest cell populations.

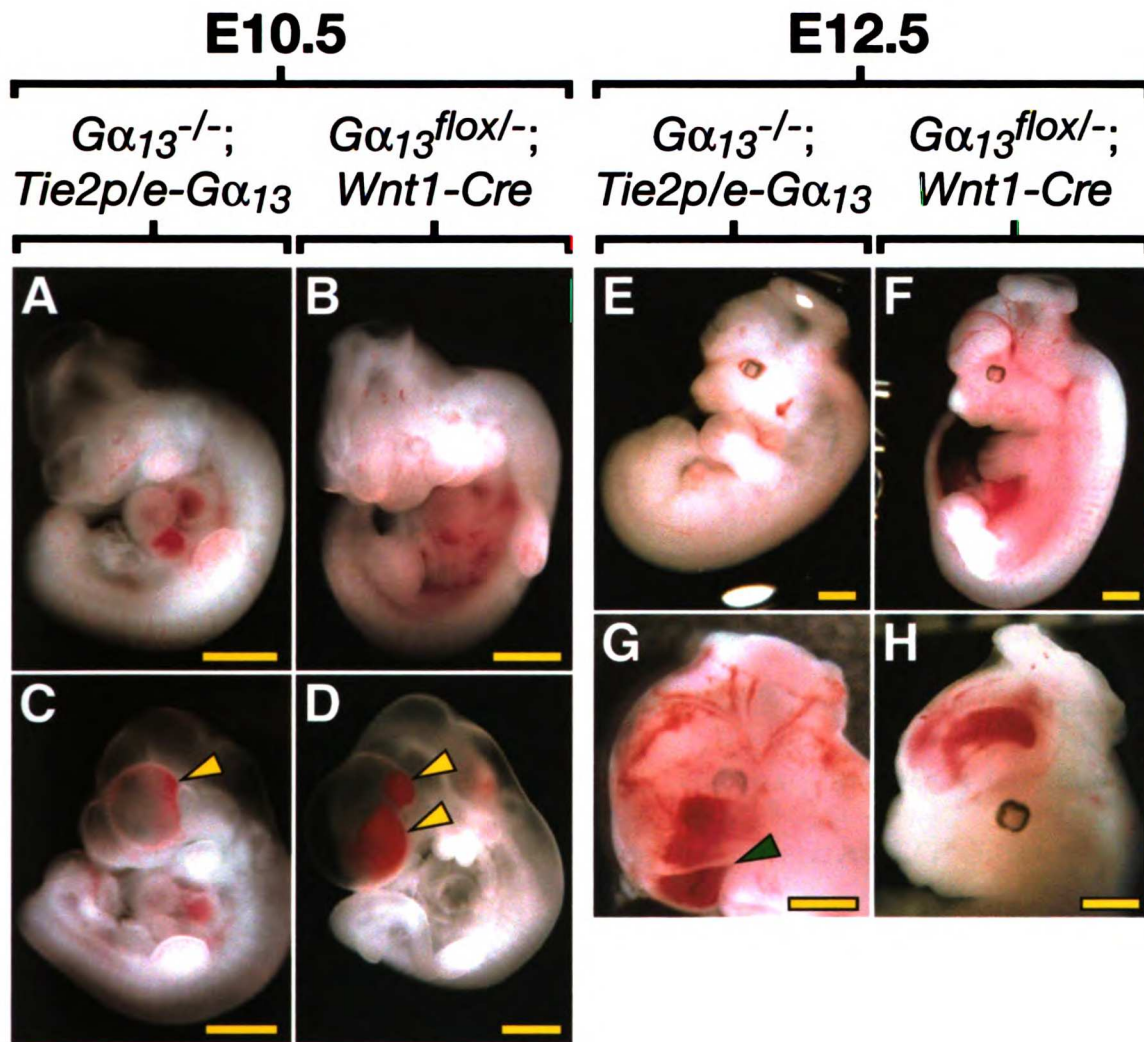


Figure 12 Legend:

Conditional excision of $G\alpha_{13}$ in *Wnt1*-expressing tissue recapitulates the phenotype of endothelium-rescued $G\alpha_{13}^{-/-}$ embryos. *Tie2p/e-G\alpha_{13}^{Tg/o}; G\alpha_{13}^{+/-} (A,C,E,G) and *Wnt1-CreTg/o; G\alpha_{13}^{flox/-} (B,D,F,H) embryos exhibit similar defects. At E10.5 (A-D), there is evidence of neural tube closure defects (A,B) and bleeding into the telencephalon (C,D) in both genotypes (yellow arrowheads). By E12.5 (E-H), embryos of both genotypes exhibit variable exencephaly and craniofacial hemorrhage. Occasional embryos also exhibited craniofacial abnormalities, such as the midline facial cleft seen in G (green arrowhead).**

(Yellow bars = 1 mm.)

1
2
3
4
5
6
7
8
9
10
11
12
13
14
15
16
17
18
19
20
21
22
23
24
25
26
27
28
29
30
31
32
33
34
35
36
37
38
39
40
41
42
43
44
45
46
47
48
49
50
51
52
53
54
55
56
57
58
59
60
61
62
63
64
65
66
67
68
69
70
71
72
73
74
75
76
77
78
79
80
81
82
83
84
85
86
87
88
89
90
91
92
93
94
95
96
97
98
99
100

$G\alpha_{13}^{-/-}$ endothelial cells are defective in network formation in vitro:

Our results strongly suggest that $G\alpha_{13}$ signaling in endothelial cells plays a critical role in vascular development. What function(s) might it serve in this context? $G\alpha_{13}$ links G protein-coupled receptors to Rho activation and perhaps to other effector pathways. Toward exploring the effect of $G\alpha_{13}$ deficiency on endothelial cell responses and behaviors, we ablated $G\alpha_{13}$ function in cultured mouse microvascular endothelial cells. Cells were immunopurified from the skin of $G\alpha_{13}^{lox/lox}$ neonatal mice and infected with adenovirus directing expression of *Cre* plus green fluorescent protein (*GFP*), or *GFP* alone.²⁶⁹ Southern and Northern blot analysis of such cultures suggested an efficiency of >95% for $G\alpha_{13}$ excision (see Figure 6 C, and data not shown). Curiously, $G\alpha_{13}$ excision had no detectable effect on Rho activation or changes in endothelial cell shape or stress fiber formation in response to PAR1 agonist. In addition, no effect was detected in assays of endothelial cell movement on coverslips, adhesion on various matrices or contraction of collagen gels (data not shown). There was, however, a reproducible difference in the behavior of cells cultured on Matrigel. When Ad-*GFP*⁺ infected wild-type or Ad-*GFP*⁺ infected $G\alpha_{13}^{lox/lox}$ endothelial cells were plated on Matrigel, they formed a monolayer that remodeled to become a “network” of cords and tubes (Figure 13 a,c). When Ad-*Cre*⁺-*GFP*⁺ $G\alpha_{13}^{lox/lox}$ endothelial cells were plated on Matrigel at the same density, the monolayer formed normally but showed decreased remodeling (Figure 13b). The different remodeling behaviors depended upon the $G\alpha_{13}$ genotype in that no differences were seen between wild-type cells infected with the Ad-*Cre*⁺-*GFP*⁺ vs. Ad-

WU LIBRARY

D

1. The first part of the document is a list of names and addresses, which appears to be a directory or a list of contacts. The names are written in a cursive hand, and the addresses are listed below them. The list includes names such as "Mr. J. H. Smith", "Mrs. A. B. Jones", and "Mr. C. D. Brown".

2. The second part of the document is a series of short, handwritten notes or entries. These notes are arranged in a list format, with each entry starting with a number or a letter. The notes are written in a cursive hand and appear to be related to the names and addresses listed above.

3. The third part of the document is a series of short, handwritten notes or entries, similar to the second part. These notes are also arranged in a list format and are written in a cursive hand.

4. The fourth part of the document is a series of short, handwritten notes or entries, similar to the previous parts. These notes are arranged in a list format and are written in a cursive hand.

5. The fifth part of the document is a series of short, handwritten notes or entries, similar to the previous parts. These notes are arranged in a list format and are written in a cursive hand.

6. The sixth part of the document is a series of short, handwritten notes or entries, similar to the previous parts. These notes are arranged in a list format and are written in a cursive hand.

7. The seventh part of the document is a series of short, handwritten notes or entries, similar to the previous parts. These notes are arranged in a list format and are written in a cursive hand.

8. The eighth part of the document is a series of short, handwritten notes or entries, similar to the previous parts. These notes are arranged in a list format and are written in a cursive hand.

9. The ninth part of the document is a series of short, handwritten notes or entries, similar to the previous parts. These notes are arranged in a list format and are written in a cursive hand.

10. The tenth part of the document is a series of short, handwritten notes or entries, similar to the previous parts. These notes are arranged in a list format and are written in a cursive hand.



Figure 13: $G\alpha_{13}$ -deficient endothelial cells fail to form a network on Matrigel

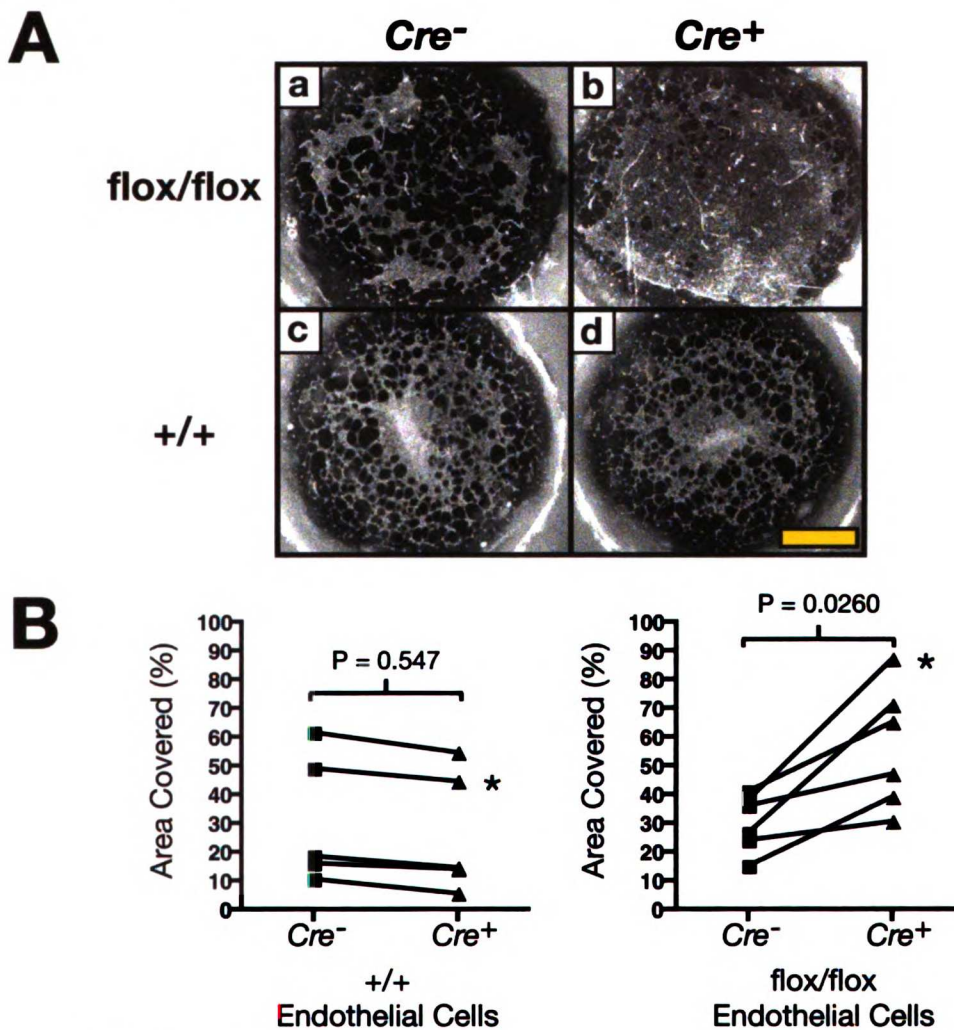


Figure 13 Legend:

A. $G\alpha_{13}^{flox/flox}$ endothelial cells infected with GFP^+ -adenovirus (Cre^-) (**a**) formed an interconnected network of cords and tubes after plating on Matrigel, whereas endothelial cells infected with a GFP^+ - Cre^+ -adenovirus (Cre^+) (**b**) remained primarily as a sheet of cells (see **Figure 6C** for the efficiency of adenoviral Cre excision in $G\alpha_{13}^{flox/flox}$ endothelial cells). In parallel control experiments, endothelial cells isolated from $G\alpha_{13}^{+/+}$ mice formed similar networks whether infected with the Cre^- (**c**) or Cre^+ adenovirus (**d**). (Bar = 4.5 mm.)

B. The percent of the Matrigel surface covered with cells was calculated for 5 $G\alpha_{13}^{+/+}$ and 6 $G\alpha_{13}^{flox/flox}$ experiments (a total of 10 $G\alpha_{13}^{+/+}$ and 12 $G\alpha_{13}^{flox/flox}$ samples) and is expressed as "Area Covered (%)". Connected points indicate paired samples from a single endothelial cell preparation one half of which was infected with Cre^+ virus and other half infected with Cre^- virus. Asterisks mark the samples shown in (**A**). Note that network formation decreased (and hence the area of Matrigel surface covered by cells increased) in association with Cre expression in $G\alpha_{13}^{flox/flox}$ but not $G\alpha_{13}^{+/+}$ endothelial cells. P values were calculated with the Mann-Whitney test.

1
2
3
4
5
6
7
8
9
10
11
12
13
14
15
16
17
18
19
20
21
22
23
24
25
26
27
28
29
30
31
32
33
34
35
36
37
38
39
40
41
42
43
44
45
46
47
48
49
50
51
52
53
54
55
56
57
58
59
60
61
62
63
64
65
66
67
68
69
70
71
72
73
74
75
76
77
78
79
80
81
82
83
84
85
86
87
88
89
90
91
92
93
94
95
96
97
98
99
100

Chapter III:
DISCUSSION

While there are over 300 non-odorant G protein-coupled receptors in mammals, they signal via only four classes of heterotrimeric G proteins: $G\alpha_s$, $G\alpha_{i/o}$, $G\alpha_{q/11}$, and $G\alpha_{12/13}$. The role of G protein-coupled receptors in embryonic development is relatively unexplored, and the absolute number of these receptors and the partially redundant functions of some family members make a systematic study of the necessary roles of GPCRs in development a daunting proposition. Probing for roles of GPCR signaling by ablation of their common G protein signaling pathways is a more tractable alternative.^{254, 270-272} This study focused on $G\alpha_{13}$, and our results imply a key role for G protein-coupled receptor signaling via $G\alpha_{13}$ in several distinct cell types and developmental processes.

The observation that *Tie2p/e-Cre*-mediated excision of the floxed $G\alpha_{13}$ allele caused abnormal vascular structures and embryonic death beginning at E9.5 strongly suggests a key role for $G\alpha_{13}$ in a *Tie2p/e-Cre*-expressing lineage. *Tie2p/e-Cre* can mediate excision of floxed alleles in both endothelium and in hematopoietic lineages (see reference²⁷³ and data not shown). However, several observations point to an endothelial rather than hematopoietic defect as the cause of embryonic death in the *Tie2p/e-Cre*^{Tg/o}; $G\alpha_{13}^{\text{lox}}$ embryos. While the majority of endothelial cells in $G\alpha_{13}^{+/lacZ}$ knockin embryos showed β -galactosidase staining at E9.5-10.5 (Figure 2), less than 2% circulating embryonic blood cells were β -galactosidase-positive at this time (data not shown). Thus,

1
2
3
4
5
6
7
8
9
10
11
12
13
14
15
16
17
18
19
20
21
22
23
24
25
26
27
28
29
30
31
32
33
34
35
36
37
38
39
40
41
42
43
44
45
46
47
48
49
50
51
52
53
54
55
56
57
58
59
60
61
62
63
64
65
66
67
68
69
70
71
72
73
74
75
76
77
78
79
80
81
82
83
84
85
86
87
88
89
90
91
92
93
94
95
96
97
98
99
100

$G\alpha_{13}$ may not be expressed in most embryonic blood cells. It is formally possible that $G\alpha_{13}$ is important in stem cells that represent only a small fraction circulating cells, and that loss of $G\alpha_{13}$ from such cells would have a profound effect. However, while defects in hematopoiesis can cause death of the embryo between E10.5 and 12.5, typically such affected embryos are morphologically indistinguishable from their wild-type littermates except for pallor.^{49, 274-278} Specifically, these embryos do not exhibit the abnormal vascular structures, failed remodeling of blood vessels and pericardial dilatation that were already present in most *Tie2^{p/e}-Cre^{Tg}⁰; G α_{13} ^{flox/-}* embryos at E9.5. One notable exception is SCL/TAL1, loss of which was shown to cause developmental arrest at E9.5 with both failed yolk sac hematopoiesis and abnormal vasculature.^{47, 278} The observed vascular phenotype was latter shown to be due to a role for SCL/TAL1 in endothelial cells since expression of SCL/TAL1 in hematopoietic cells from a GATA1 promoter-driven transgene rescued hematopoiesis but did not prevent vascular abnormalities or death.⁴⁹ Thus, our results are most consistent with the hypothesis that $G\alpha_{13}$ function in endothelial cells is necessary for proper vascular development.

The observation that *Wnt1-Cre* mediated excision of $G\alpha_{13}$ caused intracranial hemorrhage and exencephaly and at least grossly phenocopied $G\alpha_{13}$ ^{-/-} embryos that were rescued by the *Tie2^{p/e}-G α_{13}* transgene strongly suggests a necessary role for $G\alpha_{13}$ in neural crest or its derivatives. *Wnt1-Cre* mediates excision of floxed alleles in both neural crest cells and in the developing CNS. *Nestin-Cre* is not active in neural crest. *Nestin-Cre* caused virtually complete excision of the floxed $G\alpha_{13}$ allele in the brains of $G\alpha_{13}$ ^{flox/-} mice without causing any obvious developmental abnormality, but the onset of

11
12
13
14
15
16
17
18
19
20
21
22
23
24
25
26
27
28
29
30
31
32
33
34
35
36
37
38
39
40
41
42
43
44
45
46
47
48
49
50
51
52
53
54
55
56
57
58
59
60
61
62
63
64
65
66
67
68
69
70
71
72
73
74
75
76
77
78
79
80
81
82
83
84
85
86
87
88
89
90
91
92
93
94
95
96
97
98
99
100



101
102
103
104
105
106
107
108
109
110
111
112
113
114
115
116
117
118
119
120
121
122
123
124
125
126
127
128
129
130
131
132
133
134
135
136
137
138
139
140
141
142
143
144
145
146
147
148
149
150
151
152
153
154
155
156
157
158
159
160
161
162
163
164
165
166
167
168
169
170
171
172
173
174
175
176
177
178
179
180
181
182
183
184
185
186
187
188
189
190
191
192
193
194
195
196
197
198
199
200

201
202
203
204
205
206
207
208
209
210
211
212
213
214
215
216
217
218
219
220
221
222
223
224
225
226
227
228
229
230
231
232
233
234
235
236
237
238
239
240
241
242
243
244
245
246
247
248
249
250
251
252
253
254
255
256
257
258
259
260
261
262
263
264
265
266
267
268
269
270
271
272
273
274
275
276
277
278
279
280
281
282
283
284
285
286
287
288
289
290
291
292
293
294
295
296
297
298
299
300

Nestin-Cre-mediated excision was later than that driven by *Wnt1-Cre*. While we cannot exclude the possibility that the difference between the *Wnt1-Cre* and *Nestin-Cre* phenotypes might be due to the earlier loss of $G\alpha_{13}$ function in *Wnt1*-expressing cells, several considerations suggest that the *Wnt1-Cre* conditional phenotype is due to loss of $G\alpha_{13}$ function specifically in neural crest and its derivatives. Analysis of $G\alpha_{13}^{lacZ}$ knockin embryos revealed relatively high expression of $G\alpha_{13}$ in the dorsal neural tube in presumptive neural crest precursor cells, and the details of the *Wnt1-Cre^{Tg/o}; Gα₁₃^{lox/-}* phenotype are consistent with a role for $G\alpha_{13}$ signaling in neural crest. Failed migration of non-neuronal neural crest cells in other mutant mouse strains such as *PDGFRα* knockout mice and *Patch* mutant mice (in which there is, among other genetic abnormalities, a deletion in the *PDGFRα* gene)* is associated with cranial cystic malformations/blebs, hemorrhage, and craniofacial malformations²⁷⁹ like those seen in *Wnt1-Cre^{Tg/o}; Gα₁₃^{lox/-}* embryos. Alterations in neural crest cell function can also be associated with neural tube closure defects^{264, 279, 280} and this is the likely cause of the exencephaly seen in *Wnt1-Cre^{Tg/o}; Gα₁₃^{lox/-}* embryos.

Exactly how $G\alpha_{13}$ functions in vascular endothelial and neural crest cells relate to the observed phenotypes is unknown. $G\alpha_{13}$ contributes to regulation of the small GTPase

* *N.B.*: The genetic defect in *Patch* mutant mice (which is on chromosome 5) is completely distinct from the *Patched* gene (which is on chromosome 13) that is involved in Hedgehog signaling. Interestingly, the *Patch* mutation is a large genomic deletion that includes the *PDGFRα*, *Kit*, and *Flk1* loci. The name "Patch" derives from the observation that mice harboring this mutation have a white patch on their rump that results from the defective migration of a subset of melanocytes. [Brunkow, M. E., Nagle, D. L., Bernstein, A., Bucan, M. A 1.8-Mb YAC contig spanning three members of the receptor tyrosine kinase gene family (*Pdgfra*, *Kit*, and *Flk1*) on mouse chromosome 5, *Genomics* 25, 421-32 (1995).]



Rho by G protein-coupled receptors via Lsc/p115RhoGEF,^{251, 252} and Rho plays a key role in regulation of the actin cytoskeleton.^{282, 283} Additionally, the Rho family member RhoA has been shown to be involved in regulating the assembly of endothelial cells into vessels in the adult mouse²⁸⁴ and RhoB has been found to support endothelial cell survival and sprouting morphogenesis in the adult mouse retina.²⁸⁵ However, despite extensive studies of $G\alpha_{13}$ -null endothelial cells in culture, we were unable to detect gross defects in Rho activation, or in agonist-induced changes in cell shape or movement (data not shown).

The heterotrimeric G proteins $G\alpha_{12}$ and $G\alpha_{q/11}$ are also capable of regulating Rho²⁸⁶⁻²⁸⁹ therefore it is possible that partial redundancy with these or other G proteins masked effects in these assays. Indeed, while $G\alpha_{12}^{-/-}$ and compound $G\alpha_{12}^{+/-}; G\alpha_{13}^{+/-}$ embryos are phenotypically normal, $G\alpha_{12}^{-/-}; G\alpha_{13}^{-/-}$ embryos show a more severe, earlier vascular phenotype than global $G\alpha_{13}^{-/-}$ embryos; and $G\alpha_{12}^{-/-}; G\alpha_{13}^{+/-}$ embryos show a less severe vascular phenotype than global $G\alpha_{13}^{-/-}$ embryos and are able to develop about a day longer than $G\alpha_{13}^{-/-}$ embryos. These results suggest redundancy in $G\alpha_{12}$ and $G\alpha_{13}$ signaling pathways in vascular development.²⁸⁸ Redundancy of $G\alpha_{12}$ and $G\alpha_{13}$ signaling pathways is not observed in all cell types or all processes since $G\alpha_{13}$ but not $G\alpha_{12}$ signaling in platelets is required for platelet activation.²⁹⁰ $G\alpha_q^{-/-}$ mice survive to adulthood but have a bleeding diathesis resulting from defective platelet activation.²⁷⁰ $G\alpha_{12}^{-/-}; G\alpha_q^{-/-}$ embryos exhibit clear defects by E13.5 including defects in digitation of the foot and hand plates but show no obvious vascular defects. $G\alpha_{12}$ and $G\alpha_q$ were expressed by the endothelial cells in our endothelial cell cultures (data not shown) and perhaps they show partial redundancy with $G\alpha_{13}$ functions in endothelial cells.

11
12
13
14
15
16
17
18
19
20
21
22
23
24
25
26
27
28
29
30
31
32
33
34
35
36
37
38
39
40
41
42
43
44
45
46
47
48
49
50
51
52
53
54
55
56
57
58
59
60
61
62
63
64
65
66
67
68
69
70
71
72
73
74
75
76
77
78
79
80
81
82
83
84
85
86
87
88
89
90
91
92
93
94
95
96
97
98
99
100
101
102
103
104
105
106
107
108
109
110
111
112
113
114
115
116
117
118
119
120
121
122
123
124
125
126
127
128
129
130
131
132
133
134
135
136
137
138
139
140
141
142
143
144
145
146
147
148
149
150
151
152
153
154
155
156
157
158
159
160
161
162
163
164
165
166
167
168
169
170
171
172
173
174
175
176
177
178
179
180
181
182
183
184
185
186
187
188
189
190
191
192
193
194
195
196
197
198
199
200
201
202
203
204
205
206
207
208
209
210
211
212
213
214
215
216
217
218
219
220
221
222
223
224
225
226
227
228
229
230
231
232
233
234
235
236
237
238
239
240
241
242
243
244
245
246
247
248
249
250
251
252
253
254
255
256
257
258
259
260
261
262
263
264
265
266
267
268
269
270
271
272
273
274
275
276
277
278
279
280
281
282
283
284
285
286
287
288
289
290
291
292
293
294
295
296
297
298
299
300
301
302
303
304
305
306
307
308
309
310
311
312
313
314
315
316
317
318
319
320
321
322
323
324
325
326
327
328
329
330
331
332
333
334
335
336
337
338
339
340
341
342
343
344
345
346
347
348
349
350
351
352
353
354
355
356
357
358
359
360
361
362
363
364
365
366
367
368
369
370
371
372
373
374
375
376
377
378
379
380
381
382
383
384
385
386
387
388
389
390
391
392
393
394
395
396
397
398
399
400
401
402
403
404
405
406
407
408
409
410
411
412
413
414
415
416
417
418
419
420
421
422
423
424
425
426
427
428
429
430
431
432
433
434
435
436
437
438
439
440
441
442
443
444
445
446
447
448
449
450
451
452
453
454
455
456
457
458
459
460
461
462
463
464
465
466
467
468
469
470
471
472
473
474
475
476
477
478
479
480
481
482
483
484
485
486
487
488
489
490
491
492
493
494
495
496
497
498
499
500
501
502
503
504
505
506
507
508
509
510
511
512
513
514
515
516
517
518
519
520
521
522
523
524
525
526
527
528
529
530
531
532
533
534
535
536
537
538
539
540
541
542
543
544
545
546
547
548
549
550
551
552
553
554
555
556
557
558
559
560
561
562
563
564
565
566
567
568
569
570
571
572
573
574
575
576
577
578
579
580
581
582
583
584
585
586
587
588
589
590
591
592
593
594
595
596
597
598
599
600
601
602
603
604
605
606
607
608
609
610
611
612
613
614
615
616
617
618
619
620
621
622
623
624
625
626
627
628
629
630
631
632
633
634
635
636
637
638
639
640
641
642
643
644
645
646
647
648
649
650
651
652
653
654
655
656
657
658
659
660
661
662
663
664
665
666
667
668
669
670
671
672
673
674
675
676
677
678
679
680
681
682
683
684
685
686
687
688
689
690
691
692
693
694
695
696
697
698
699
700
701
702
703
704
705
706
707
708
709
710
711
712
713
714
715
716
717
718
719
720
721
722
723
724
725
726
727
728
729
730
731
732
733
734
735
736
737
738
739
740
741
742
743
744
745
746
747
748
749
750
751
752
753
754
755
756
757
758
759
760
761
762
763
764
765
766
767
768
769
770
771
772
773
774
775
776
777
778
779
780
781
782
783
784
785
786
787
788
789
790
791
792
793
794
795
796
797
798
799
800
801
802
803
804
805
806
807
808
809
810
811
812
813
814
815
816
817
818
819
820
821
822
823
824
825
826
827
828
829
830
831
832
833
834
835
836
837
838
839
840
841
842
843
844
845
846
847
848
849
850
851
852
853
854
855
856
857
858
859
860
861
862
863
864
865
866
867
868
869
870
871
872
873
874
875
876
877
878
879
880
881
882
883
884
885
886
887
888
889
890
891
892
893
894
895
896
897
898
899
900
901
902
903
904
905
906
907
908
909
910
911
912
913
914
915
916
917
918
919
920
921
922
923
924
925
926
927
928
929
930
931
932
933
934
935
936
937
938
939
940
941
942
943
944
945
946
947
948
949
950
951
952
953
954
955
956
957
958
959
960
961
962
963
964
965
966
967
968
969
970
971
972
973
974
975
976
977
978
979
980
981
982
983
984
985
986
987
988
989
990
991
992
993
994
995
996
997
998
999
1000

A reproducible effect of $G\alpha_{13}$ -deficiency was seen only when endothelial cells were examined for a more complex behavior: the ability to form networks on Matrigel. $G\alpha_{13}$ null endothelial cells tended to remain organized as sheets rather than reorienting to form networks of cords and tubes. Thus, the signaling defect in endothelial cells lacking only $G\alpha_{13}$ may be relatively subtle and involve cell-cell and/or cell-matrix interactions. In this regard, it is interesting to consider analogies between $G\alpha_{13}$ phenotypes and the *concertina* gastrulation defect. *Concertina* is the *Drosophila* homolog of vertebrate $G\alpha_{13}$.²⁹¹ Gastrulation in fly embryos creates mesoderm and endoderm from a uniform blastula, and furrow formation and inward migration of cells occurs at sites along the length of the embryo rather than through a single blastopore as in mouse.²⁹² *Concertina* mutant embryos begin furrow formation by forming a zone of tightly apposed cells, as do wild-type embryos, and constrict the apices of some of these cells - though ultimately not enough cells constrict to form an organized groove. Thus, *concertina*/ $G\alpha_{13}$ is not necessary for the initiation of gastrulation in *Drosophila* but plays a necessary role in coordinating or propagating changes in cell shape and movement. Furthermore, loss of function of DRhoGEF (a *Drosophila* Lsc/p115RhoGEF homologue) and *Drosophila* Rho signal downstream of *concertina* and loss of any member of this signaling cascade results in similar gastrulation defects.^{293, 294} This appears to be similar to the endothelial defects seen in the studies presented here; endothelial cells form an initial plexus but fail to properly reorganize it. Detailed studies of the cytoskeletal rearrangements in endothelial cells and their movement during vertebrate vasculogenesis and angiogenesis are needed.

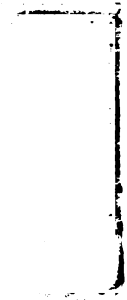


4/28
72
1
2
3
4
5
6
7
8
9
10
11
12
13
14
15
16
17
18
19
20
21
22
23
24
25
26
27
28
29
30
31
32
33
34
35
36
37
38
39
40
41
42
43
44
45
46
47
48
49
50
51
52
53
54
55
56
57
58
59
60
61
62
63
64
65
66
67
68
69
70
71
72
73
74
75
76
77
78
79
80
81
82
83
84
85
86
87
88
89
90
91
92
93
94
95
96
97
98
99
100

Studies of the signaling molecules that orchestrate the behavior of endothelial cells during blood vessel development have focused mainly on growth factors and receptor tyrosine kinases. Our results emphasize a role for G protein-coupled receptors in this process. Our group previously showed that knockout of *Par1*, a G protein-coupled receptor for thrombin, caused a partially penetrant embryonic lethality at midgestation that could be attributed to a role for PAR1 in endothelial cells.^{235, 236} This phenotype was similar in time of onset and general features to that observed in *Tie2p/e-Cre^{Tg/o}; Gα₁₃^{flox}* embryos in the present study, but the *Par1*^{-/-} phenotype was less penetrant. Similarly, knockout of *Edg1*, a Gα_i-coupled receptor for sphingosine-1 phosphate,¹⁵⁸ caused lethality that began at ~E12.5 and was attributable to a necessary function in endothelial cells.¹⁵⁹ Combined-deficiency of this receptor along with knockouts of *Edg3* and *Edg5*, which couple to Gα_i, Gα_q, and Gα_{12/13}, yielded earlier phenotypes.^{169, 170} Interestingly, combined deficiency of the Gα_{12/13}-coupled *Edg3* and *Edg5* receptors resulted in a partially penetrant vascular phenotype observed after E13.5. Thus, multiple GPCRs and heterotrimeric G proteins play both unique and partially redundant roles in helping to orchestrate endothelial cell function during blood vessel development, and signaling via Gα₁₃ plays a key role in this process.

How might Gα₁₃ signaling regulate vascular processes? Gα_{12/13} has been shown to interact with the cytoplasmic tail of N-cadherin and acts to upregulate β-catenin-mediated transcriptional activation by destabilizing β-catenin binding to cadherins.^{295, 296} This interaction appears to also down-regulate cadherin-mediated cell adhesion.²⁹⁷ Thrombin activation of PAR1 has been shown to induce the endocytosis of the TGFβ1 binding

11/12/77
12
13
14
15
16
17
18
19
20
21
22
23
24
25
26
27
28
29
30
31
32
33
34
35
36
37
38
39
40
41
42
43
44
45
46
47
48
49
50
51
52
53
54
55
56
57
58
59
60
61
62
63
64
65
66
67
68
69
70
71
72
73
74
75
76
77
78
79
80
81
82
83
84
85
86
87
88
89
90
91
92
93
94
95
96
97
98
99
100



101
102
103
104
105
106
107
108
109
110
111
112
113
114
115
116
117
118
119
120
121
122
123
124
125
126
127
128
129
130
131
132
133
134
135
136
137
138
139
140
141
142
143
144
145
146
147
148
149
150
151
152
153
154
155
156
157
158
159
160
161
162
163
164
165
166
167
168
169
170
171
172
173
174
175
176
177
178
179
180
181
182
183
184
185
186
187
188
189
190
191
192
193
194
195
196
197
198
199
200

201
202
203
204
205
206
207
208
209
210
211
212
213
214
215
216
217
218
219
220
221
222
223
224
225
226
227
228
229
230
231
232
233
234
235
236
237
238
239
240
241
242
243
244
245
246
247
248
249
250
251
252
253
254
255
256
257
258
259
260
261
262
263
264
265
266
267
268
269
270
271
272
273
274
275
276
277
278
279
280
281
282
283
284
285
286
287
288
289
290
291
292
293
294
295
296
297
298
299
300

membrane protein Endoglin thus leading to a reduction in TGF β 1 signaling in endothelial cells, though it is not yet known whether G α_{13} is required for this. These results suggest that G $\alpha_{12/13}$ could be involved in EC/VSMC and/or EC/EC association (see the Introduction for a discussion of this). There are also reports that G $\alpha_{12/13}$ signaling through Sonic Hedgehog/Smoothed to RhoA activation and down-stream transcriptional changes in neuronal cells is responsible for smoothed-induced inhibition of neurite outgrowth.²⁹⁸ Due to the severe vascular defects seen in embryos with inactivating mutations in Hedgehog signaling pathways it is formally possible that this Hedgehog/Smoothed/G $\alpha_{12/13}$ signaling axis has implications in understanding the observed phenotypes or in the defects we observe in *Wnt1-Cre^{Tg/o}; G α_{13} ^{lox/-}* embryos. These possibilities are speculative but might suggest future experiments to better define the function of G α_{13} in the vasculature.

Our studies also suggest a key role for G α_{13} signaling in neural crest cells. Defects in neural crest cell function in mice lacking the G α_{13} -coupled Endothelin Receptors ET_A and ET_B (and in related knockouts) have been reported (see the Introduction for details) and have been attributed, at least in part, to loss of G $\alpha_{q/11}$ activation by these receptors.^{272, 299} These knockouts survived to birth with phenotypes quite distinct from the embryonic phenotypes seen with knockout of G α_{13} function in *Wnt1*-expressing cells. Mice in which G $\alpha_{12/13}$ is deleted in neural crest cells using a different *Cre*-expressing transgene, *PO-Cre*, do not have neuronal or craniofacial defects but rather defects in the cardiac outflow tract.²⁷² The *PO-Cre* transgene drives expression in neural crest populations that give rise to the spinal dorsal root ganglia, the sympathetic

1
2
3
4
5
6
7
8
9
10
11
12
13
14
15
16
17
18
19
20
21
22
23
24
25
26
27
28
29
30
31
32
33
34
35
36
37
38
39
40
41
42
43
44
45
46
47
48
49
50
51
52
53
54
55
56
57
58
59
60
61
62
63
64
65
66
67
68
69
70
71
72
73
74
75
76
77
78
79
80
81
82
83
84
85
86
87
88
89
90
91
92
93
94
95
96
97
98
99
100

and enteric nervous systems, and in the ventral craniofacial mesenchyme. These results suggest that Endothelin Receptors do not signal through $G\alpha_{12/13}$ in neural crest cells that contribute to certain craniofacial structures. Our results with the *Wnt1-Cre* transgene imply that $G\alpha_{12/13}$ signaling is, however, required in other neural crest cell populations. Intriguingly, RhoB is selectively expressed in delaminating neural crest cells in chick embryos.³⁰⁰ It would be interesting to explore whether defective $G\alpha_{13}$ signaling to RhoB in mouse neural crest cells is responsible for the defects we observed in *Wnt1-Cre^{Tg/o}*; *Gα₁₃^{lox/}* embryos. Thus, our results suggest a broader role for GPCR signaling in the development of neural crest-derived tissues and will stimulate efforts to identify the receptors and ligands involved.

1/2
1/3
1/4
1/5
1/6
1/7
1/8
1/9
1/10

1	1
2	1
3	1
4	1
5	1
6	1
7	1
8	1
9	1
10	1

1/11
1/12
1/13
1/14
1/15
1/16
1/17
1/18
1/19
1/20

MATERIALS AND METHODS

Mutant Mouse Strains

Generation of the $G\alpha_{13}^{\text{lacZ}}$ allele:

BAC-125h06 containing the $G\alpha_{13}$ gene (also known as *gna13*) was obtained by screening a mouse 129/SvJae genomic library with two PCR primer pairs (F1/R1 and F2/R2 primer pairs; see Table 5 for all oligonucleotides and primer pairs described here). The F1/R1 pair was designed to amplify sequences in $G\alpha_{13}$ exon 1 and the F2/R2 pair was designed to amplify sequences in $G\alpha_{13}$ exon 4. To facilitate construction of the targeting vector (Figure 1A), two $G\alpha_{13}$ gene fragments from BAC-125h06 were subcloned into pBC-SK (Stratagene) for sequencing and restriction site mapping. The first was a *Bam*HI fragment containing ~0.2-kb of 5' untranslated sequence, exons 1 and 2, and ~6.0-kb of 3' intronic sequence. The second was an *Eco*RI/*Xho*I fragment containing ~3.0-kb of 5' untranslated sequence, exon 1, and a portion of intronic sequence downstream of exon 1. To construct the targeting vector portions of these subcloned fragments were PCR amplified and introduced into pNTK,³⁰¹ which contains a loxP-flanked neomycin-resistance cassette (floxed-*neo*) and a thymidine kinase cassette (*tk*). The 5' homologous arm of the vector contained 1.7-kb of 5' untranslated sequence and the first 45 base pairs of exon 1, including the start codon, and was amplified by PCR (Primers: F3/R3) from BAC-125h06 with *Pfx* proofreading polymerase and cloned into pCRII-TOPO-Blunt (Invitrogen). A plasmid containing a *lacZ*-Sv40pA cassette (in which all the *Eco*RI and *Xba*I sites in the MCS and the Sv40 polyadenylation sequence had been deleted) was cut with *Hind*III and *Nru*I and the similarly cut 5' homologous arm was inserted such that the

11
12
13
14
15
16
17
18
19
20
21
22
23
24
25
26
27
28
29
30
31
32
33
34
35
36
37
38
39
40
41
42
43
44
45
46
47
48
49
50
51
52
53
54
55
56
57
58
59
60
61
62
63
64
65
66
67
68
69
70
71
72
73
74
75
76
77
78
79
80
81
82
83
84
85
86
87
88
89
90
91
92
93
94
95
96
97
98
99
100

THE
FIRST
PART
OF
THE
HISTORY
OF
THE
CITY
OF
LONDON
FROM
THE
BEGINNING
TO
THE
PRESENT
TIME
BY
JOHN
STOW
1597

3' end of the arm (*i.e.*, the 45-bp of $G\alpha_{13}$ coding sequence) was fused in frame to the *lacZ* gene via the *NruI* site. The 3' homologous arm included the last 120-bp of exon 1, 2.5-kb of intron 1, and the first 29-bp of exon 2. It was PCR amplified (Primers: F4/R4) from BAC-125h06 and subcloned in the same manner as the 5' homologous arm. It was then excised from pCRII-TOPO-Blunt with *BamHI* and *MfeI* and inserted between the floxed-*neo'* and *tk* cassettes in similarly cut pNTK. Finally, the 5' homologous arm *lacZ-Sv40pA* fusion was released from its plasmid backbone with *SaI* and inserted 5' of the floxed-*neo'* cassette in the similarly cut 3' homologous arm pNTK construct. The linearized vector was electroporated into RF8 ES cells, which were selected as described.^{302, 303} 463 ES clones were screened by Southern hybridization; 3 were correctly targeted at both the 5' and 3' ends. Mice generated from one of these, clone 51, were used for the studies presented. The loxP-flanked *neo'* cassette was excised *in vivo* by crossing mice heterozygous for the $G\alpha_{13}^{lacZ-Neo+}$ allele to mice carrying a β -actin promoter-*Cre* transgene (see Figure 1B).³⁰⁴

Generation of a floxed $G\alpha_{13}$ allele:

BAC-125h06 was again used as a source of $G\alpha_{13}$ gene fragments. Two additional fragments were subcloned from BAC-125h06 into pBC-SK. The first was an *EcoRV* fragment containing most of exon 4 and 2.6-kb of 3' untranslated sequence. The second was an *EcoRI* fragment containing exons 3 and 4, 7.9-kb of intronic sequence upstream of exon 3, and 290-bp of 3' untranslated sequence. The targeting vector (Figure 5) contained a 5' homologous arm corresponding to a 2.3-kb *SpeI/XhoI* fragment in intron 3, exon 4 (0.57-kb), and a 3' homologous arm corresponding to 2.0-kb of 3' untranslated



sequence. The 2.3-kb 5' homologous arm was excised from the *EcoRI* BAC-125h06 subclone with *SpeI* and *XhoI* and inserted into a similarly cut modified pBC-SK plasmid (in which the native multi-cloning site (MCS) had been replaced by an oligonucleotide linker (F5/R5) containing the following sites: 5'-*NotI-SpeI-XhoI-KpnI-EcoRI*-3'). Next, another oligonucleotide linker (F6/R6) was inserted into the *XhoI* and *KpnI* sites at the 3' end of the 5' homologous arm (i.e., the *XhoI* and *KpnI* sites in the new MCS created by F5/R5, above) thus destroying the *XhoI* and *KpnI* sites and adding the following sites: 5'-*SacII-KpnI-EcoRV-XhoI*-3'. A *SacII/KpnI* fragment from pK11 (pBS-SK-FRT-PGKNeo-FRT-LoxP; G. Martin, UCSF) containing an FRT-flanked *neo'* cassette with a single 3' loxP site was inserted into the 3' end of the 5' homologous arm sequence with *SacII* and *KpnI* (in the same orientation as the native *Gα₁₃* gene). To generate the 3' homologous arm, a 2.7-kb *XhoI/SacI* fragment containing the 3' end of exon 4 and 1.7-kb of 3' untranslated sequence was excised from the *EcoRV* BAC125h06 subclone and inserted into similarly cut pBC-SK. An oligonucleotide linker containing a loxP sequence and an associated *EcoRV* site (F7/R7) was then inserted into the *StuI/EcoRI* sites 290-bp downstream of the stop codon, destroying the *EcoRI* site. To complete the 3' homologous arm, another oligonucleotide linker (F8/R8) was inserted into the *SacI* site at the 3' end of the 3' homologous arm loxP construct, destroying the *SacI* site and introducing an *EcoRI* site. The 3' homologous arm/loxP construct was cut with *XhoI* and *EcoRI* and inserted into the similarly cut 5' homologous arm FRT-*neo'*-loxP construct (described above). A 0.45-kb *XhoI* fragment spanning the 3' end of the intron and 5' end of exon 4 was excised from the *EcoRI* BAC-125h06 subclone and inserted into the *XhoI* site at the 5' end of the 3' homologous arm. To assemble the final vector, a modified

1
2
3
4
5
6
7
8
9
10
11
12
13
14
15
16
17
18
19
20
21
22
23
24
25
26
27
28
29
30
31
32
33
34
35
36
37
38
39
40
41
42
43
44
45
46
47
48
49
50
51
52
53
54
55
56
57
58
59
60
61
62
63
64
65
66
67
68
69
70
71
72
73
74
75
76
77
78
79
80
81
82
83
84
85
86
87
88
89
90
91
92
93
94
95
96
97
98
99
100



THE
FEDERAL
BUREAU OF
INVESTIGATION
OF THE
DEPARTMENT OF JUSTICE
WASHINGTON, D. C. 20535

101
102
103
104
105
106
107
108
109
110
111
112
113
114
115
116
117
118
119
120
121
122
123
124
125
126
127
128
129
130
131
132
133
134
135
136
137
138
139
140
141
142
143
144
145
146
147
148
149
150
151
152
153
154
155
156
157
158
159
160
161
162
163
164
165
166
167
168
169
170
171
172
173
174
175
176
177
178
179
180
181
182
183
184
185
186
187
188
189
190
191
192
193
194
195
196
197
198
199
200

pNTK plasmid was first generated in which the *NotI* site in the linearization MCS was **deleted** by *NotI* digest followed by fill-in with Klenow fragment polymerase and **religation**. Next, the floxed-*neo'* cassette was deleted by digestion with *XhoI* and *SpeI*, **and** insertion of an oligonucleotide linker (F9/R9) that also destroyed the *XhoI* and *SpeI* **sites** and inserted *MfeI* and *NotI* sites. In order to introduce a *tk* selection cassette, all **relevant** sequences that had been assembled in pBC-SK (*i.e.*, everything above) were **excised** as a single unit with *EcoRI* and *NotI* and inserted into the *MfeI/NotI* sites in the **modified** pNTK plasmid thus destroying the insert-derived *EcoRI* site and allowing for **linearization** with *EcoRI*. All $G\alpha_{13}$ coding sequences and fragment junctions in the final **targeting** vector were sequenced. The linearized vector was electroporated into RF8 ES cells and 42 ES clones were selected and screened. Two were correctly targeted at both the 5' and 3' ends. Mice generated from one of these, clone 9C3, were used in the studies shown. The FRT-flanked *neo'* cassette was removed by crossing mice heterozygous for the $G\alpha_{13}^{\text{lox-Neo}}$ allele to mice bearing a transgene in which a modified *FLP*-recombinase ("*FLPe*") gene is driven by a β -actin promoter.³⁰⁴⁻³⁰⁶ Excision of the *neo'* cassette was confirmed by *EcoRV* digest and Southern analysis with a *SpeI* fragment termed "5' Probe" (see Figure 5). Studies were done in mixed C57BL/6:129SvJae or C57BL/6:129SvJae:ICR backgrounds and used littermate controls.

Generation of *Tie2p/e-G\alpha_{13}* transgenic mice:

A transgene to direct $G\alpha_{13}$ expression to endothelium was generated in a manner analogous to the *Tie2p/e-Par1* transgene previously described.²³⁶ Briefly, $G\alpha_{13}$ coding sequence from pCDNA1- $G\alpha_{13}$ (provided by Dr. Henry Bourne, UCSF) was ligated, along

1
2
3
4
5
6
7
8
9
10
11
12
13
14
15
16
17
18
19
20
21
22
23
24
25
26
27
28
29
30
31
32
33
34
35
36
37
38
39
40
41
42
43
44
45
46
47
48
49
50
51
52
53
54
55
56
57
58
59
60
61
62
63
64
65
66
67
68
69
70
71
72
73
74
75
76
77
78
79
80
81
82
83
84
85
86
87
88
89
90
91
92
93
94
95
96
97
98
99
100

with an internal ribosome entry sequence³⁰⁷ (from Dr. Marc Tessier-Lavigne, UCSF), into **pBS-Tie2p/e-lacZ** (from Dr. Thomas Sato, UT Southwestern) such that the $G\alpha_{13}$ -IRES cassette was 3' of the Tie2 promoter sequence and 5' of the β -galactosidase coding sequence, polyA, and Tie2 enhancer. A restriction fragment containing the Tie2p/e- $G\alpha_{13}$ -IRES-lacZ insert was purified and introduced by pronuclear injection into fertilized oocytes from ICR strain mice. Two independent transgenic lines that showed endothelium-specific β -galactosidase staining in E8.5-E11.5 embryos were selected for study.

Other mouse strains used: Tie2p/e-Cre transgenic mice were a gift of Dr. M. Yanagisawa (University of Texas, Southwestern).²⁵⁹ Wnt1-Cre mice were a gift of Dr. A. McMahon (Harvard University).^{266, 267} Tie2p/e-lacZ transgenic mice were a gift of Dr. T. Sato (University of Texas, Southwestern).²⁶⁰ β -actin-Cre transgenic mice and FLPe-recombinase transgenic mice were from J. Miyazaki (Osaka University Medical School)²⁵⁸ and S.M. Dymecki (Carnegie Institute of Washington),³⁰⁶ respectively. The ROSA26R Cre reporter strain³⁰⁸ and Nestin-Cre transgenic mice²⁶⁸ were from Jackson Laboratories. $G\alpha_{13}^{+/-}$ (exon 1 deletion) mice were a gift of Dr. M. Simon (California Institute of Technology).²⁵⁴

Genotyping of mutant mouse strains:

Genomic DNA from ES cell clones, embryonic tissue, or mouse tail samples was isolated as described.²³⁶ $G\alpha_{13}^{lacZ}$ and $G\alpha_{13}^{lacZ-Neo+}$ alleles were genotyped by NcoI digestion and Southern hybridization with the Exon 1 probe (see Figure 1). $G\alpha_{13}^{lox}$, $G\alpha_{13}^{FRT-Neo+}$, and

1
2
3
4
5
6
7
8
9
10
11
12
13
14
15
16
17
18
19
20
21
22
23
24
25
26
27
28
29
30
31
32
33
34
35
36
37
38
39
40
41
42
43
44
45
46
47
48
49
50
51
52
53
54
55
56
57
58
59
60
61
62
63
64
65
66
67
68
69
70
71
72
73
74
75
76
77
78
79
80
81
82
83
84
85
86
87
88
89
90
91
92
93
94
95
96
97
98
99
100

101
102
103
104
105
106
107
108
109
110
111
112
113
114
115
116
117
118
119
120
121
122
123
124
125
126
127
128
129
130
131
132
133
134
135
136
137
138
139
140
141
142
143
144
145
146
147
148
149
150
151
152
153
154
155
156
157
158
159
160
161
162
163
164
165
166
167
168
169
170
171
172
173
174
175
176
177
178
179
180
181
182
183
184
185
186
187
188
189
190
191
192
193
194
195
196
197
198
199
200

1
2
3
4
5
6
7
8
9
10
11
12
13
14
15
16
17
18
19
20
21
22
23
24
25
26
27
28
29
30
31
32
33
34
35
36
37
38
39
40
41
42
43
44
45
46
47
48
49
50
51
52
53
54
55
56
57
58
59
60
61
62
63
64
65
66
67
68
69
70
71
72
73
74
75
76
77
78
79
80
81
82
83
84
85
86
87
88
89
90
91
92
93
94
95
96
97
98
99
100

101
102
103
104
105
106
107
108
109
110
111
112
113
114
115
116
117
118
119
120
121
122
123
124
125
126
127
128
129
130
131
132
133
134
135
136
137
138
139
140
141
142
143
144
145
146
147
148
149
150
151
152
153
154
155
156
157
158
159
160
161
162
163
164
165
166
167
168
169
170
171
172
173
174
175
176
177
178
179
180
181
182
183
184
185
186
187
188
189
190
191
192
193
194
195
196
197
198
199
200

201
202
203
204
205
206
207
208
209
210
211
212
213
214
215
216
217
218
219
220
221
222
223
224
225
226
227
228
229
230
231
232
233
234
235
236
237
238
239
240
241
242
243
244
245
246
247
248
249
250
251
252
253
254
255
256
257
258
259
260
261
262
263
264
265
266
267
268
269
270
271
272
273
274
275
276
277
278
279
280
281
282
283
284
285
286
287
288
289
290
291
292
293
294
295
296
297
298
299
300

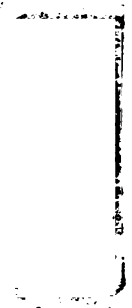
$G\alpha_{13}$ alleles were genotyped by digestion with *EcoRV* and *NcoI* and Southern hybridization with Exon 1 and Exon 4 probes (see Figure 5 and Figure 6A). These probes were PCR-amplified from BAC-125h06 DNA (see Table 6 for PCR primer sequences). The *Tie2p/e-G\alpha_{13}* and *Tie2p/e-lacZ* transgenes were detected by Southern blot analysis using a *lacZ* cDNA probe. The *Tie2p/e-Cre*, *Wnt1-Cre*, *Nestin-Cre*, and β -*actin-Cre* transgenes were detected either by PCR or by Southern blot using the *Cre* sequence amplified by the same primer pair (see Table 6 for the *Cre* PCR primer sequences).

Generation of homozygous $G\alpha_{13}^{lacZ}$ ES cells and chimeric embryos:

The heterozygous $G\alpha_{13}^{lacZ}$ Neo ES cell clone #51 was grown on STO feeder cells in 2.5mg/ml G418 for 10 days to promote gene conversion. 144 ES clones were screened by Southern hybridization to Exon 1 probe, and 29 (20.1%) were homozygous for the $G\alpha_{13}^{lacZ-Neo+}$ allele. To remove the loxP-flanked *neo'* cassette, clone 4A2 was electroporated with a plasmid containing both a puromycin-resistance cassette and a *Cre*-expression cassette (pCAGGS-NLS-CRE-PGKPuro/cg; a gift from Dr. Gail Martin, UCSF), and were grown on puromycin-resistant STO cells. Approximately 50% of the puromycin resistant clones showed excision of the floxed *neo'* cassette from both $G\alpha_{13}^{lacZ-Neo+}$ alleles. Two of these, "4A3" and "4C1", were used for the production of embryonic chimeras. A heterozygous $G\alpha_{13}^{lacZ}$ ES clone, "B3", was generated by electroporation of ES clone #51 with pCAGGS-NLS-CRE-PGKPuro/cg followed by puromycin selection as above. Chimeric embryos were generated by micro-injection of ES cells into Wt E3.5 blastocysts using standard techniques.³⁰²

7-111
7-112
7-113
7-114
7-115
7-116
7-117
7-118
7-119
7-120

7-121
7-122
7-123
7-124
7-125



7-126
7-127
7-128
7-129
7-130
7-131
7-132
7-133
7-134
7-135
7-136
7-137
7-138
7-139
7-140
7-141
7-142
7-143
7-144
7-145
7-146
7-147
7-148
7-149
7-150
7-151
7-152
7-153
7-154
7-155
7-156
7-157
7-158
7-159
7-160
7-161
7-162
7-163
7-164
7-165
7-166
7-167
7-168
7-169
7-170
7-171
7-172
7-173
7-174
7-175
7-176
7-177
7-178
7-179
7-180
7-181
7-182
7-183
7-184
7-185
7-186
7-187
7-188
7-189
7-190
7-191
7-192
7-193
7-194
7-195
7-196
7-197
7-198
7-199
7-200

7-111
7-112
7-113
7-114
7-115
7-116
7-117
7-118
7-119
7-120
7-121
7-122
7-123
7-124
7-125
7-126
7-127
7-128
7-129
7-130
7-131
7-132
7-133
7-134
7-135
7-136
7-137
7-138
7-139
7-140
7-141
7-142
7-143
7-144
7-145
7-146
7-147
7-148
7-149
7-150
7-151
7-152
7-153
7-154
7-155
7-156
7-157
7-158
7-159
7-160
7-161
7-162
7-163
7-164
7-165
7-166
7-167
7-168
7-169
7-170
7-171
7-172
7-173
7-174
7-175
7-176
7-177
7-178
7-179
7-180
7-181
7-182
7-183
7-184
7-185
7-186
7-187
7-188
7-189
7-190
7-191
7-192
7-193
7-194
7-195
7-196
7-197
7-198
7-199
7-200

Embryo dissection, immunostaining and X-gal staining:

Noon of the day a plug was observed was defined as E0.5. After euthanasia, the uterine horns of the pregnant female were removed and embryonic and extraembryonic tissues were dissected free. The yolk sac was photographed and its properties noted, then the embryo was dissected. The presence of a heartbeat and other phenotypic characteristics were recorded before dissecting the next embryo. Whole-mount X-gal staining for β -galactosidase activity was performed as described.²⁶² X-gal-stained yolk sacs and embryos were embedded in paraffin or plastic, sectioned, and counter-stained with nuclear fast red. For analysis of β -galactosidase activity in the adult, tissues were dissected and fixed as above except on ice for 30 to 60 minutes, then rinsed in PBS and equilibrated in 18% sucrose overnight at 4°C before processing for frozen sectioning. Frozen sections were then stained with X-gal at 37°C for 1-2 days. Immunostaining for PECAM1 used rat anti-mouse CD31 (Pharmlngen) and Cy3-conjugated goat anti-rat secondary antibody (Jackson ImmunoResearch) while immunostaining for Endoglin used rat anti-mouse CD105 (Pharmlngen) and an HRP-conjugated goat anti-rat secondary antibody.

Southern and Northern analysis

For Northern analysis of $G\alpha_{13}$ expression in purified adenoviral-infected mouse endothelial cells, total RNA was prepared using Trizol (Invitrogen) according to the manufacturer. 10 μ g of RNA was separated in 1% agarose gels and transferred to a

Hybond-N membrane. Samples were hybridized in Sigma Perfect-Hyb to a DNA probe for $G\alpha_{13}$ exon 4 (corresponding to nucleotides 703-1144 of the $G\alpha_{13}$ coding sequence). **All** Southern and Northern probes were labeled with ^{32}P -dCTP using random primer labeling kits according to manufacturer's instructions (Amersham Rediprime II); hybridization was detected by scanning Southern and Northern membranes using a Storm PhosphorImager (Molecular Dynamics).

Isolation and adenoviral infection of neonatal endothelial cells

Microvascular endothelial cells were isolated from the skin of $G\alpha_{13}^{\text{flax/flax}}$ mice as described.²⁵⁶ Over 95% of cells in these preparations expressed the endothelial markers PECAM1 and ICAM2.²⁵⁶ Immediately after the second round of immunopurification, cells were subjected to 2 successive rounds of infection with ~100 IFU/ml of Cre⁺GFP⁺ or control (GFP⁺ only) adenovirus (a gift from Dr. Hilary Beggs, UCSF) for 24 hr each.^{269, 309} One to 6 days after the second infection, the cells were used for experiments.

Matrigel assay

400-500 μl of Matrigel (Beckton Dickinson, Catalogue #354234) was gelled in 18mm cylindrical holes in an agarose gel for 1-2 hr at 37°C. 1×10^5 endothelial cells that had been infected with the appropriate adenovirus, were plated onto the Matrigel surface and incubated 14-16 hr at 37°C in DME with 20% fetal bovine serum and 50 $\mu\text{g}/\text{mL}$ endothelial cell growth supplement (BTI, Stoughton, MA). Planimetry to calculate Network Area % was calculated using Adobe Photoshop 7.0.

11
12
13
14
15
16
17
18
19
20
21
22
23
24
25
26
27
28
29
30
31
32
33
34
35
36
37
38
39
40
41
42
43
44
45
46
47
48
49
50
51
52
53
54
55
56
57
58
59
60
61
62
63
64
65
66
67
68
69
70
71
72
73
74
75
76
77
78
79
80
81
82
83
84
85
86
87
88
89
90
91
92
93
94
95
96
97
98
99
100

1
2
3
4
5
6
7
8
9
10
11
12
13
14
15
16
17
18
19
20
21
22
23
24
25
26
27
28
29
30
31
32
33
34
35
36
37
38
39
40
41
42
43
44
45
46
47
48
49
50
51
52
53
54
55
56
57
58
59
60
61
62
63
64
65
66
67
68
69
70
71
72
73
74
75
76
77
78
79
80
81
82
83
84
85
86
87
88
89
90
91
92
93
94
95
96
97
98
99
100

1
2
3
4
5
6
7
8
9
10
11
12
13
14
15
16
17
18
19
20
21
22
23
24
25
26
27
28
29
30
31
32
33
34
35
36
37
38
39
40
41
42
43
44
45
46
47
48
49
50
51
52
53
54
55
56
57
58
59
60
61
62
63
64
65
66
67
68
69
70
71
72
73
74
75
76
77
78
79
80
81
82
83
84
85
86
87
88
89
90
91
92
93
94
95
96
97
98
99
100

Table 6. Oligonucleotides used for the generation and genotyping of mice. Each is shown in a 5'-3' direction. Internal restriction endonuclease sites are shown in bold; overhangs are marked with a dotted line and the restriction enzyme that generates the compatible overhang is shown.

F1	AGCAGCGCAAGTCCAAGGAGATCG
R1	GATCTCGTTGCTGTAGATGGTGGG
F2	AATCGGGTTTTTCAGCAACGT CTC
R2	CTGCAGCATGAGCTGCTTCAGG
F3	AAGCTTT ATTGTTTACTGCAGCCAGTGTAGTGAGTGAGTC
	<i>HindIII</i>
R3	TCGCGAGCGAAGCACACGGACAGCACGGAGCG
	<i>NruI</i>
F4	CAATTGA ATAGATAGAGCGGCAAGTCCACCTTCC
	<i>MfeI</i>
R4	GGATCCT CTCTCGGGCATCTACCAGCAC
	<i>BamHI</i>
F5	GCGGCCGC-ACTAGTCGGCTCGAGATTGGTACC-GAATTCGTAC
	<i>NotI</i> <i>SpeI</i> <i>XhoI</i> <i>KpnI</i> <i>EcoRI</i> <i>KpnI</i>
R5	GAATTCGGTACCAATCTCGAGCCGACTAGTGCGGCCGCAGCT
	<i>SacI</i>
F6	TCGACCCGCGGGGAGGTACC-GATATC-CTCGAGCGTAC
	<i>XhoI</i> <i>SacI</i> <i>KpnI</i> <i>EcoRV</i> <i>XhoI</i> <i>KpnI</i>
R6	GCTCGAGGATATCGGTACCTCCCCGCGG
F7	CCTGATATCATAACTTCGTATAGCATACATTATACGAAGTTAT
	<i>EcoRV</i> <i>loxP</i>
R7	AATTATAACTTCGTATAATGTATGCTATACGAAGTTATGATATCAGG
	<i>EcoRI</i>
F8	TGGGCG AATTCGGGAAGCT
	<i>EcoRI</i> <i>SacI</i>
R8	TCCCGAATTCGCCCAAGCT
	<i>SacI</i>
F9	TCGACAATTGAAGGAAAAAAGCGGCCGC
	<i>XhoI</i> <i>MfeI</i> <i>NotI</i>
R9	GATCGCGGCCGCTTTTTTCTTCAATTG
	<i>BamHI</i>
5' Exon 1 Probe	GTTTTTGCCTGAGCAGCGTC
3' Exon 1 Probe	TCCTGTTACATCCACTGAGACCG
5' Exon 4 Probe	TTACAGACAGATATCTGGGTGGCA
3' Exon 4 Probe	GATTACTTACATGCCGTCTCCACA
5' Cre PCR Primer	GATATCTCACGTA CTGACGGT
3' Cre PCR Primer	GCCGGCTAATCGCCATCTTC

REFERENCES

1. Risau, W. Mechanisms of angiogenesis. *Nature* 386, 671-4 (1997).
2. Vajkoczy, P. et al. Multistep nature of microvascular recruitment of ex vivo-expanded embryonic endothelial progenitor cells during tumor angiogenesis. *J Exp Med* 197, 1755-65 (2003).
3. Rumpold, H., Wolf, D., Koeck, R. & Gunsilius, E. Endothelial progenitor cells: a source for therapeutic vasculogenesis? *J Cell Mol Med* 8, 509-18 (2004).
4. Tepper, O. M. et al. Adult vasculogenesis occurs through in situ recruitment, proliferation, and tubulization of circulating bone marrow-derived cells. *Blood* 105, 1068-77 (2005).
5. Djonov, V., Baum, O. & Burri, P. H. Vascular remodeling by intussusceptive angiogenesis. *Cell Tissue Res* 314, 107-17 (2003).
6. Augustin, H. G. Tubes, branches, and pillars: the many ways of forming a new vasculature. *Circ Res* 89, 645-7 (2001).
7. Carmeliet, P. Mechanisms of angiogenesis and arteriogenesis. *Nat Med* 6, 389-95 (2000).
8. Risau, W. & Flamme, I. Vasculogenesis. *Annu Rev Cell Dev Biol* 11, 73-91 (1995).
9. Sabin, F. Preliminary note on the differentiation of angioblasts and the method by which they produce blood-vessels, blood-plasma, and red blood-cells as seen in the living chick. *Anatomical Record* 13, 199-204 (1917).
10. Choi, K., Kennedy, M., Kazarov, A., Papadimitriou, J. C. & Keller, G. A common precursor for hematopoietic and endothelial cells. *Development* 125, 725-32 (1998).
11. Kennedy, M. et al. A common precursor for primitive erythropoiesis and definitive haematopoiesis. *Nature* 386, 488-93 (1997).
12. Fehling, H. J. et al. Tracking mesoderm induction and its specification to the hemangioblast during embryonic stem cell differentiation. *Development* 130, 4217-27 (2003).
13. Drake, C. J. & Fleming, P. A. Vasculogenesis in the day 6.5 to 9.5 mouse embryo. *Blood* 95, 1671-9 (2000).
14. Dooley, K. A., Davidson, A. J. & Zon, L. I. Zebrafish scl functions independently in hematopoietic and endothelial development. *Dev Biol* 277, 522-36 (2005).
15. Giles, P. B. et al. VEGF directs newly gastrulated mesoderm to the endothelial lineage. *Dev Biol* 279, 169-78 (2005).
16. Yamaguchi, T. P., Harpal, K., Henkemeyer, M. & Rossant, J. fgfr-1 is required for embryonic growth and mesodermal patterning during mouse gastrulation. *Genes Dev* 8, 3032-44 (1994).
17. Deng, C. X. et al. Murine FGFR-1 is required for early postimplantation growth and axial organization. *Genes Dev* 8, 3045-57 (1994).

12
13
14
15
16
17
18
19
20
21
22
23
24
25
26
27
28
29
30
31
32
33
34
35
36
37
38
39
40
41
42
43
44
45
46
47
48
49
50
51
52
53
54
55
56
57
58
59
60
61
62
63
64
65
66
67
68
69
70
71
72
73
74
75
76
77
78
79
80
81
82
83
84
85
86
87
88
89
90
91
92
93
94
95
96
97
98
99
100
101
102
103
104
105
106
107
108
109
110
111
112
113
114
115
116
117
118
119
120
121
122
123
124
125
126
127
128
129
130
131
132
133
134
135
136
137
138
139
140
141
142
143
144
145
146
147
148
149
150
151
152
153
154
155
156
157
158
159
160
161
162
163
164
165
166
167
168
169
170
171
172
173
174
175
176
177
178
179
180
181
182
183
184
185
186
187
188
189
190
191
192
193
194
195
196
197
198
199
200
201
202
203
204
205
206
207
208
209
210
211
212
213
214
215
216
217
218
219
220
221
222
223
224
225
226
227
228
229
230
231
232
233
234
235
236
237
238
239
240
241
242
243
244
245
246
247
248
249
250
251
252
253
254
255
256
257
258
259
260
261
262
263
264
265
266
267
268
269
270
271
272
273
274
275
276
277
278
279
280
281
282
283
284
285
286
287
288
289
290
291
292
293
294
295
296
297
298
299
300
301
302
303
304
305
306
307
308
309
310
311
312
313
314
315
316
317
318
319
320
321
322
323
324
325
326
327
328
329
330
331
332
333
334
335
336
337
338
339
340
341
342
343
344
345
346
347
348
349
350
351
352
353
354
355
356
357
358
359
360
361
362
363
364
365
366
367
368
369
370
371
372
373
374
375
376
377
378
379
380
381
382
383
384
385
386
387
388
389
390
391
392
393
394
395
396
397
398
399
400
401
402
403
404
405
406
407
408
409
410
411
412
413
414
415
416
417
418
419
420
421
422
423
424
425
426
427
428
429
430
431
432
433
434
435
436
437
438
439
440
441
442
443
444
445
446
447
448
449
450
451
452
453
454
455
456
457
458
459
460
461
462
463
464
465
466
467
468
469
470
471
472
473
474
475
476
477
478
479
480
481
482
483
484
485
486
487
488
489
490
491
492
493
494
495
496
497
498
499
500
501
502
503
504
505
506
507
508
509
510
511
512
513
514
515
516
517
518
519
520
521
522
523
524
525
526
527
528
529
530
531
532
533
534
535
536
537
538
539
540
541
542
543
544
545
546
547
548
549
550
551
552
553
554
555
556
557
558
559
560
561
562
563
564
565
566
567
568
569
570
571
572
573
574
575
576
577
578
579
580
581
582
583
584
585
586
587
588
589
590
591
592
593
594
595
596
597
598
599
600
601
602
603
604
605
606
607
608
609
610
611
612
613
614
615
616
617
618
619
620
621
622
623
624
625
626
627
628
629
630
631
632
633
634
635
636
637
638
639
640
641
642
643
644
645
646
647
648
649
650
651
652
653
654
655
656
657
658
659
660
661
662
663
664
665
666
667
668
669
670
671
672
673
674
675
676
677
678
679
680
681
682
683
684
685
686
687
688
689
690
691
692
693
694
695
696
697
698
699
700
701
702
703
704
705
706
707
708
709
710
711
712
713
714
715
716
717
718
719
720
721
722
723
724
725
726
727
728
729
730
731
732
733
734
735
736
737
738
739
740
741
742
743
744
745
746
747
748
749
750
751
752
753
754
755
756
757
758
759
760
761
762
763
764
765
766
767
768
769
770
771
772
773
774
775
776
777
778
779
780
781
782
783
784
785
786
787
788
789
790
791
792
793
794
795
796
797
798
799
800
801
802
803
804
805
806
807
808
809
810
811
812
813
814
815
816
817
818
819
820
821
822
823
824
825
826
827
828
829
830
831
832
833
834
835
836
837
838
839
840
841
842
843
844
845
846
847
848
849
850
851
852
853
854
855
856
857
858
859
860
861
862
863
864
865
866
867
868
869
870
871
872
873
874
875
876
877
878
879
880
881
882
883
884
885
886
887
888
889
890
891
892
893
894
895
896
897
898
899
900
901
902
903
904
905
906
907
908
909
910
911
912
913
914
915
916
917
918
919
920
921
922
923
924
925
926
927
928
929
930
931
932
933
934
935
936
937
938
939
940
941
942
943
944
945
946
947
948
949
950
951
952
953
954
955
956
957
958
959
960
961
962
963
964
965
966
967
968
969
970
971
972
973
974
975
976
977
978
979
980
981
982
983
984
985
986
987
988
989
990
991
992
993
994
995
996
997
998
999
1000

18. Poole, T. J., Finkelstein, E. B. & Cox, C. M. The role of FGF and VEGF in angioblast induction and migration during vascular development. *Dev Dyn* 220, 1-17 (2001).
19. Chang, H. et al. Smad5 knockout mice die at mid-gestation due to multiple embryonic and extraembryonic defects. *Development* 126, 1631-42 (1999).
20. Dyer, M. A., Farrington, S. M., Mohn, D., Munday, J. R. & Baron, M. H. Indian hedgehog activates hematopoiesis and vasculogenesis and can respecify prospective neurectodermal cell fate in the mouse embryo. *Development* 128, 1717-30 (2001).
21. Huber, T. L., Kouskoff, V., Fehling, H. J., Palis, J. & Keller, G. Haemangioblast commitment is initiated in the primitive streak of the mouse embryo. *Nature* 432, 625-30 (2004).
22. Patterson, L. J., Gering, M. & Patient, R. Scl is required for dorsal aorta as well as blood formation in zebrafish embryos. *Blood* 105, 3502-11 (2005).
23. Mandal, L., Banerjee, U. & Hartenstein, V. Evidence for a fruit fly hemangioblast and similarities between lymph-gland hematopoiesis in fruit fly and mammal aorta-gonadal-mesonephros mesoderm. *Nat Genet* 36, 1019-23 (2004).
24. Ferguson, J. E., 3rd, Kelley, R. W. & Patterson, C. Mechanisms of Endothelial Differentiation in Embryonic Vasculogenesis. *Arterioscler Thromb Vasc Biol* (2005).
25. Haar, J. L. & Ackerman, G. A. A phase and electron microscopic study of vasculogenesis and erythropoiesis in the yolk sac of the mouse. *Anatomical Record* 170, 199-223 (1971).
26. McGrath, K. E., Koniski, A. D., Malik, J. & Palis, J. Circulation is established in a stepwise pattern in the mammalian embryo. *Blood* 101, 1669-76 (2003).
27. Ji, R. P. et al. Onset of cardiac function during early mouse embryogenesis coincides with entry of primitive erythroblasts into the embryo proper. *Circ Res* 92, 133-5 (2003).
28. Yoshida, H., Sato, M., Kasukawa, R. & Yoshida, T. Properties of vascular permeability factor in human sera for guinea-pig skin. *Experientia* 35, 676-8 (1979).
29. Keck, P. J. et al. Vascular permeability factor, an endothelial cell mitogen related to PDGF. *Science* 246, 1309-12 (1989).
30. Robinson, C. J. & Stringer, S. E. The splice variants of vascular endothelial growth factor (VEGF) and their receptors. *J Cell Sci* 114, 853-65 (2001).
31. de Vries, C. et al. The fms-like tyrosine kinase, a receptor for vascular endothelial growth factor. *Science* 255, 989-91 (1992).
32. Peters, K. G., De Vries, C. & Williams, L. T. Vascular endothelial growth factor receptor expression during embryogenesis and tissue repair suggests a role in endothelial differentiation and blood vessel growth. *Proc Natl Acad Sci U S A* 90, 8915-9 (1993).
33. Quinn, T. P., Peters, K. G., De Vries, C., Ferrara, N. & Williams, L. T. Fetal liver kinase 1 is a receptor for vascular endothelial growth factor and is selectively expressed in vascular endothelium. *Proc Natl Acad Sci U S A* 90, 7533-7 (1993).



34. Kaipainen, A. et al. Expression of the *fms*-like tyrosine kinase 4 gene becomes restricted to lymphatic endothelium during development. *Proc Natl Acad Sci U S A* 92, 3566-70 (1995).
35. Karkkainen, M. J., Makinen, T. & Alitalo, K. Lymphatic endothelium: a new frontier of metastasis research. *Nat Cell Biol* 4, E2-5 (2002).
36. Soker, S., Takashima, S., Miao, H. Q., Neufeld, G. & Klagsbrun, M. Neuropilin-1 is expressed by endothelial and tumor cells as an isoform-specific receptor for vascular endothelial growth factor. *Cell* 92, 735-45 (1998).
37. Kawasaki, T. et al. A requirement for neuropilin-1 in embryonic vessel formation. *Development* 126, 4895-902 (1999).
38. Takashima, S. et al. Targeting of both mouse neuropilin-1 and neuropilin-2 genes severely impairs developmental yolk sac and embryonic angiogenesis. *Proc Natl Acad Sci U S A* 99, 3657-62 (2002).
39. Yuan, L. et al. Abnormal lymphatic vessel development in neuropilin 2 mutant mice. *Development* 129, 4797-806 (2002).
40. Carmeliet, P. et al. Abnormal blood vessel development and lethality in embryos lacking a single VEGF allele. *Nature* 380, 435-9 (1996).
41. Ferrara, N. et al. Heterozygous embryonic lethality induced by targeted inactivation of the VEGF gene. *Nature* 380, 439-42 (1996).
42. Gerber, H. P. et al. VEGF is required for growth and survival in neonatal mice. *Development* 126, 1149-59 (1999).
43. Shalaby, F. et al. Failure of blood-island formation and vasculogenesis in *Flk-1*-deficient mice. *Nature* 376, 62-6 (1995).
44. Sakurai, Y., Ohgimoto, K., Kataoka, Y., Yoshida, N. & Shibuya, M. Essential role of *Flk-1* (VEGF receptor 2) tyrosine residue 1173 in vasculogenesis in mice. *Proc Natl Acad Sci U S A* 102, 1076-81 (2005).
45. Shalaby, F. et al. A requirement for *Flk1* in primitive and definitive hematopoiesis and vasculogenesis. *Cell* 89, 981-90 (1997).
46. Gerhardt, H. et al. VEGF guides angiogenic sprouting utilizing endothelial tip cell filopodia. *J Cell Biol* 161, 1163-77 (2003).
47. Robb, L. et al. Absence of yolk sac hematopoiesis from mice with a targeted disruption of the *scl* gene. *Proc Natl Acad Sci U S A* 92, 7075-9 (1995).
48. Sanchez, M. et al. An *SCL* 3' enhancer targets developing endothelium together with embryonic and adult haematopoietic progenitors. *Development* 126, 3891-904 (1999).
49. Visvader, J. E., Fujiwara, Y. & Orkin, S. H. Unsuspected role for the T-cell leukemia protein *SCL/tal-1* in vascular development. *Genes and Development* 12, 473-9 (1998).
50. Gering, M., Rodaway, A. R., Gottgens, B., Patient, R. K. & Green, A. R. The *SCL* gene specifies haemangioblast development from early mesoderm. *Embo J* 17, 4029-45 (1998).
51. Hall, M. A. et al. The critical regulator of embryonic hematopoiesis, *SCL*, is vital in the adult for megakaryopoiesis, erythropoiesis, and lineage choice in *CFU-S12*. *Proc Natl Acad Sci U S A* 100, 992-7 (2003).

11
12
13
14
15
16
17
18
19
20
21
22
23
24
25
26
27
28
29
30
31
32
33
34
35
36
37
38
39
40
41
42
43
44
45
46
47
48
49
50
51
52
53
54
55
56
57
58
59
60
61
62
63
64
65
66
67
68
69
70
71
72
73
74
75
76
77
78
79
80
81
82
83
84
85
86
87
88
89
90
91
92
93
94
95
96
97
98
99
100
101
102
103
104
105
106
107
108
109
110
111
112
113
114
115
116
117
118
119
120
121
122
123
124
125
126
127
128
129
130
131
132
133
134
135
136
137
138
139
140
141
142
143
144
145
146
147
148
149
150
151
152
153
154
155
156
157
158
159
160
161
162
163
164
165
166
167
168
169
170
171
172
173
174
175
176
177
178
179
180
181
182
183
184
185
186
187
188
189
190
191
192
193
194
195
196
197
198
199
200
201
202
203
204
205
206
207
208
209
210
211
212
213
214
215
216
217
218
219
220
221
222
223
224
225
226
227
228
229
230
231
232
233
234
235
236
237
238
239
240
241
242
243
244
245
246
247
248
249
250
251
252
253
254
255
256
257
258
259
260
261
262
263
264
265
266
267
268
269
270
271
272
273
274
275
276
277
278
279
280
281
282
283
284
285
286
287
288
289
290
291
292
293
294
295
296
297
298
299
300
301
302
303
304
305
306
307
308
309
310
311
312
313
314
315
316
317
318
319
320
321
322
323
324
325
326
327
328
329
330
331
332
333
334
335
336
337
338
339
340
341
342
343
344
345
346
347
348
349
350
351
352
353
354
355
356
357
358
359
360
361
362
363
364
365
366
367
368
369
370
371
372
373
374
375
376
377
378
379
380
381
382
383
384
385
386
387
388
389
390
391
392
393
394
395
396
397
398
399
400
401
402
403
404
405
406
407
408
409
410
411
412
413
414
415
416
417
418
419
420
421
422
423
424
425
426
427
428
429
430
431
432
433
434
435
436
437
438
439
440
441
442
443
444
445
446
447
448
449
450
451
452
453
454
455
456
457
458
459
460
461
462
463
464
465
466
467
468
469
470
471
472
473
474
475
476
477
478
479
480
481
482
483
484
485
486
487
488
489
490
491
492
493
494
495
496
497
498
499
500
501
502
503
504
505
506
507
508
509
510
511
512
513
514
515
516
517
518
519
520
521
522
523
524
525
526
527
528
529
530
531
532
533
534
535
536
537
538
539
540
541
542
543
544
545
546
547
548
549
550
551
552
553
554
555
556
557
558
559
560
561
562
563
564
565
566
567
568
569
570
571
572
573
574
575
576
577
578
579
580
581
582
583
584
585
586
587
588
589
590
591
592
593
594
595
596
597
598
599
600
601
602
603
604
605
606
607
608
609
610
611
612
613
614
615
616
617
618
619
620
621
622
623
624
625
626
627
628
629
630
631
632
633
634
635
636
637
638
639
640
641
642
643
644
645
646
647
648
649
650
651
652
653
654
655
656
657
658
659
660
661
662
663
664
665
666
667
668
669
670
671
672
673
674
675
676
677
678
679
680
681
682
683
684
685
686
687
688
689
690
691
692
693
694
695
696
697
698
699
700
701
702
703
704
705
706
707
708
709
710
711
712
713
714
715
716
717
718
719
720
721
722
723
724
725
726
727
728
729
730
731
732
733
734
735
736
737
738
739
740
741
742
743
744
745
746
747
748
749
750
751
752
753
754
755
756
757
758
759
760
761
762
763
764
765
766
767
768
769
770
771
772
773
774
775
776
777
778
779
780
781
782
783
784
785
786
787
788
789
790
791
792
793
794
795
796
797
798
799
800
801
802
803
804
805
806
807
808
809
810
811
812
813
814
815
816
817
818
819
820
821
822
823
824
825
826
827
828
829
830
831
832
833
834
835
836
837
838
839
840
841
842
843
844
845
846
847
848
849
850
851
852
853
854
855
856
857
858
859
860
861
862
863
864
865
866
867
868
869
870
871
872
873
874
875
876
877
878
879
880
881
882
883
884
885
886
887
888
889
890
891
892
893
894
895
896
897
898
899
900
901
902
903
904
905
906
907
908
909
910
911
912
913
914
915
916
917
918
919
920
921
922
923
924
925
926
927
928
929
930
931
932
933
934
935
936
937
938
939
940
941
942
943
944
945
946
947
948
949
950
951
952
953
954
955
956
957
958
959
960
961
962
963
964
965
966
967
968
969
970
971
972
973
974
975
976
977
978
979
980
981
982
983
984
985
986
987
988
989
990
991
992
993
994
995
996
997
998
999
1000

52. Kappel, A. et al. Role of SCL/Tal-1, GATA, and ets transcription factor binding sites for the regulation of flk-1 expression during murine vascular development. *Blood* 96, 3078-85 (2000).
53. Ciruna, B. G., Schwartz, L., Harpal, K., Yamaguchi, T. P. & Rossant, J. Chimeric analysis of fibroblast growth factor receptor-1 (Fgfr1) function: a role for FGFR1 in morphogenetic movement through the primitive streak. *Development* 124, 2829-41 (1997).
54. Madiari, F. & Hackshaw, K. Expression of the mouse FGF-1 and FGF-1.A mRNAs during embryonic development and in the aging heart. *Res Commun Mol Pathol Pharmacol* 112, 139-44 (2002).
55. Faloon, P. et al. Basic fibroblast growth factor positively regulates hematopoietic development. *Development* 127, 1931-41 (2000).
56. Magnusson, P. et al. Deregulation of Flk-1/vascular endothelial growth factor receptor-2 in fibroblast growth factor receptor-1-deficient vascular stem cell development. *J Cell Sci* 117, 1513-23 (2004).
57. Parker, L. & Stainier, D. Y. Cell-autonomous and non-autonomous requirements for the zebrafish gene cloche in hematopoiesis. *Development* 126, 2643-51 (1999).
58. Liao, E. C. et al. SCL/Tal-1 transcription factor acts downstream of cloche to specify hematopoietic and vascular progenitors in zebrafish. *Genes Dev* 12, 621-6 (1998).
59. Liao, W. et al. The zebrafish gene cloche acts upstream of a flk-1 homologue to regulate endothelial cell differentiation. *Development* 124, 381-9 (1997).
60. Fong, G. H., Rossant, J., Gertsenstein, M. & Breitman, M. L. Role of the Flt-1 receptor tyrosine kinase in regulating the assembly of vascular endothelium. *Nature* 376, 66-70 (1995).
61. Fong, G. H., Zhang, L., Bryce, D. M. & Peng, J. Increased hemangioblast commitment, not vascular disorganization, is the primary defect in flt-1 knock-out mice. *Development* 126, 3015-25 (1999).
62. Hiratsuka, S., Minowa, O., Kuno, J., Noda, T. & Shibuya, M. Flt-1 lacking the tyrosine kinase domain is sufficient for normal development and angiogenesis in mice. *Proc Natl Acad Sci U S A* 95, 9349-54 (1998).
63. Hirashima, M. et al. A chemically defined culture of VEGFR2+ cells derived from embryonic stem cells reveals the role of VEGFR1 in tuning the threshold for VEGF in developing endothelial cells. *Blood* 101, 2261-7 (2003).
64. Matsumura, K. et al. Modulation of VEGFR-2-mediated endothelial-cell activity by VEGF-C/VEGFR-3. *Blood* 101, 1367-74 (2003).
65. Kukk, E. et al. VEGF-C receptor binding and pattern of expression with VEGFR-3 suggests a role in lymphatic vascular development. *Development* 122, 3829-37 (1996).
66. Akuzawa, N., Kurabayashi, M., Ohyama, Y., Arai, M. & Nagai, R. Zinc finger transcription factor Egr-1 activates Flt-1 gene expression in THP-1 cells on induction for macrophage differentiation. *Arterioscler Thromb Vasc Biol* 20, 377-84 (2000).



67. Vidal, F., Aragones, J., Alfranca, A. & de Landazuri, M. O. Up-regulation of vascular endothelial growth factor receptor Flt-1 after endothelial denudation: role of transcription factor Egr-1. *Blood* 95, 3387-95 (2000).
68. Takeda, N. et al. Endothelial PAS domain protein 1 gene promotes angiogenesis through the transactivation of both vascular endothelial growth factor and its receptor, Flt-1. *Circ Res* 95, 146-53 (2004).
69. Barleon, B. et al. Vascular endothelial growth factor up-regulates its receptor fms-like tyrosine kinase 1 (FLT-1) and a soluble variant of FLT-1 in human vascular endothelial cells. *Cancer Res* 57, 5421-5 (1997).
70. Partanen, J. et al. A novel endothelial cell surface receptor tyrosine kinase with extracellular epidermal growth factor homology domains. *Mol Cell Biol* 12, 1698-707 (1992).
71. Dumont, D. J., Yamaguchi, T. P., Conlon, R. A., Rossant, J. & Breitman, M. L. tek, a novel tyrosine kinase gene located on mouse chromosome 4, is expressed in endothelial cells and their presumptive precursors. *Oncogene* 7, 1471-80 (1992).
72. Schnurch, H. & Risau, W. Expression of tie-2, a member of a novel family of receptor tyrosine kinases, in the endothelial cell lineage. *Development* 119, 957-68 (1993).
73. Korhonen, J. et al. Enhanced expression of the tie receptor tyrosine kinase in endothelial cells during neovascularization. *Blood* 80, 2548-55 (1992).
74. Sato, T. N., Qin, Y., Kozak, C. A. & Audus, K. L. Tie-1 and tie-2 define another class of putative receptor tyrosine kinase genes expressed in early embryonic vascular system. *Proc Natl Acad Sci U S A* 90, 9355-8 (1993).
75. Partanen, J. et al. Cell autonomous functions of the receptor tyrosine kinase TIE in a late phase of angiogenic capillary growth and endothelial cell survival during murine development. *Development* 122, 3013-21 (1996).
76. Puri, M. C., Rossant, J., Alitalo, K., Bernstein, A. & Partanen, J. The receptor tyrosine kinase TIE is required for integrity and survival of vascular endothelial cells. *Embo J* 14, 5884-91 (1995).
77. Dumont, D. J. et al. Dominant-negative and targeted null mutations in the endothelial receptor tyrosine kinase, tek, reveal a critical role in vasculogenesis of the embryo. *Genes Dev* 8, 1897-909 (1994).
78. Sato, T. N. et al. Distinct roles of the receptor tyrosine kinases Tie-1 and Tie-2 in blood vessel formation. *Nature* 376, 70-4 (1995).
79. Jones, N. et al. Rescue of the early vascular defects in Tek/Tie2 null mice reveals an essential survival function. *EMBO Rep* 2, 438-45 (2001).
80. Puri, M. C., Partanen, J., Rossant, J. & Bernstein, A. Interaction of the TEK and TIE receptor tyrosine kinases during cardiovascular development. *Development* 126, 4569-80 (1999).
81. Patan, S. TIE1 and TIE2 receptor tyrosine kinases inversely regulate embryonic angiogenesis by the mechanism of intussusceptive microvascular growth. *Microvasc Res* 56, 1-21 (1998).
82. Tachibana, K., Jones, N., Dumont, D. J., Puri, M. C. & Bernstein, A. Selective role of a distinct tyrosine residue on Tie2 in heart development and early hematopoiesis. *Mol Cell Biol* 25, 4693-702 (2005).

1942
1943
1944
1945
1946
1947
1948
1949
1950
1951
1952
1953
1954
1955
1956
1957
1958
1959
1960
1961
1962
1963
1964
1965
1966
1967
1968
1969
1970
1971
1972
1973
1974
1975
1976
1977
1978
1979
1980
1981
1982
1983
1984
1985
1986
1987
1988
1989
1990
1991
1992
1993
1994
1995
1996
1997
1998
1999
2000
2001
2002
2003
2004
2005
2006
2007
2008
2009
2010
2011
2012
2013
2014
2015
2016
2017
2018
2019
2020
2021
2022
2023
2024
2025

1942
1943
1944
1945
1946
1947
1948
1949
1950
1951
1952
1953
1954
1955
1956
1957
1958
1959
1960
1961
1962
1963
1964
1965
1966
1967
1968
1969
1970
1971
1972
1973
1974
1975
1976
1977
1978
1979
1980
1981
1982
1983
1984
1985
1986
1987
1988
1989
1990
1991
1992
1993
1994
1995
1996
1997
1998
1999
2000
2001
2002
2003
2004
2005
2006
2007
2008
2009
2010
2011
2012
2013
2014
2015
2016
2017
2018
2019
2020
2021
2022
2023
2024
2025

83. Sundberg, C., Kowanetz, M., Brown, L. F., Detmar, M. & Dvorak, H. F. Stable expression of angiopoietin-1 and other markers by cultured pericytes: phenotypic similarities to a subpopulation of cells in maturing vessels during later stages of angiogenesis *in vivo*. *Lab Invest* 82, 387-401 (2002).
84. Davis, S. et al. Isolation of angiopoietin-1, a ligand for the TIE2 receptor, by secretion-trap expression cloning. *Cell* 87, 1161-9 (1996).
85. Suri, C. et al. Requisite role of angiopoietin-1, a ligand for the TIE2 receptor, during embryonic angiogenesis [see comments]. *Cell* 87, 1171-80 (1996).
86. Wong, A. L. et al. Tie2 expression and phosphorylation in angiogenic and quiescent adult tissues. *Circ Res* 81, 567-74 (1997).
87. Thurston, G. et al. Leakage-resistant blood vessels in mice transgenically overexpressing angiopoietin-1. *Science* 286, 2511-4 (1999).
88. Vikkula, M. et al. Vascular dysmorphogenesis caused by an activating mutation in the receptor tyrosine kinase TIE2. *Cell* 87, 1181-90 (1996).
89. Teichert-Kuliszewska, K. et al. Biological action of angiopoietin-2 in a fibrin matrix model of angiogenesis is associated with activation of Tie2. *Cardiovasc Res* 49, 659-70 (2001).
90. Maisonpierre, P. C. et al. Angiopoietin-2, a natural antagonist for Tie2 that disrupts *in vivo* angiogenesis. *Science* 277, 55-60 (1997).
91. Gale, N. W. et al. Angiopoietin-2 is required for postnatal angiogenesis and lymphatic patterning, and only the latter role is rescued by Angiopoietin-1. *Dev Cell* 3, 411-23 (2002).
92. Gerhardt, H., Wolburg, H. & Redies, C. N-cadherin mediates pericytic-endothelial interaction during brain angiogenesis in the chicken. *Dev Dyn* 218, 472-9 (2000).
93. Armulik, A., Abramsson, A. & Betsholtz, C. Endothelial/pericyte interactions. *Circ Res* 97, 512-23 (2005).
94. Hungerford, J. E. & Little, C. D. Developmental biology of the vascular smooth muscle cell: building a multilayered vessel wall. *J Vasc Res* 36, 2-27 (1999).
95. Etchevers, H. C., Vincent, C., Le Douarin, N. M. & Couly, G. F. The cephalic neural crest provides pericytes and smooth muscle cells to all blood vessels of the face and forebrain. *Development* 128, 1059-68 (2001).
96. Vrancken Peeters, M. P., Gittenberger-de Groot, A. C., Mentink, M. M. & Poelmann, R. E. Smooth muscle cells and fibroblasts of the coronary arteries derive from epithelial-mesenchymal transformation of the epicardium. *Anat Embryol (Berl)* 199, 367-78 (1999).
97. DeRuiter, M. C. et al. Embryonic endothelial cells transdifferentiate into mesenchymal cells expressing smooth muscle actins *in vivo* and *in vitro*. *Circ Res* 80, 444-51 (1997).
98. Shull, M. M. et al. Targeted disruption of the mouse transforming growth factor-beta 1 gene results in multifocal inflammatory disease. *Nature* 359, 693-9 (1992).
99. Kulkarni, A. B. et al. Transforming growth factor beta 1 null mutation in mice causes excessive inflammatory response and early death. *Proc Natl Acad Sci U S A* 90, 770-4 (1993).

100. Dickson, M. C. et al. Defective haematopoiesis and vasculogenesis in transforming growth factor-beta 1 knock out mice. *Development* 121, 1845-54 (1995).
101. Agah, R. et al. Cardiovascular overexpression of transforming growth factor-beta(1) causes abnormal yolk sac vasculogenesis and early embryonic death. *Circ Res* 86, 1024-30 (2000).
102. Kaartinen, V. et al. Abnormal lung development and cleft palate in mice lacking TGF-beta 3 indicates defects of epithelial-mesenchymal interaction. *Nat Genet* 11, 415-21 (1995).
103. Proetzel, G. et al. Transforming growth factor-beta 3 is required for secondary palate fusion. *Nat Genet* 11, 409-14 (1995).
104. Sanford, L. P. et al. TGFbeta2 knockout mice have multiple developmental defects that are non-overlapping with other TGFbeta knockout phenotypes. *Development* 124, 2659-70 (1997).
105. Oshima, M., Oshima, H. & Taketo, M. M. TGF-beta receptor type II deficiency results in defects of yolk sac hematopoiesis and vasculogenesis. *Dev Biol* 179, 297-302 (1996).
106. Goumans, M. J. et al. Transforming growth factor-beta signalling in extraembryonic mesoderm is required for yolk sac vasculogenesis in mice. *Development* 126, 3473-83 (1999).
107. Larsson, J. et al. Abnormal angiogenesis but intact hematopoietic potential in TGF-beta type I receptor-deficient mice. *Embo J* 20, 1663-73 (2001).
108. Oh, S. P. et al. Activin receptor-like kinase 1 modulates transforming growth factor-beta 1 signaling in the regulation of angiogenesis. *Proc Natl Acad Sci U S A* 97, 2626-31 (2000).
109. Urness, L. D., Sorensen, L. K. & Li, D. Y. Arteriovenous malformations in mice lacking activin receptor-like kinase-1. *Nat Genet* 26, 328-31 (2000).
110. Roman, B. L. et al. Disruption of *acvr11* increases endothelial cell number in zebrafish cranial vessels. *Development* 129, 3009-19 (2002).
111. Johnson, D. W. et al. Mutations in the activin receptor-like kinase 1 gene in hereditary haemorrhagic telangiectasia type 2. *Nat Genet* 13, 189-95 (1996).
112. Lechleider, R. J. et al. Targeted mutagenesis of *Smad1* reveals an essential role in chorioallantoic fusion. *Dev Biol* 240, 157-67 (2001).
113. Barbara, N. P., Wrana, J. L. & Letarte, M. Endoglin is an accessory protein that interacts with the signaling receptor complex of multiple members of the transforming growth factor-beta superfamily. *J Biol Chem* 274, 584-94 (1999).
114. Derynck, R. & Zhang, Y. E. Smad-dependent and Smad-independent pathways in TGF-beta family signalling. *Nature* 425, 577-84 (2003).
115. McAllister, K. A. et al. Endoglin, a TGF-beta binding protein of endothelial cells, is the gene for hereditary haemorrhagic telangiectasia type 1. *Nat Genet* 8, 345-51 (1994).
116. Li, D. Y. et al. Defective angiogenesis in mice lacking endoglin. *Science* 284, 1534-7 (1999).
117. Bourdeau, A., Dumont, D. J. & Letarte, M. A murine model of hereditary hemorrhagic telangiectasia. *J Clin Invest* 104, 1343-51 (1999).

118. Arthur, H. M. et al. Endoglin, an ancillary TGFbeta receptor, is required for extraembryonic angiogenesis and plays a key role in heart development. *Dev Biol* 217, 42-53 (2000).
119. Sorensen, L. K., Brooke, B. S., Li, D. Y. & Urness, L. D. Loss of distinct arterial and venous boundaries in mice lacking endoglin, a vascular-specific TGFbeta coreceptor. *Dev Biol* 261, 235-50 (2003).
120. Goumans, M. J. et al. Balancing the activation state of the endothelium via two distinct TGF-beta type I receptors. *Embo J* 21, 1743-53 (2002).
121. Pece-Barbara, N. et al. Endoglin null endothelial cells proliferate faster and are more responsive to transforming growth factor beta1 with higher affinity receptors and an activated Alk1 pathway. *J Biol Chem* 280, 27800-8 (2005).
122. Lebrin, F. et al. Endoglin promotes endothelial cell proliferation and TGF-beta/ALK1 signal transduction. *Embo J* 23, 4018-28 (2004).
123. Carvalho, R. L. et al. Defective paracrine signalling by TGFbeta in yolk sac vasculature of endoglin mutant mice: a paradigm for hereditary haemorrhagic telangiectasia. *Development* 131, 6237-47 (2004).
124. Wurdak, H. et al. Inactivation of TGFbeta signaling in neural crest stem cells leads to multiple defects reminiscent of DiGeorge syndrome. *Genes Dev* 19, 530-5 (2005).
125. Antonelli-Orlidge, A., Saunders, K. B., Smith, S. R. & D'Amore, P. A. An activated form of transforming growth factor beta is produced by cocultures of endothelial cells and pericytes. *Proc Natl Acad Sci U S A* 86, 4544-8 (1989).
126. Sato, Y., Tsuboi, R., Lyons, R., Moses, H. & Rifkin, D. B. Characterization of the activation of latent TGF-beta by co-cultures of endothelial cells and pericytes or smooth muscle cells: a self-regulating system. *J Cell Biol* 111, 757-63 (1990).
127. Gilula, N. B., Reeves, O. R. & Steinbach, A. Metabolic coupling, ionic coupling and cell contacts. *Nature* 235, 262-5 (1972).
128. Revel, J. P. & Karnovsky, M. J. Hexagonal array of subunits in intercellular junctions of the mouse heart and liver. *J Cell Biol* 33, C7-C12 (1967).
129. Walker, D. L., Vacha, S. J., Kirby, M. L. & Lo, C. W. Connexin43 deficiency causes dysregulation of coronary vasculogenesis. *Dev Biol* 284, 479-98 (2005).
130. Hirschi, K. K., Burt, J. M., Hirschi, K. D. & Dai, C. Gap junction communication mediates transforming growth factor-beta activation and endothelial-induced mural cell differentiation. *Circ Res* 93, 429-37 (2003).
131. Krtiger, O. et al. Defective vascular development in connexin 45-deficient mice. *Development* 127, 4179-93 (2000).
132. Soriano, P. Abnormal kidney development and hematological disorders in PDGF beta-receptor mutant mice. *Genes Dev* 8, 1888-96 (1994).
133. Leveen, P. et al. Mice deficient for PDGF B show renal, cardiovascular, and hematological abnormalities. *Genes Dev* 8, 1875-87 (1994).
134. Lindahl, P., Johansson, B. R., Levéen, P. & Betsholtz, C. Pericyte loss and microaneurysm formation in PDGF-B-deficient mice. *Science* 277, 242-5 (1997).
135. Hellström, M., Kaln, M., Lindahl, P., Abramsson, A. & Betsholtz, C. Role of PDGF-B and PDGFR-beta in recruitment of vascular smooth muscle cells and pericytes during embryonic blood vessel formation in the mouse. *Development* 126, 3047-55 (1999).

11
12
13
14
15
16
17
18
19
20
21
22
23
24
25
26
27
28
29
30
31
32
33
34
35
36
37
38
39
40
41
42
43
44
45
46
47
48
49
50
51
52
53
54
55
56
57
58
59
60
61
62
63
64
65
66
67
68
69
70
71
72
73
74
75
76
77
78
79
80
81
82
83
84
85
86
87
88
89
90
91
92
93
94
95
96
97
98
99
100
101
102
103
104
105
106
107
108
109
110
111
112
113
114
115
116
117
118
119
120
121
122
123
124
125
126
127
128
129
130
131
132
133
134
135
136
137
138
139
140
141
142
143
144
145
146
147
148
149
150
151
152
153
154
155
156
157
158
159
160
161
162
163
164
165
166
167
168
169
170
171
172
173
174
175
176
177
178
179
180
181
182
183
184
185
186
187
188
189
190
191
192
193
194
195
196
197
198
199
200
201
202
203
204
205
206
207
208
209
210
211
212
213
214
215
216
217
218
219
220
221
222
223
224
225
226
227
228
229
230
231
232
233
234
235
236
237
238
239
240
241
242
243
244
245
246
247
248
249
250
251
252
253
254
255
256
257
258
259
260
261
262
263
264
265
266
267
268
269
270
271
272
273
274
275
276
277
278
279
280
281
282
283
284
285
286
287
288
289
290
291
292
293
294
295
296
297
298
299
300
301
302
303
304
305
306
307
308
309
310
311
312
313
314
315
316
317
318
319
320
321
322
323
324
325
326
327
328
329
330
331
332
333
334
335
336
337
338
339
340
341
342
343
344
345
346
347
348
349
350
351
352
353
354
355
356
357
358
359
360
361
362
363
364
365
366
367
368
369
370
371
372
373
374
375
376
377
378
379
380
381
382
383
384
385
386
387
388
389
390
391
392
393
394
395
396
397
398
399
400
401
402
403
404
405
406
407
408
409
410
411
412
413
414
415
416
417
418
419
420
421
422
423
424
425
426
427
428
429
430
431
432
433
434
435
436
437
438
439
440
441
442
443
444
445
446
447
448
449
450
451
452
453
454
455
456
457
458
459
460
461
462
463
464
465
466
467
468
469
470
471
472
473
474
475
476
477
478
479
480
481
482
483
484
485
486
487
488
489
490
491
492
493
494
495
496
497
498
499
500
501
502
503
504
505
506
507
508
509
510
511
512
513
514
515
516
517
518
519
520
521
522
523
524
525
526
527
528
529
530
531
532
533
534
535
536
537
538
539
540
541
542
543
544
545
546
547
548
549
550
551
552
553
554
555
556
557
558
559
560
561
562
563
564
565
566
567
568
569
570
571
572
573
574
575
576
577
578
579
580
581
582
583
584
585
586
587
588
589
590
591
592
593
594
595
596
597
598
599
600
601
602
603
604
605
606
607
608
609
610
611
612
613
614
615
616
617
618
619
620
621
622
623
624
625
626
627
628
629
630
631
632
633
634
635
636
637
638
639
640
641
642
643
644
645
646
647
648
649
650
651
652
653
654
655
656
657
658
659
660
661
662
663
664
665
666
667
668
669
670
671
672
673
674
675
676
677
678
679
680
681
682
683
684
685
686
687
688
689
690
691
692
693
694
695
696
697
698
699
700
701
702
703
704
705
706
707
708
709
710
711
712
713
714
715
716
717
718
719
720
721
722
723
724
725
726
727
728
729
730
731
732
733
734
735
736
737
738
739
740
741
742
743
744
745
746
747
748
749
750
751
752
753
754
755
756
757
758
759
760
761
762
763
764
765
766
767
768
769
770
771
772
773
774
775
776
777
778
779
780
781
782
783
784
785
786
787
788
789
790
791
792
793
794
795
796
797
798
799
800
801
802
803
804
805
806
807
808
809
810
811
812
813
814
815
816
817
818
819
820
821
822
823
824
825
826
827
828
829
830
831
832
833
834
835
836
837
838
839
840
841
842
843
844
845
846
847
848
849
850
851
852
853
854
855
856
857
858
859
860
861
862
863
864
865
866
867
868
869
870
871
872
873
874
875
876
877
878
879
880
881
882
883
884
885
886
887
888
889
890
891
892
893
894
895
896
897
898
899
900
901
902
903
904
905
906
907
908
909
910
911
912
913
914
915
916
917
918
919
920
921
922
923
924
925
926
927
928
929
930
931
932
933
934
935
936
937
938
939
940
941
942
943
944
945
946
947
948
949
950
951
952
953
954
955
956
957
958
959
960
961
962
963
964
965
966
967
968
969
970
971
972
973
974
975
976
977
978
979
980
981
982
983
984
985
986
987
988
989
990
991
992
993
994
995
996
997
998
999
1000

136. Crosby, J. R., Seifert, R. A., Soriano, P. & Bowen-Pope, D. F. Chimaeric analysis reveals role of Pdgf receptors in all muscle lineages. *Nature Genetics* 18, 385-8 (1998).
137. Bjarnegard, M. et al. Endothelium-specific ablation of PDGFB leads to pericyte loss and glomerular, cardiac and placental abnormalities. *Development* 131, 1847-57 (2004).
138. Enge, M. et al. Endothelium-specific platelet-derived growth factor-B ablation mimics diabetic retinopathy. *Embo J* 21, 4307-16 (2002).
139. Hammes, H. P. et al. Pericytes and the pathogenesis of diabetic retinopathy. *Diabetes* 51, 3107-12 (2002).
140. Lindblom, P. et al. Endothelial PDGF-B retention is required for proper investment of pericytes in the microvessel wall. *Genes Dev* 17, 1835-40 (2003).
141. Abramsson, A., Lindblom, P. & Betsholtz, C. Endothelial and nonendothelial sources of PDGF-B regulate pericyte recruitment and influence vascular pattern formation in tumors. *J Clin Invest* 112, 1142-51 (2003).
142. Park, J. E., Keller, G. A. & Ferrara, N. The vascular endothelial growth factor (VEGF) isoforms: differential deposition into the subepithelial extracellular matrix and bioactivity of extracellular matrix-bound VEGF. *Mol Biol Cell* 4, 1317-26 (1993).
143. Carmeliet, P. et al. Impaired myocardial angiogenesis and ischemic cardiomyopathy in mice lacking the vascular endothelial growth factor isoforms VEGF164 and VEGF188. *Nat Med* 5, 495-502 (1999).
144. Lehti, K. et al. An MT1-MMP-PDGF receptor-beta axis regulates mural cell investment of the microvasculature. *Genes Dev* 19, 979-91 (2005).
145. Mu, D. et al. The integrin alpha(v)beta8 mediates epithelial homeostasis through MT1-MMP-dependent activation of TGF-beta1. *J Cell Biol* 157, 493-507 (2002).
146. Zhu, J. et al. beta8 integrins are required for vascular morphogenesis in mouse embryos. *Development* 129, 2891-903 (2002).
147. Heuchel, R. et al. Platelet-derived growth factor beta receptor regulates interstitial fluid homeostasis through phosphatidylinositol-3' kinase signaling. *Proc Natl Acad Sci U S A* 96, 11410-5 (1999).
148. Tallquist, M. D. et al. Retention of PDGFR-beta function in mice in the absence of phosphatidylinositol 3'-kinase and phospholipase Cgamma signaling pathways. *Genes Dev* 14, 3179-90 (2000).
149. Tallquist, M. D., French, W. J. & Soriano, P. Additive effects of PDGF receptor beta signaling pathways in vascular smooth muscle cell development. *PLoS Biol* 1, E52 (2003).
150. Henkemeyer, M. et al. Vascular system defects and neuronal apoptosis in mice lacking ras GTPase-activating protein. *Nature* 377, 695-701 (1995).
151. Eerola, I. et al. Capillary malformation-arteriovenous malformation, a new clinical and genetic disorder caused by RASA1 mutations. *Am J Hum Genet* 73, 1240-9 (2003).
152. Hla, T. & Maciag, T. An abundant transcript induced in differentiating human endothelial cells encodes a polypeptide with structural similarities to G-protein-coupled receptors. *J Biol Chem* 265, 9308-13 (1990).

10
11
12
13
14
15
16
17
18
19
20
21
22
23
24
25
26
27
28
29
30
31
32
33
34
35
36
37
38
39
40
41
42
43
44
45
46
47
48
49
50
51
52
53
54
55
56
57
58
59
60
61
62
63
64
65
66
67
68
69
70
71
72
73
74
75
76
77
78
79
80
81
82
83
84
85
86
87
88
89
90
91
92
93
94
95
96
97
98
99
100



101
102
103
104
105
106
107
108
109
110
111
112
113
114
115
116
117
118
119
120
121
122
123
124
125
126
127
128
129
130
131
132
133
134
135
136
137
138
139
140
141
142
143
144
145
146
147
148
149
150
151
152
153
154
155
156
157
158
159
160
161
162
163
164
165
166
167
168
169
170
171
172
173
174
175
176
177
178
179
180
181
182
183
184
185
186
187
188
189
190
191
192
193
194
195
196
197
198
199
200

201
202
203
204
205
206
207
208
209
210
211
212
213
214
215
216
217
218
219
220
221
222
223
224
225
226
227
228
229
230
231
232
233
234
235
236
237
238
239
240
241
242
243
244
245
246
247
248
249
250
251
252
253
254
255
256
257
258
259
260
261
262
263
264
265
266
267
268
269
270
271
272
273
274
275
276
277
278
279
280
281
282
283
284
285
286
287
288
289
290
291
292
293
294
295
296
297
298
299
300

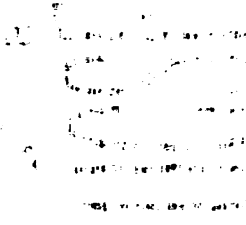
153. An, S. et al. Identification of cDNAs encoding two G protein-coupled receptors for lysosphingolipids. *FEBS Lett* 417, 279-82 (1997).
154. Lee, M. J. et al. Sphingosine-1-phosphate as a ligand for the G protein-coupled receptor EDG-1. *Science* 279, 1552-5 (1998).
155. Toman, R. E. & Spiegel, S. Lysophospholipid receptors in the nervous system. *Neurochem Res* 27, 619-27 (2002).
156. Idzko, M. et al. Sphingosine 1-phosphate induces chemotaxis of immature and modulates cytokine-release in mature human dendritic cells for emergence of Th2 immune responses. *Faseb J* 16, 625-7 (2002).
157. Im, D. S. et al. Molecular cloning and characterization of a lysophosphatidic acid receptor, Edg-7, expressed in prostate. *Mol Pharmacol* 57, 753-9 (2000).
158. Liu, Y. et al. Edg-1, the G protein-coupled receptor for sphingosine-1-phosphate, is essential for vascular maturation. *J Clin Invest* 106, 951-61 (2000).
159. Allende, M. L., Yamashita, T. & Proia, R. L. G-protein-coupled receptor S1P1 acts within endothelial cells to regulate vascular maturation. *Blood* 102, 3665-7 (2003).
160. Paik, J. H. et al. Sphingosine 1-phosphate receptor regulation of N-cadherin mediates vascular stabilization. *Genes Dev* 18, 2392-403 (2004).
161. Carmeliet, P. et al. Targeted deficiency or cytosolic truncation of the VE-cadherin gene in mice impairs VEGF-mediated endothelial survival and angiogenesis. *Cell* 98, 147-57 (1999).
162. Navarro, P., Ruco, L. & Dejana, E. Differential localization of VE- and N-cadherins in human endothelial cells: VE-cadherin competes with N-cadherin for junctional localization. *J Cell Biol* 140, 1475-84 (1998).
163. Crosby, C. V. et al. VE-cadherin is not required for the formation of nascent blood vessels but acts to prevent their disassembly. *Blood* 105, 2771-6 (2005).
164. Cattelino, A. et al. The conditional inactivation of the beta-catenin gene in endothelial cells causes a defective vascular pattern and increased vascular fragility. *J Cell Biol* 162, 1111-22 (2003).
165. Radice, G. L. et al. Developmental defects in mouse embryos lacking N-cadherin. *Dev Biol* 181, 64-78 (1997).
166. Kupperman, E., An, S., Osborne, N., Waldron, S. & Stainier, D. Y. A sphingosine-1-phosphate receptor regulates cell migration during vertebrate heart development. *Nature* 406, 192-5 (2000).
167. Ishii, I. et al. Marked perinatal lethality and cellular signaling deficits in mice null for the two sphingosine 1-phosphate (S1P) receptors, S1P(2)/LP(B2)/EDG-5 and S1P(3)/LP(B3)/EDG-3. *J Biol Chem* 277, 25152-9 (2002).
168. MacLennan, A. J. et al. An essential role for the H218/AGR16/Edg-5/LP(B2) sphingosine 1-phosphate receptor in neuronal excitability. *Eur J Neurosci* 14, 203-9 (2001).
169. Kono, M. et al. The sphingosine-1-phosphate receptors S1P1, S1P2, and S1P3 function coordinately during embryonic angiogenesis. *J Biol Chem* 279, 29367-73 (2004).
170. Ancellin, N. & Hla, T. Differential pharmacological properties and signal transduction of the sphingosine 1-phosphate receptors EDG-1, EDG-3, and EDG-5. *J Biol Chem* 274, 18997-9002 (1999).



171. Chae, S. S., Paik, J. H., Allende, M. L., Proia, R. L. & Hla, T. Regulation of limb development by the sphingosine 1-phosphate receptor S1p1/EDG-1 occurs via the hypoxia/VEGF axis. *Dev Biol* 268, 441-7 (2004).
172. Lee, M. J. et al. Vascular endothelial cell adherens junction assembly and morphogenesis induced by sphingosine-1-phosphate. *Cell* 99, 301-12 (1999).
173. Esser, S., Lampugnani, M. G., Corada, M., Dejana, E. & Risau, W. Vascular endothelial growth factor induces VE-cadherin tyrosine phosphorylation in endothelial cells. *J Cell Sci* 111 (Pt 13), 1853-65 (1998).
174. Lee, M. J. et al. Akt-mediated phosphorylation of the G protein-coupled receptor EDG-1 is required for endothelial cell chemotaxis. *Mol Cell* 8, 693-704 (2001).
175. Usui, S. et al. Blood lipid mediator sphingosine 1-phosphate potently stimulates platelet-derived growth factor-A and -B chain expression through S1P1-Gi-Ras-MAPK-dependent induction of Kruppel-like factor 5. *J Biol Chem* 279, 12300-11 (2004).
176. Ryu, Y. et al. Sphingosine-1-phosphate, a platelet-derived lysophospholipid mediator, negatively regulates cellular Rac activity and cell migration in vascular smooth muscle cells. *Circ Res* 90, 325-32 (2002).
177. Olivera, A. & Spiegel, S. Sphingosine-1-phosphate as second messenger in cell proliferation induced by PDGF and FCS mitogens. *Nature* 365, 557-60 (1993).
178. Isaac, D. D. & Andrew, D. J. Tubulogenesis in *Drosophila*: a requirement for the trachealess gene product. *Genes Dev* 10, 103-17 (1996).
179. Jarecki, J., Johnson, E. & Krasnow, M. A. Oxygen regulation of airway branching in *Drosophila* is mediated by branchless FGF. *Cell* 99, 211-20 (1999).
180. Ryan, H. E., Lo, J. & Johnson, R. S. HIF-1 alpha is required for solid tumor formation and embryonic vascularization. *Embo J* 17, 3005-15 (1998).
181. Iyer, N. V. et al. Cellular and developmental control of O₂ homeostasis by hypoxia-inducible factor 1 alpha. *Genes Dev* 12, 149-62 (1998).
182. Kozak, K. R., Abbott, B. & Hankinson, O. ARNT-deficient mice and placental differentiation. *Dev Biol* 191, 297-305 (1997).
183. Maltepe, E., Schmidt, J. V., Baunoch, D., Bradfield, C. A. & Simon, M. C. Abnormal angiogenesis and responses to glucose and oxygen deprivation in mice lacking the protein ARNT. *Nature* 386, 403-7 (1997).
184. Shweiki, D., Itin, A., Soffer, D. & Keshet, E. Vascular endothelial growth factor induced by hypoxia may mediate hypoxia-initiated angiogenesis. *Nature* 359, 843-5 (1992).
185. Tsuzuki, Y. et al. Vascular endothelial growth factor (VEGF) modulation by targeting hypoxia-inducible factor-1alpha--> hypoxia response element--> VEGF cascade differentially regulates vascular response and growth rate in tumors. *Cancer Res* 60, 6248-52 (2000).
186. Oosthuysen, B. et al. Deletion of the hypoxia-response element in the vascular endothelial growth factor promoter causes motor neuron degeneration. *Nat Genet* 28, 131-8 (2001).
187. Ema, M. et al. A novel bHLH-PAS factor with close sequence similarity to hypoxia-inducible factor 1alpha regulates the VEGF expression and is potentially involved in lung and vascular development. *Proc Natl Acad Sci U S A* 94, 4273-8 (1997).

Handwritten notes on the left margin, including numbers and symbols such as 1, 2, 3, 4, 5, 6, 7, 8, 9, 10, 11, 12, 13, 14, 15, 16, 17, 18, 19, 20, 21, 22, 23, 24, 25, 26, 27, 28, 29, 30, 31, 32, 33, 34, 35, 36, 37, 38, 39, 40, 41, 42, 43, 44, 45, 46, 47, 48, 49, 50, 51, 52, 53, 54, 55, 56, 57, 58, 59, 60, 61, 62, 63, 64, 65, 66, 67, 68, 69, 70, 71, 72, 73, 74, 75, 76, 77, 78, 79, 80, 81, 82, 83, 84, 85, 86, 87, 88, 89, 90, 91, 92, 93, 94, 95, 96, 97, 98, 99, 100.

Printed text in the left margin, appearing as a list or index of items, possibly related to the handwritten notes.



188. Kappel, A. et al. Identification of vascular endothelial growth factor (VEGF) receptor-2 (Flk-1) promoter/enhancer sequences sufficient for angioblast and endothelial cell-specific transcription in transgenic mice. *Blood* 93, 4284-92 (1999).
189. Elvert, G. et al. Cooperative interaction of hypoxia-inducible factor-2alpha (HIF-2alpha) and Ets-1 in the transcriptional activation of vascular endothelial growth factor receptor-2 (Flk-1). *J Biol Chem* 278, 7520-30 (2003).
190. Eliceiri, B. P. & Cheresh, D. A. The role of alphav integrins during angiogenesis: insights into potential mechanisms of action and clinical development. *J Clin Invest* 103, 1227-30 (1999).
191. Schneller, M., Vuori, K. & Ruoslahti, E. Alphavbeta3 integrin associates with activated insulin and PDGFbeta receptors and potentiates the biological activity of PDGF. *Embo J* 16, 5600-7 (1997).
192. Cowden Dahl, K. D., Robertson, S. E., Weaver, V. M. & Simon, M. C. Hypoxia-inducible factor regulates alphavbeta3 integrin cell surface expression. *Mol Biol Cell* 16, 1901-12 (2005).
193. Soldi, R. et al. Role of alphavbeta3 integrin in the activation of vascular endothelial growth factor receptor-2. *Embo J* 18, 882-92 (1999).
194. Byzova, T. V. et al. A mechanism for modulation of cellular responses to VEGF: activation of the integrins. *Molecular Cell* 6, 851-60 (2000).
195. Bader, B. L., Rayburn, H., Crowley, D. & Hynes, R. O. Extensive vasculogenesis, angiogenesis, and organogenesis precede lethality in mice lacking all alpha v integrins. *Cell* 95, 507-19 (1998).
196. McCarty, J. H. et al. Selective ablation of alphav integrins in the central nervous system leads to cerebral hemorrhage, seizures, axonal degeneration and premature death. *Development* 132, 165-76 (2005).
197. McHugh, K. P. et al. Mice lacking beta3 integrins are osteosclerotic because of dysfunctional osteoclasts. *J Clin Invest* 105, 433-40 (2000).
198. Reynolds, L. E. et al. Enhanced pathological angiogenesis in mice lacking beta3 integrin or beta3 and beta5 integrins. *Nat Med* 8, 27-34 (2002).
199. Gu, C. et al. Neuropilin-1 conveys semaphorin and VEGF signaling during neural and cardiovascular development. *Dev Cell* 5, 45-57 (2003).
200. Toyofuku, T. et al. Dual roles of Sema6D in cardiac morphogenesis through region-specific association of its receptor, Plexin-A1, with off-track and vascular endothelial growth factor receptor type 2. *Genes Dev* 18, 435-47 (2004).
201. Krebs, L. T. et al. Notch signaling is essential for vascular morphogenesis in mice. *Genes Dev* 14, 1343-52 (2000).
202. Uyttendaele, H., Ho, J., Rossant, J. & Kitajewski, J. Vascular patterning defects associated with expression of activated Notch4 in embryonic endothelium. *Proc Natl Acad Sci U S A* 98, 5643-8 (2001).
203. Xue, Y. et al. Embryonic lethality and vascular defects in mice lacking the Notch ligand Jagged1. *Hum Mol Genet* 8, 723-30 (1999).
204. Gale, N. W. et al. Haploinsufficiency of delta-like 4 ligand results in embryonic lethality due to major defects in arterial and vascular development. *Proc Natl Acad Sci U S A* 101, 15949-54 (2004).

11
12
13
14
15
16
17
18
19
20
21
22
23
24
25
26
27
28
29
30
31
32
33
34
35
36
37
38
39
40
41
42
43
44
45
46
47
48
49
50
51
52
53
54
55
56
57
58
59
60
61
62
63
64
65
66
67
68
69
70
71
72
73
74
75
76
77
78
79
80
81
82
83
84
85
86
87
88
89
90
91
92
93
94
95
96
97
98
99
100

1
2
3
4
5
6
7
8
9
10
11
12
13
14
15
16
17
18
19
20
21
22
23
24
25
26
27
28
29
30
31
32
33
34
35
36
37
38
39
40
41
42
43
44
45
46
47
48
49
50
51
52
53
54
55
56
57
58
59
60
61
62
63
64
65
66
67
68
69
70
71
72
73
74
75
76
77
78
79
80
81
82
83
84
85
86
87
88
89
90
91
92
93
94
95
96
97
98
99
100

101
102
103
104
105
106
107
108
109
110
111
112
113
114
115
116
117
118
119
120
121
122
123
124
125
126
127
128
129
130
131
132
133
134
135
136
137
138
139
140
141
142
143
144
145
146
147
148
149
150
151
152
153
154
155
156
157
158
159
160
161
162
163
164
165
166
167
168
169
170
171
172
173
174
175
176
177
178
179
180
181
182
183
184
185
186
187
188
189
190
191
192
193
194
195
196
197
198
199
200

205. Duarte, A. et al. Dosage-sensitive requirement for mouse Dll4 in artery development. *Genes Dev* 18, 2474-8 (2004).
206. Fischer, A., Schumacher, N., Maier, M., Sendtner, M. & Gessler, M. The Notch target genes *Hey1* and *Hey2* are required for embryonic vascular development. *Genes Dev* 18, 901-11 (2004).
207. Zhong, T. P., Childs, S., Leu, J. P. & Fishman, M. C. Gridlock signalling pathway fashions the first embryonic artery. *Nature* 414, 216-20 (2001).
208. Pereira, F. A., Qiu, Y., Zhou, G., Tsai, M. J. & Tsai, S. Y. The orphan nuclear receptor COUP-TFII is required for angiogenesis and heart development. *Genes Dev* 13, 1037-49 (1999).
209. You, L. R. et al. Suppression of Notch signalling by the COUP-TFII transcription factor regulates vein identity. *Nature* 435, 98-104 (2005).
210. Domenga, V. et al. Notch3 is required for arterial identity and maturation of vascular smooth muscle cells. *Genes Dev* 18, 2730-5 (2004).
211. Joutel, A., Monet, M., Domenga, V., Riant, F. & Tournier-Lasserre, E. Pathogenic mutations associated with cerebral autosomal dominant arteriopathy with subcortical infarcts and leukoencephalopathy differently affect Jagged1 binding and Notch3 activity via the RBP/JK signaling Pathway. *Am J Hum Genet* 74, 338-47 (2004).
212. Tessier-Lavigne, M. Eph receptor tyrosine kinases, axon repulsion, and the development of topographic maps. *Cell* 82, 345-8 (1995).
213. Gerety, S. S., Wang, H. U., Chen, Z. F. & Anderson, D. J. Symmetrical mutant phenotypes of the receptor EphB4 and its specific transmembrane ligand ephrin-B2 in cardiovascular development. *Mol Cell* 4, 403-14 (1999).
214. Wang, H. U., Chen, Z. F. & Anderson, D. J. Molecular distinction and angiogenic interaction between embryonic arteries and veins revealed by ephrin-B2 and its receptor Eph-B4. *Cell* 93, 741-53 (1998).
215. Adams, R. H. et al. Roles of ephrinB ligands and EphB receptors in cardiovascular development: demarcation of arterial/venous domains, vascular morphogenesis, and sprouting angiogenesis. *Genes and Development* 13, 295-306 (1999).
216. Gerety, S. S. & Anderson, D. J. Cardiovascular ephrinB2 function is essential for embryonic angiogenesis. *Development* 129, 1397-1410 (2002).
217. Othman-Hassan, K. et al. Arterial identity of endothelial cells is controlled by local cues. *Dev Biol* 237, 398-409 (2001).
218. Helbling, P. M., Saulnier, D. M. & Brandli, A. W. The receptor tyrosine kinase EphB4 and ephrin-B ligands restrict angiogenic growth of embryonic veins in *Xenopus laevis*. *Development* 127, 269-78 (2000).
219. Yanagisawa, M. et al. A novel potent vasoconstrictor peptide produced by vascular endothelial cells. *Nature* 332, 411-5 (1988).
220. Levin, E. R. Endothelins. *N Engl J Med* 333, 356-63 (1995).
221. Hosoda, K. et al. Targeted and natural (piebald-lethal) mutations of endothelin-B receptor gene produce megacolon associated with spotted coat color in mice. *Cell* 79, 1267-76 (1994).
222. Clouthier, D. E. et al. Cranial and cardiac neural crest defects in endothelin-A receptor-deficient mice. *Development* 125, 813-24 (1998).



223. Yanagisawa, H. et al. Disruption of ECE-1 and ECE-2 reveals a role for endothelin-converting enzyme-2 in murine cardiac development. *J Clin Invest* 105, 1373-82 (2000).
224. Yanagisawa, H. et al. Role of Endothelin-1/Endothelin-A receptor-mediated signaling pathway in the aortic arch patterning in mice [see comments]. *Journal of Clinical Investigation* 102, 22-33 (1998).
225. Tachibana, K. et al. The chemokine receptor CXCR4 is essential for vascularization of the gastrointestinal tract. *Nature* 393, 591-4 (1998).
226. Zou, Y. R., Kottmann, A. H., Kuroda, M., Taniuchi, I. & Littman, D. R. Function of the chemokine receptor CXCR4 in haematopoiesis and in cerebellar development. *Nature* 393, 595-9 (1998).
227. Nagasawa, T. et al. Defects of B-cell lymphopoiesis and bone-marrow myelopoiesis in mice lacking the CXC chemokine PBSF/SDF-1. *Nature* 382, 635-8 (1996).
228. Salvucci, O. et al. Regulation of endothelial cell branching morphogenesis by endogenous chemokine stromal-derived factor-1. *Blood* 99, 2703-11 (2002).
229. McMahon, A. P. More surprises in the Hedgehog signaling pathway. *Cell* 100, 185-8 (2000).
230. DeCamp, D. L., Thompson, T. M., de Sauvage, F. J. & Lerner, M. R. Smoothed activates Galphai-mediated signaling in frog melanophores. *J Biol Chem* 275, 26322-7 (2000).
231. Vokes, S. A. et al. Hedgehog signaling is essential for endothelial tube formation during vasculogenesis. *Development* 131, 4371-80 (2004).
232. Byrd, N. et al. Hedgehog is required for murine yolk sac angiogenesis. *Development* 129, 361-72 (2002).
233. Lawson, N. D., Vogel, A. M. & Weinstein, B. M. sonic hedgehog and vascular endothelial growth factor act upstream of the Notch pathway during arterial endothelial differentiation. *Dev Cell* 3, 127-36 (2002).
234. Byrd, N. & Grabel, L. Hedgehog signaling in murine vasculogenesis and angiogenesis. *Trends Cardiovasc Med* 14, 308-13 (2004).
235. Connolly, A. J., Ishihara, H., Kahn, M. L., Farese, R. V., Jr. & Coughlin, S. R. Role of the thrombin receptor in development and evidence for a second receptor. *Nature* 381, 516-9 (1996).
236. Griffin, C. T., Srinivasan, Y., Zheng, Y. W., Huang, W. & Coughlin, S. R. A role for thrombin receptor signaling in endothelial cells during embryonic development. [Comment In: *Science*. 2001 Aug 31;293(5535):1602-4 UI: 21425318]. *Science* 293, 1666-70 (2001).
237. Rahman, A. et al. Galpha(q) and Gbetagamma regulate PAR-1 signaling of thrombin-induced NF-kappaB activation and ICAM-1 transcription in endothelial cells. *Circ Res* 91, 398-405 (2002).
238. Marinissen, M. J., Servitja, J. M., Offermanns, S., Simon, M. I. & Gutkind, J. S. Thrombin protease-activated receptor-1 signals through Gq- and G13-initiated MAPK cascades regulating c-Jun expression to induce cell transformation. *J Biol Chem* 278, 46814-25 (2003).

239. Vanhauwe, J. F. et al. Thrombin receptors activate G(o) proteins in endothelial cells to regulate intracellular calcium and cell shape changes. *J Biol Chem* 277, 34143-9 (2002).
240. Ponimaskin, E. et al. Acylation of Galpha(13) is important for its interaction with thrombin receptor, transforming activity and actin stress fiber formation. *FEBS Lett* 478, 173-7 (2000).
241. Strathmann, M. P. & Simon, M. I. G alpha 12 and G alpha 13 subunits define a fourth class of G protein alpha subunits. *Proc Natl Acad Sci U S A* 88, 5582-6 (1991).
242. Gohla, A., Offermanns, S., Wilkie, T. M. & Schultz, G. Differential involvement of Galpha12 and Galpha13 in receptor-mediated stress fiber formation. *Journal of Biological Chemistry* 274, 17901-7 (1999).
243. Gohla, A., Harhammer, R. & Schultz, G. The G-protein G13 but not G12 mediates signaling from lysophosphatidic acid receptor via epidermal growth factor receptor to Rho. *J Biol Chem* 273, 4653-9 (1998).
244. Needham, L. K. & Rozengurt, E. Galpha12 and Galpha13 stimulate Rho-dependent tyrosine phosphorylation of focal adhesion kinase, paxillin, and p130 Crk-associated substrate. *J Biol Chem* 273, 14626-32 (1998).
245. Vexler, Z. S., Symons, M. & Barber, D. L. Activation of Na⁺-H⁺ exchange is necessary for RhoA-induced stress fiber formation. *Journal of Biological Chemistry* 271, 22281-4 (1996).
246. Mao, J., Yuan, H., Xie, W., Simon, M. I. & Wu, D. Specific involvement of G proteins in regulation of serum response factor-mediated gene transcription by different receptors. *J Biol Chem* 273, 27118-23 (1998).
247. Liu, J. L., Blakesley, V. A., Gutkind, J. S. & LeRoith, D. The constitutively active mutant Galpha13 transforms mouse fibroblast cells deficient in insulin-like growth factor-I receptor. *J Biol Chem* 272, 29438-41 (1997).
248. Zohn, I. E. et al. G2A is an oncogenic G protein-coupled receptor. *Oncogene* 19, 3866-77 (2000).
249. Althoefer, H., Eversole-Cire, P. & Simon, M. I. Constitutively active Galphaq and Galpha13 trigger apoptosis through different pathways. *J Biol Chem* 272, 24380-6 (1997).
250. Berestetskaya, Y. V., Faure, M. P., Ichijo, H. & Voyno-Yasenetskaya, T. A. Regulation of apoptosis by alpha-subunits of G12 and G13 proteins via apoptosis signal-regulating kinase-1. *J Biol Chem* 273, 27816-23 (1998).
251. Hart, M. J. et al. Direct stimulation of the guanine nucleotide exchange activity of p115 RhoGEF by Galpha13 [see comments]. *Science* 280, 2112-4 (1998).
252. Kozasa, T. et al. p115 RhoGEF, a GTPase activating protein for Galpha12 and Galpha13 [see comments]. *Science* 280, 2109-11 (1998).
253. Xu, J. et al. Divergent signals and cytoskeletal assemblies regulate self-organizing polarity in neutrophils. *Cell* 114, 201-14 (2003).
254. Offermanns, S., Mancino, V., Revel, J. P. & Simon, M. I. Vascular system defects and impaired cell chemokinesis as a result of Galpha13 deficiency. *Science* 275, 533-6 (1997).

255. Spicher, K. et al. G12 and G13 alpha-subunits are immunochemically detectable in most membranes of various mammalian cells and tissues. *Biochem Biophys Res Commun* 198, 906-14 (1994).
256. Kataoka, H. et al. Protease-activated receptors 1 and 4 mediate thrombin signaling in endothelial cells. *Blood* 102, 3224-31 (2003).
257. Mortensen, R. M., Conner, D. A., Chao, S., Geisterfer-Lowrance, A. A. & Seidman, J. G. Production of homozygous mutant ES cells with a single targeting construct. *Mol Cell Biol* 12, 2391-5 (1992).
258. Sakai, K. & Miyazaki, J. A transgenic mouse line that retains Cre recombinase activity in mature oocytes irrespective of the cre transgene transmission. *Biochem Biophys Res Commun* 237, 318-24 (1997).
259. Kisanuki, Y. Y. et al. Tie2-Cre transgenic mice: a new model for endothelial cell-lineage analysis in vivo. *Dev Biol* 230, 230-42 (2001).
260. Schlaeger, T. M. et al. Uniform vascular-endothelial-cell-specific gene expression in both embryonic and adult transgenic mice. *Proceedings of the National Academy of Sciences of the United States of America* 94, 3058-63 (1997).
261. Soriano, P. Generalized lacZ expression with the ROSA26 Cre reporter strain [letter]. *Nature Genetics* 21, 70-1 (1999).
262. Schlaeger, T. M., Qin, Y., Fujiwara, Y., Magram, J. & Sato, T. N. Vascular endothelial cell lineage-specific promoter in transgenic mice. *Development* 121, 1089-98 (1995).
263. Danielian, P. S., Muccino, D., Rowitch, D. H., Michael, S. K. & McMahon, A. P. Modification of gene activity in mouse embryos in utero by a tamoxifen-inducible form of Cre recombinase. *Curr Biol* 8, 1323-6 (1998).
264. Brewer, S., Feng, W., Huang, J., Sullivan, S. & Williams, T. Wnt1-Cre-mediated deletion of AP-2alpha causes multiple neural crest-related defects. *Dev Biol* 267, 135-52 (2004).
265. Chi, C. L., Martinez, S., Wurst, W. & Martin, G. R. The isthmus organizer signal FGF8 is required for cell survival in the prospective midbrain and cerebellum. *Development* 130, 2633-44 (2003).
266. Brault, V. et al. Inactivation of the beta-catenin gene by Wnt1-Cre-mediated deletion results in dramatic brain malformation and failure of craniofacial development. *Development* 128, 1253-64 (2001).
267. Jiang, X., Rowitch, D. H., Soriano, P., McMahon, A. P. & Sucov, H. M. Fate of the mammalian cardiac neural crest. *Development* 127, 1607-16 (2000).
268. Tronche, F. et al. Disruption of the glucocorticoid receptor gene in the nervous system results in reduced anxiety. *Nat Genet* 23, 99-103 (1999).
269. Beggs, H. E. et al. FAK deficiency in cells contributing to the basal lamina results in cortical abnormalities resembling congenital muscular dystrophies. *Neuron* 40, 501-14 (2003).
270. Offermanns, S., Toombs, C. F., Hu, Y. H. & Simon, M. I. Defective platelet activation in G alpha(q)-deficient mice. *Nature* 389, 183-6 (1997).
271. Offermanns, S. et al. Embryonic cardiomyocyte hypoplasia and craniofacial defects in G alpha q/G alpha 11-mutant mice. *Embo Journal* 17, 4304-12 (1998).

272. Dettlaff-Swiercz, D. A., Wettschureck, N., Moers, A., Huber, K. & Offermanns, S. Characteristic defects in neural crest cell-specific Galphaq/Galpha11- and Galpha12/Galpha13-deficient mice. *Dev Biol* 282, 174-82 (2005).
273. Gitler, A. D. et al. Tie2-Cre-induced inactivation of a conditional mutant Nf1 allele in mouse results in a myeloproliferative disorder that models juvenile myelomonocytic leukemia. *Pediatr Res* 55, 581-4 (2004).
274. Crispino, J. D. et al. Proper coronary vascular development and heart morphogenesis depend on interaction of GATA-4 with FOG cofactors. *Genes Dev* 15, 839-44 (2001).
275. Fujiwara, Y., Browne, C. P., Cunniff, K., Goff, S. C. & Orkin, S. H. Arrested development of embryonic red cell precursors in mouse embryos lacking transcription factor GATA-1. *Proc Natl Acad Sci U S A* 93, 12355-8 (1996).
276. Tsai, F. Y. et al. An early haematopoietic defect in mice lacking the transcription factor GATA-2. *Nature* 371, 221-6 (1994).
277. Shimizu, R., Ohneda, K., Engel, J. D., Trainor, C. D. & Yamamoto, M. Transgenic rescue of GATA-1-deficient mice with GATA-1 lacking a FOG-1 association site phenocopies patients with X-linked thrombocytopenia. *Blood* 103, 2560-7 (2004).
278. Shivdasani, R. A., Mayer, E. L. & Orkin, S. H. Absence of blood formation in mice lacking the T-cell leukaemia oncoprotein tal-1/SCL. *Nature* 373, 432-4 (1995).
279. Soriano, P. The PDGF alpha receptor is required for neural crest cell development and for normal patterning of the somites. *Development* 124, 2691-700 (1997).
280. Inoue, T. et al. Mouse Zic5 deficiency results in neural tube defects and hypoplasia of cephalic neural crest derivatives. *Dev Biol* 270, 146-62 (2004).
281. Girkontaite, I. et al. Lsc is required for marginal zone B cells, regulation of lymphocyte motility and immune responses. *Nat Immunol* 2, 855-62 (2001).
282. Hall, A. Rho GTPases and the actin cytoskeleton. *Science* 279, 509-14 (1998).
283. Kranenburg, O. et al. Activation of RhoA by lysophosphatidic acid and Galpha12/13 subunits in neuronal cells: induction of neurite retraction. *Mol Biol Cell* 10, 1851-7 (1999).
284. Hoang, M. V., Whelan, M. C. & Senger, D. R. Rho activity critically and selectively regulates endothelial cell organization during angiogenesis. *Proc Natl Acad Sci U S A* 101, 1874-9 (2004).
285. Adini, I., Rabinovitz, I., Sun, J. F., Prendergast, G. C. & Benjamin, L. E. RhoB controls Akt trafficking and stage-specific survival of endothelial cells during vascular development. *Genes Dev* 17, 2721-32 (2003).
286. Gohla, A., Offermanns, S., Wilkie, T. M. & Schultz, G. Differential involvement of Galpha12 and Galpha13 in receptor-mediated stress fiber formation. *J Biol Chem* 274, 17901-7 (1999).
287. Gratacap, M. P., Payraastre, B., Nieswandt, B. & Offermanns, S. Differential regulation of Rho and Rac through heterotrimeric G- proteins and cyclic nucleotides. *J Biol Chem* 276, 47906-13 (2001).
288. Gu, J. L., Muller, S., Mancino, V., Offermanns, S. & Simon, M. I. Interaction of G alpha(12) with G alpha(13) and G alpha(q) signaling pathways. *Proc Natl Acad Sci U S A* 99, 9352-7 (2002).



289. Vogt, S., Grosse, R., Schultz, G. & Offermanns, S. Receptor-dependent RhoA activation in G12/G13-deficient cells: genetic evidence for an involvement of Gq/G11. *J Biol Chem* 278, 28743-9 (2003).
290. Moers, A. et al. G13 is an essential mediator of platelet activation in hemostasis and thrombosis. *Nat Med* 9, 1418-22 (2003).
291. Parks, S. & Wieschaus, E. The *Drosophila* gastrulation gene *concertina* encodes a G alpha-like protein. *Cell* 64, 447-58 (1991).
292. Sweeton, D., Parks, S., Costa, M. & Wieschaus, E. Gastrulation in *Drosophila*: the formation of the ventral furrow and posterior midgut invaginations. *Development* 112, 775-89 (1991).
293. Hacker, U. & Perrimon, N. DRhoGEF2 encodes a member of the Dbl family of oncogenes and controls cell shape changes during gastrulation in *Drosophila*. *Genes Dev* 12, 274-84 (1998).
294. Magie, C. R., Meyer, M. R., Gorsuch, M. S. & Parkhurst, S. M. Mutations in the Rho1 small GTPase disrupt morphogenesis and segmentation during early *Drosophila* development. *Development* 126, 5353-64 (1999).
295. Meigs, T. E., Fields, T. A., McKee, D. D. & Casey, P. J. Interaction of Galpha 12 and Galpha 13 with the cytoplasmic domain of cadherin provides a mechanism for beta -catenin release. *Proc Natl Acad Sci U S A* 98, 519-24 (2001).
296. Krakstad, B. F., Ardawatia, V. V. & Aragay, A. M. A role for Galpha12/Galalpha13 in p120ctn regulation. *Proc Natl Acad Sci U S A* 101, 10314-9 (2004).
297. Meigs, T. E., Fedor-Chaikin, M., Kaplan, D. D., Brackenbury, R. & Casey, P. J. Galpha12 and Galpha13 negatively regulate the adhesive functions of cadherin. *J Biol Chem* 277, 24594-600 (2002).
298. Kasai, K. et al. The G12 family of heterotrimeric G proteins and Rho GTPase mediate Sonic hedgehog signalling. *Genes Cells* 9, 49-58 (2004).
299. Ivey, K. et al. Galphaq and Galpha11 proteins mediate endothelin-1 signaling in neural crest-derived pharyngeal arch mesenchyme. *Dev Biol* 255, 230-7 (2003).
300. Liu, J. P. & Jessell, T. M. A role for rhoB in the delamination of neural crest cells from the dorsal neural tube. *Development* 125, 5055-67 (1998).
301. Mortensen, R. in *Current Protocols in Molecular Biology* (ed. Ausubel, F. M. e. a.) 9.16.1 (J. Wiley & Sons, Inc., New York, 1993).
302. Hogan, B., Beddington, R., Constantini, F. & Lacy, E. *Manipulating the mouse embryo* (Cold Spring Harbor Laboratory Press, 1994).
303. Meiner, V. L. et al. Disruption of the acyl-CoA:cholesterol acyltransferase gene in mice: evidence suggesting multiple cholesterol esterification enzymes in mammals. *Proc Natl Acad Sci U S A* 93, 14041-6 (1996).
304. Meyers, E. N., Lewandoski, M. & Martin, G. R. An Fgf8 mutant allelic series generated by Cre- and Flp-mediated recombination. *Nat Genet* 18, 136-41 (1998).
305. Dymecki, S. M. A modular set of Flp, FRT and lacZ fusion vectors for manipulating genes by site-specific recombination. *Gene* 171, 197-201 (1996).
306. Rodríguez, C. I. et al. High-efficiency deleter mice show that FLPe is an alternative to Cre-loxP [letter]. *Nature Genetics* 25, 139-40 (2000).
307. Plump, A. S. et al. Slit1 and Slit2 cooperate to prevent premature midline crossing of retinal axons in the mouse visual system. *Neuron* 33, 219-32 (2002).



308. Soriano, P. Generalized lacZ expression with the ROSA26 Cre reporter strain. *Nat Genet* 21, 70-1 (1999).
309. He, T. C. et al. A simplified system for generating recombinant adenoviruses. *Proc Natl Acad Sci U S A* 95, 2509-14 (1998).



THE
OFFICE
OF THE
SECRETARY
OF THE
TREASURY
WASHINGTON
D. C.

RECEIVED
MAY 10 1917
U. S. DEPARTMENT OF THE TREASURY

FRANCIS

REAR

ADMIRAL

U. S. NAVY

WASHINGTON

MAY 10 1917

MAY 10 1917

MAY 10 1917

MAY 10 1917

MAY 10 1917

MAY 10 1917

MAY 10 1917

UC
 LIBRARY
 SAN FRANCISCO
 UNIVERSITY
 OF THE
 EASTERN
 SHORE
 STATE
 COLLEGE

100
 101
 102
 103
 104
 105
 106
 107
 108
 109
 110

111
 112
 113
 114
 115
 116
 117
 118
 119
 120

UC
 Fra
 RE
 Y
 121
 122
 123
 124
 125
 126
 127
 128
 129
 130

LIBRARY

LIBRARY

7486916



3 1378 00748 6916

For reference

Not to be taken from the room.

